

INTERPRETATION OF SUBSURFACE TEMPERATURE
MEASUREMENTS IN THE MOSFELLSSVEIT AND
ÖLFUSDALUR GEOTHERMAL AREAS, SW-ICELAND

Zhou Xi-Xiang*,
UNU Geothermal Training Programme,
National Energy Authority,
Grensasvegur 9, 108 Reykjavik, Iceland.

*Permanent address:
Chengdu Geological College,
Chengdu,
People's Republic of China.

ABSTRACT

The report presents analyses and interpretation of temperature measurements from drillholes in two important geothermal fields in SW-Iceland. In the Mosfellssveit low temperature field, temperature profiles from 38 wells are studied, and data from 8 wells form the basis of interpretation of the Ölfusdalur high temperature field. It is found that the repeatability of the measurements in the low temperature field is within 0.3°C, and the corresponding value for the high temperature field is 2°C. Both fields are found to be characterized by negative temperature gradients. This is interpreted as due to a horizontal component of the hot water flow in these two geothermal systems. Tentative thermal models are presented for the two fields, with generalized temperature distributions and flow directions as deduced from the temperature data.

LIST OF CONTENTS

	Page
ABSTRACT	3
PREFACE	9
I MOSFELLSSVEIT LOW TEMPERATURE AREA	11
1 INTRODUCTION	11
2 GEOLOGICAL SITUATION OF THE AREA	11
3 INSTRUMENTATION	13
4 ERRORS, FLUCTUATIONS AND DISTURBANCE EFFECTS IN THE TEMPERATURE MEASUREMENTS	15
5 INTERPRETATION	18
6 CONCLUSION AND DISCUSSION	20
II ÖLFUSDALUR HIGH TEMPERATURE AREA	21
1 INTRODUCTION	21
2 INSTRUMENTATION	22
3 ERRORS, FLUCTUATIONS AND DISTURBANCES IN THE TEMPERATURE MEASUREMENTS	23
4 INTERPRETATION	26
5 CONCLUSION AND DISCUSSION	27
ACKNOWLEDGEMENTS	29
REFERENCES	30
FIGURES	33-102

LIST OF FIGURES

1. Geological situation of the Mosfellssveit and the Ölfusdalur geothermal field
2. Boreholes in Mosfellssveit
3. Calibration curve for thermistors (1)
4. Calibration curve for thermistors (2)
5. Temperature profile of well MG-1
6. " " MG-2
7. " " MG-3
8. " " MG-4
9. " " MG-5
10. " " MG-6
11. " " MG-7
12. " " MG-8
13. " " MG-9
14. " " MG-10
15. " " MG-11
16. Temperature profile and simplified geological section of well MG-12
17. " " MG-13
18. " " MG-14
19. " " MG-15
20. " " MG-16
21. " " MG-17
22. " " MG-18
23. " " MG-19
24. " " MG-20
25. " " MG-21
26. " " MG-22
27. Temperature profile of well MG-23
28. " " MG-24
29. Temperature profile and simplified geological section of well MG-25
30. " " MG-27
31. " " MG-28
32. " " MG-29
33. " " MG-30
34. " " MG-31

35. Temperature profile and simplified geological section of well MG-32
36. " " MG-33
37. " " MG-34
38. " " MG-35
39. " " MG-36
40. " " MG-37
41. " " MG-38
42. " " MG-39
43. Temperature profile NW-SE, S-Reykir, Mosfellssveit
44. " " N - S, " "
45. " " W - E, N-Reykir, "
46. " " N - S, " "
47. a, b. Maps showing maximum temperature and depth of maximum temperature at S-Reykir, Mosfellssveit.
48. Isotherms at 100 m depth, S-Reykir, Mosfellssveit
49. " 300 m " "
50. " 500 m " "
51. " 700 m " "
52. " 900 m " "
53. " 1100 m " "
54. " 1300 m " "
55. " 1500 m " "
56. Map showing maximum temperature in Mosfellssveit
57. A model of geothermal water in Mosfellssveit
58. Ölfusdalur high temperature field
59. Temperature profile of well G-8, Ölfusdalur
60. " " G-1, "
61. " " G-7, "
62. " " G-7, "
63. " " G-6, "
64. " " G-3, "
65. " " G-5, "
66. " " G-2, "
67. " " G-4, "
68. Temperature profile NW-SE, Ölfusdalur
69. The preliminary model of hot water flow, Ölfusdalur

LIST OF TABLES

	Page
1. Occurrence of aquifers in different rock types of 29 drillholes	12
2. Chemical composition in ppm of thermal water	13
3. Calibration values for a termistor	14
4. Temperature in Mg-2	16
5. Chemical composition of thermal water in G-2	21
6. Temperature measurements in well G-3	24

PREFACE

The author was awarded a United Nations University Fellowship to attend the UNU Geothermal Training Programme at the National Energy Authority in Iceland in 1980. The training started with an introductory lecture course lasting for 4 weeks on a wide range of topics related to geothermal energy, including geothermal energy around the world, geology, geophysics, geochemistry, borehole geology, borehole geophysics, reservoir engineering and utilization of geothermal resources etc. For me the lecture course provides a general background knowledge concerning most aspects of geothermal energy. After the lecture course I received specialized training in borehole geophysics lasting about 5 months.

From 1980.06.23 to 1980.07.05 we went on a geological field excursion to the main geothermal fields in Iceland. We visited the State Horticultural College, greenhouses, a wool washing factory and a fish drying factory utilizing geothermal water in Hveragerdi, the Fludir low temperature field, the Geysir geothermal field, the Nesjavellir steam field, the Leira geothermal field, the Deildartunga hot spring area, the seaweeds drying plant at Reykholar, hot spring area in Hrutafjordur and several low temperature areas in N-Iceland (Reykir at Reykjabraut, Skutudalur, Dalvik, Akureyri and Hveravellir), a diatomite factory utilizing geothermal steam at Myvatn and the high temperature fields at Namafjall and Krafla and the Krafla power station. During the excursion we studied geological situation and some exploration methods in several typical low and high temperature geothermal fields and seminars were held at the various localities .

Except these activities and short visits to view volcanic eruptions in Krafla and Hekla most of my time was devoted to training in borehole geophysics, which included actual borehole logging in wells (3 weeks), theoretical aspect of temperature and pressure logs, differential temperature, self-potential, resistivity and caliper logs as well as neutron and gamma logs (3 weeks). In view of the present status of geothermal development in China the main emphasis in my training was on temperature and pressure logs. The training was conducted so that I might later train geophysicists in applying these methods. The research work for this report was mainly carried out during the last 10 weeks and includes analyses of temperature

data from two important geothermal fields in SW Iceland. One is the Mosfellssveit low temperature field, which is one of the main sources of hot water for the Reykjavík district heating system. The other is the Ölfusdalur high temperature area.

I M O S F E L L S S V E I T L O W T E M P E R A T U R E A R E A

1 I T R O D U C T I O N

The Mosfellssveit geothermal field is one of the main sources of hot water for the Reykjavik district heating system, which serves about 120.000 inhabitants. It is located 15-20 km NE of Reykjavik (Fig. 1) (Palmason et al 1979). Prior to 1933, when exploration drilling was started in the area, natural hot springs discharged approximately 120 l/s of thermal water. From 1933-1955, there were drilled about 70 wells 100-628 m in depth with a diameter of 11-15 cm. The total free flow was about 340 l/s in 1970 when drilling was started again. In 1942 a pipeline about 15 km long was built from the field to Reykjavik. Since 1970 there have been drilled 39 wells 800-2045 m deep and 22-32 cm wide. All but one of these wells have been economically harnessable. The pumping capacity of the individual wells ranges from 23-100 l/s of 63°-100°C water with a draw down of a few tens of meters. Larger pumps than 100 l/s could be used in some of the wells. The total capacity of the Mosfellssveit field using pumps is estimated 2000-2200 l/s of about 86°C water (Thorsteinsson, 1975).

From 1970 until now temperature measurements have been carried out in these 39 wells of 800-2045 m. These data have been collected and drawn into diagram in this report. The study of temperature distribution in the area is made in order to try to find out how the hot water flows in the reservoir. If we know the behaviour of the geothermal system we can find out where to locate new drillholes and we can predict what will be the temperature in the new wells.

2 G E O L O G I C A L S I T U A T I O N O F T H E A R E A

The Mosfellssveit field is divided into two subareas, S-Reykir and N-Reykir (see Fig. 2), each at an elevation of 40-80 meters above mean sea level. The subareas are 2-3 km apart and are separated by hills which rise to an elevation of 220-250 meters above mean sea level.

Geologically the field is located on the western flank of the neovolcanic zone in Southwest Iceland and close to a Plio-Pleistocene central volcano (Fridleifsson, 1973, 1977) (see Fig. 1). The rocks in the area range in age from about 2.8 to 1.8 m.y. Plio-Pleistocene strata reaches down to a depth of at least 2000 meters. The stratigraphic succession is characterized by sequences of subaerial lava flows intercalated by volcanic hyaloclastites and morainic horizons at intervals corresponding to glaciations. Usually hyaloclastites are dominant to about 1000 m depth. Below, there are mostly lavas, but hyaloclastite horizons are found to the bottom of holes. Dykes are rare in the uppermost 1000 m, but their number tend to increase with depth (Tomasson et al 1975).

Aquifers are irregularly distributed through the geological section but are commonly at contacts between individual lava flows and hyaloclastites and dolerite intrusions. Table 1 shows the occurrence of aquifers in the different rock types in the first 29 drillholes in the area.

TABLE 1

Occurrence of aquifers in different rock types of 29 drillholes
(from Tomasson et al 1975)

Rock types	Aquifers/circulation loss			Total number
	≤ 2 l/s	2-20 l/s	> 20 l/s	
Lavas	44	27	2	73
Hyaloclastites ^x	29	12	4	45
Dolerites		1	1	2
Lavas and hyaloclastites ^x	53	38	20	111
Lavas and dolerites	13	1	3	17
Hyaloclastites ^x and dolerites	5	2	1	8

^x included in this group are reworked hyaloclastites and detrital beds

The chemical compositions of the hot water in the MG-15 and MG-16 are listed in table 2.

TABLE 2

Chemical composition in ppm of thermal water

(data from Palmason et al. 1979 and Fridleifsson 1979)

	T°C	PH/C°	SiO ₂	Na	K	Ca	Mg	CO ₂	SO ₄	H ₂ S	Cl	F	Diss Solids
MG-15	85	9.82/19	91	43.2	0.9	2.38	0.01	19.0	23.0	0.6	24.9	0.68	165
MG-16	101	9.65/23	110	50.8	1.5	2.3	0.01	20.5	28.6	1.4	24.2	0.95	230

The alteration pattern in the area is very complex. Low temperature alteration is superimposed on former high-temperature alteration associated with the extinct central volcano. A retrograde transformation of chlorites has been demonstrated (Tomasson and Kristmannsdottir 1974).

3 INSTRUMENTATION

Thermistors were used to measure temperature in wells in the area. Resistivity measurement of temperature thermistors are widely used in temperature well logging in low temperature geothermal fields. They have the advantage of being of small size and the transmission from the measuring point to a surface recorder is easy. This is done through an electric cable, and the measuring value is obtained either directly by a simple resistivity meter, or indirectly by coupling the sensor into a resonant circuit. The data information is then fed through the cable as a pulsed signal where the temperature is given by the frequency of the pulses (Stefansson and Steingrímsson 1980).

Fabrication of one kind of thermistors is rather easy. For example, we have used a VECO thermistor (100 K-ohms, Victory Engineering Corporation) as a sensor welded on a two conductor cable. For isolation the thermistor is placed into a plastic tube and the tube filled with silastic (732 RTV adhesive/sealant) and with E-POX-E Ribbon at the top of the tube. Several hours later the tube was fixed into a brass pipe to prevent the sensor from being broken. At the end of the pipe there are some holes for the sensor to get freely in thermal contact with the water in the well.

Thermistors have negative temperature characteristics i.e. the resistivity decreases as the temperature increases. The general equation between the two values is assumed as follows:

$$R = \text{EXP} \left[A + B \left(\frac{T_0}{T} \right) + C \left(\frac{T_0}{T} \right)^2 \right] \quad (1)$$

where

R = resistivity in K-ohms

$T_0 = 273.15 \text{ } ^\circ\text{K}$

T = temperature in $^\circ\text{K}$

and A, B, and C are constants.

Reducing to logarithmic form we have

$$\text{Ln } R = A + B \left(\frac{T_0}{T} \right) + C \left(\frac{T_0}{T} \right)^2 \quad (2)$$

Before we put the thermistor into a well for measuring the temperature, we must calibrate the thermistor and calculate the coefficients A, B and C. Due to the drift of the thermistors regular recalibration is needed.

A simple calibration method is to put the thermistor into a water bath and connect the thermistor with an ohm-meter. Heating the water in heat basin we note down the temperature values from a mercury thermometer and the ohm-value from an ohm-meter. To obtain higher accuracy we heat the water slowly and stir the water continuously. A more complex calibration method is to use a computer to control the stability of the temperature and to measure automatically the calibration points. Such calibration facilities are available in Orkustofnun. Table 3 is an example of calibration result of thermistor.

TABLE 3 Calibration values for a termistor

T °C	R KΩ	Time	$\frac{1}{T}$ K ⁻¹
17.0	151.9	11.45	0.00345
35.5	65.9	13.15	0.00323
45.6	42.9	13.30	0.00314
55.1	29.2	13.43	0.00304
67.4	18.3	13.55	0.00293
75.1	13.6	14.00	0.00287
79.5	11.97	14.11	0.00284
89.1	8.67	14.25	0.00276
94.0	7.38	14.34	0.00272
57.3	26.8	14.46	0.00303
48.4	38.0	14.52	0.00311
40.2	53.4	14.58	0.00319
28.6	88.4	15.02	0.00316
17.4	148.6	15.10	0.00344

The diagram of relationship between LnR and 1/T is shown in Fig. 3. For convenience a diagram R versus temperature is shown in Fig. 4. In this example we can solve the following equations by the least square method.

$$\begin{bmatrix} n & \sum_1^n \left(\frac{T_0}{T_i}\right) & \sum_1^n \left(\frac{T_0}{T_i}\right)^2 \\ \sum_1^n \left(\frac{T_0}{T_i}\right) & \sum_1^n \left(\frac{T_0}{T_i}\right)^2 & \sum_1^n \left(\frac{T_0}{T_i}\right)^3 \\ \sum_1^n \left(\frac{T_0}{T_i}\right)^2 & \sum_1^n \left(\frac{T_0}{T_i}\right)^3 & \sum_1^n \left(\frac{T_0}{T_i}\right)^4 \end{bmatrix} \begin{bmatrix} A \\ B \\ C \end{bmatrix} = \begin{bmatrix} \sum_1^n \text{Ln } R_i \\ \sum_1^n \left[\text{Ln } R_i \left(\frac{T_0}{T_i}\right)\right] \\ \sum_1^n \left[\text{Ln } R_i \left(\frac{T_0}{T_i}\right)^2\right] \end{bmatrix}$$

and the solution is

$$\begin{aligned} A &= - 4.37 \\ B &= 19.81 \\ C &= - 2.65 \end{aligned}$$

As the temperature measurements used in this report have been made during the last ten years, various sensors have been used for the measurements. During 1970-1977 thermistors, as described above, were most frequently used, whereas the measurements in 1977-1980 have mostly been performed by a resistor coupled into a resonance circuit in the probe.

4 ERRORS, FLUCTUATIONS AND DISTURBANCE EFFECTS IN THE TEMPERATURE

MEASUREMENTS

a. Errors and fluctuations

For determining the accuracy of the temperature measurements used, and to obtain information on temperature fluctuations in the reservoir, we repeat the temperature measurement in the same well after thermal equilibrium had been reached. The completion time of MG-2 is November 11, 1963. We consider that the well has been in geothermal equilibrium for about 17 years. For the purpose of estimating measurement errors temperature measurements were made on May 8, 1980 and on July 21, 1980. The results are shown in Table 4. and Fig. 6.

TABLE 4

Temperature in well MG-2

depth (m)	temperature (°C)		$\delta = T_1 - T_2$	δ^2
	T ₁ (1980.05.08)	T ₂ (1980.07.21)		
100	68.1	69.3	- 1.2	1.44
150	70.2	71.1	- 0.9	0.81
200	72.5	73.3	- 0.8	0.64
250	75.3	76.0	- 0.7	0.49
300	78.3	78.5	- 0.2	0.04
350	80.6	80.2	0.4	0.16
400	82.4	82.9	- 0.5	0.25
450	84.8	86.1	- 1.3	1.69
500	85.9	86.0	- 0.1	0.01
550	86.4	85.4	0.5	0.25

The average square error of the measurement is

$$\sigma = \sqrt{\frac{\sum_{i=1}^n \delta_i^2}{n(n-1)}} = \sqrt{\frac{5.78}{90}} = 0.25^\circ\text{C}$$

So the accuracy of the temperature measurement is considered $\pm 0.3^\circ\text{C}$ and the temperature fluctuations are expected to be rather low.

b. Disturbance effects

The main disturbance effect in the temperature measurement is the cooling during drilling. There are large differences between the data measured at different times during drilling and the data measured in the wells a long time after drilling.

The recovery time to warm up from cooling during drilling is variable depending on the geological and geothermal conditions of the wells. Such as the permeability and the thermal conductivity of the rocks, the distribution of permeable layers as well as the temperature and pressure conditions etc.

As the rocks in the thermal area are highly permeable, and as there is a large number of aquifers, the recovery time for warming up is usually

rather short. In many cases good results have been obtained relatively shortly after drilling sometimes only a few months.

The following wells can be taken as examples:

Well MG-33 was completed on April 9, 1976. The differences between the data measured on May 14, 1976 and the data measured on September 11, 1976 are within the error of the temperature measurements. The two temperature curves can be considered the same (see Fig. 36).

Well MG-16 was completed on March 2, 1973. The two temperature curves (one was measured on October 18, 1973, the other on December 1, 1974, see Fig. 20) are almost the same except for the segments of 200-275 m depth and 50 m depth.

MG-15, MG-21, MG-32 and MG-35 (see Fig. 19, Fig. 25, Fig. 35 and Fig. 38 respectively): The differences between two curves measured at different times in these wells are about 2°-3°C.

On the other hand, some wells are close to each other and the temperature curves measured in these wells usually have the same form, for example MG-35 and MG-39. The distance between the two wells is about 200 m. The temperature curves are shown in Fig. 38 and Fig. 42 respectively. Comparing the two curves we can see that they are very similar and have almost the same maximum temperature.

The results mentioned above illustrate that the temperature data measured several months after drilling are usually reliable. But in some wells the recovery time seems to be rather long. These wells are characterized by relatively low flow rates and hence low permeability. For example MG-12, the completion time of the well is June 22, 1972. The differences between the curve measured on July 9, 1972 and the curve measured on September 20, 1972 are commonly 7°-11°C (see Fig. 16).

The completion time of MG-22 is November 9, 1973. The differences between the data measured at November 13, 1973 and the data measured at November 29, 1973 and between the data of November 29, 1973 and November 26, 1974 are about 6°C in the highest temperature intervals even larger at shallow depths (see Fig. 26).

The same results are obtained in MG-19 and especially in MG-28. Large differences have been obtained between measurements made at different times after drilling. The completion time of MG-28 is October 28, 1974. The differences in the maximum temperature part between the data measured at November 29, 1974 and at January 16, 1975 and the data of January 16, 1975 and May 25, 1976 are about 6°-8°C.

5 INTERPRETATION

There are 39 wells of 800-2045 m depth in the Mosfellssveit geothermal field. The curves for temperature with depth in most of the wells are shown in Fig. 5 to Fig. 42. These curves are usually the last measured results in the wells before pumps were installed in the wells. In most of the diagrams there are included simplified geological sections, which have been extracted from the detailed geological logs of Jens Tómasson (1975, 1977, 1978). Some diagrams show two or three sets of temperature measurements for comparison. These figures constitute the basic data for the interpretation presented here.

For interpretation some figures have been drawn to show the temperature distribution in certain cross sections (Fig. 43 to Fig. 46) and at different depths in S-Reykir (Fig. 47 to Fig. 55) as well as the distribution of the maximum temperature and of the maximum temperature with depth in S-Reykir. The main points that arise from the analyses are:

- a. From the diagrams of Fig. 5 to Fig. 42 we can see that a negative temperature gradient is observed in all the wells except for wells MG-4, MG-6, MG-7 and MG-12 which are located in the center of S-Reykir. The maximum temperatures of the curves are usually at 200-700 m depth. Deeper the temperature decreases when the depth increases. So it is quite clear that the thermal area is characterized by a certain amount of horizontal flow.
- b. In the deep part of the S-Reykir region (about > 1200 m depth) the temperature distribution is rather uniform. The temperature values are lower in the southern part and increase gradually towards the north. The horizontal gradient is about 13°C/km (Fig. 54 and Fig. 55).

- c. In the 200-1000 m depth interval the temperature also increases from south towards north. But the horizontal gradient is about 26 °C/km, twice of that in the deep part and is the highest horizontal gradient value recorded (Fig. 48 to Fig. 53). The horizontal movement of the geothermal water thus appears to be in the 200-1000 m depth interval in the area or we can say that this depth interval is the main channel of the hottest water.
- d. From two east-west cross sections, one in S-Reykir (Fig. 43) and the other in N-Reykir (Fig. 45) we can see a low temperature region in the center of these sections at about MG-4 in Fig. 43 and at MG-5 in Fig. 45. There seems to be a low-temperature belt from MG-4 to MG-5 with SW-NE direction. In wells MG-4, MG-6, MG-7 and MG-12 the positive temperature gradient is distributed in the low-temperature belt. This could possibly be due to cold water penetrating along a big fault from the surface to depth in the region.

From hydrological investigations of injection tests in the area an impermeable barrier (aquiclude) has been found to exist between the western and eastern part of the field (Thorsteinsson, 1975). So it is no wonder that most of the wells near the barrier have a rather long recovery time. Wells MG-12, MG-28 and MG-19, are examples of this. The low temperature region associated with the hydrological barrier is therefore more likely to be interpreted as due to lower heating effects from the hot water flow rather than downflow of cold surface water.

- e. The cold belt divides the thermal field into two parts (see Fig. 43 and Fig. 45). The NW thermal region is shown in more detail in Fig. 44 and the SE region is shown in Fig. 47 in more detail. It is possible that the two hot water streams are coming from different sources of hot water. One is coming from the north-west and the other from the south-east. Of course it is hard to say whether they are coming from the same inflow source or different sources by studying the temperature data alone.

6 CONCLUSIONS AND DISCUSSION

The interpretation of temperature data in the area enables us to build a geothermal model of the field. The ideal isothermal model of the maximum temperature in the field and the ideal cross section of the model are shown in Fig. 56 and Fig. 57 respectively.

We know the area is a low temperature field. The temperature of geothermal water is 60°-100°C in the field. The main horizontal flow of the hottest thermal water appears to be at the depth interval of 200-1000 m.

The temperature profiles indicate that two individual hot water channels come into the field north-west of the NE-SW barrier crossing the field and the other one from the south-east. The direction of the flow can, however, not be determined from the temperature data alone. The hot water flow is nearly horizontal in the central region of the area. There is a cold water belt with SW-NE direction through the center of the field. This colder belt is correlated with an aquiclude zone and its cause is interpreted to be a big fault. The fault disconnects aquifers and thus causes the impermeable barrier.

The temperature model suggests that new drillholes should be sited on both sides of the cold barrier towards the NW and the SE.

In this interpretation only the temperature has been taken into account. To suggest optimum exploitation of a low temperature field the combination of temperature and flow rates from aquifers at various depth intervals in the various parts of the field must be looked into. This awaits a further study.

II ÖLFUSDALUR HIGH TEMPERATURE AREA

1 INTRODUCTION

Ölfusdalur is located about 50 km east of Reykjavik and 1 km north of the village Hveragerdi (see Fig. 1 and Fig. 58). There are 8 wells of 300-1000 m depth in the area. The maximum temperature in these well is 180°-230°C. Numerous natural hot springs are distributed in and north of the drilling area. The wells were completed in 1959-1961. Temperature measurements were carried out in the wells after drilling and some have been measured again in 1979 and 1980. These data have been collected and are shown in diagrams in the report. Like in the Mosfellsveit field, the study task of the present author with the temperature data in the area is to try to find out the behaviour of the geothermal system, for example, how the hot water flows in the reservoir in the area.

Geologically the field is located on the margin of the Neovolcanic zone. All strata are late Quaternary volcanics. Early in the Brunhes-period (< 0.7 million years ago) there has been an active central volcano north of Hveragerdi (Saemundsson, 1967). But now it is extinct. Its final activity has been the formation of the many intrusions and dykes which have intruded from the roots of the volcano up to the upper strata. During and after the intrusive formation there has been great geothermal activity which has caused high temperature alteration. Then came a long period of erosion during which some hundreds of meters of strata disappeared from the top of the central volcano and its vicinity and the geothermal activity diminished. Since then the geothermal area is gradually cooling. The main geothermal activity has shifted to the west, i.e. to the Hengill area (Saemundsson, 1967).

The chemical composition of the geothermal water in one well, G-2 is listed in Table 5.

TABLE 5 Chemical composition of thermal water in well G-2. Concentrations in ppm.

	pH	SiO ₂	Na	K	Ca	Mg	CO ₂	SO ₄	H ₂ S	Cl
G-2	7.1/199	269.5	157.0	4.8	2.0	0.1	102.6	44.0	60.5	121.8

The relatively Cl-rich water is typical for this geothermal area (Saemundsson, et al 1972).

2 INSTRUMENTATION

Although resistivity thermometers (thermistors) are those most frequently used in geothermal investigations their operation temperature is limited. With ordinary types of electric insulation and electronic components problems arise at temperatures above 180°C. Maximum operation temperature of commercial high temperature electronics is well below 200°C. At such temperatures the electrical leakage of ordinary cableheads also becomes too great for any serious application of the DC method. At temperatures above 150-200°C thermistors can not be used.

In high temperature areas mechanical thermometers are mainly used. They are similar to ordinary mercury thermometers in that the data can not be transmitted to the surface. However, in the mechanical thermometers the data is recorded inside the temperature probe on a clock driven recorder. Several measuring points (20-30) can be recorded during one run in the well.

Two types of temperature sensors are used for mechanical thermometers. These are the bourdon tube (Amerada-gauge) where the boiling pressure of a special fluid is recorded, and the bimetal tube (Kuster-gauge), where the temperature expansion of the bimetal indicates the temperature.

Amerada-gauge was used in the field for temperature measurements in Ölfusdalur. The gauge consists of three basic parts i.e. the recording section, a clock and a temperature element. There is also a pressure element. If the pressure element is used instead of the temperature element, the gauge can be used for pressure measurement.

The active element in the temperature element is a helical bourdon tube, fixed at one end and free to rotate at the other. The bourdon tube is filled with a volatile liquid. The vapor pressure of the enclosed volatile liquid is directly related to its temperature and causes the free end of the bourdon tube to rotate. The resulting rotation of the end is transmitted directly to a recording stylus without the use of

gears or levers. The stylus records on a coated metal chart. The chart is carried in a removable cylindrical chart holder, the position of which is controlled by a clock. The recording mechanism is so designed that ordinary wear has no effect on the accuracy of the instrument.

The absolute accuracy of the temperature gauge used is $\pm 1^\circ\text{C}$. The sensors drift with time and need to be recalibrated regularly. But they are superior to other thermometers at high temperature and can be operated up to 350°C which is close to the highest temperature so far measured in geothermal wells. Its sensitivity and accuracy depends on the span of the temperature element and whether the temperature being measured is in the lower or upper part of the span. The sensitivity of the gauge is such that changes less than 0.2% of full scale can be detected and measured.

When a temperature measurement is done, the probe is put into the well at points of different depth levels according to need. The time measured at each point is about 5-15 minutes. Before measuring in a well the chart is put in the probe and a base line is drawn on the recorder chart. After the measurement, the chart is taken out and the distances between the deflection of the stylus and the base line are measured by a special chart scanner and the distances converted to temperature by reference to the calibration data for the element.

3 ERRORS, FLUCTUATIONS AND DISTURBANCES IN THE TEMPERATURE MEASUREMENTS

a. Errors

For determining the accuracy of the temperature measurements with the Amerada-gauge, we use the data measured at different times in the same well after equilibrium has been reached after drilling. An example is measurements in well G-3. The well was completed on November 5, 1958. The well had been closed for about 11 years, when the temperature measurement was made on October 3, 1979. The well was measured again on September 2, 1980. The results of these measurements are shown in Table 6 and Fig. 64.

TABLE 6

Temperature measurements in well G-3

depth	temperature (°C)		$\delta = T_1 - T_2$	δ^2
	T ₁ (1979.10.03)	T ₂ (1980.09.02)		
100	140.1	144.6	-4.5	20.25
200	192.9	196.6	-3.7	13.69
250	204.3	206.0	-1.7	2.89
300	206.8	210.3	-3.5	12.25
350	209.0	210.4	-0.6	0.36
400	209.0	207.1	1.9	3.61
420	209.2	207.9	1.3	1.69

The average square error of the measurement is

$$\sigma = \sqrt{\frac{\sum \delta^2}{n(n-1)}} = \sqrt{\frac{54.74}{42}} = 1.14^\circ\text{C}$$

where n is the number of measured points.

Another example is the measurements in well G-1. The completion time of the well is November 7, 1960. Two curves measured at March 23, and 25, 1961 are shown in Fig. 60. From the diagram we can see that the differences between the two curves are commonly less than 2°C.

So we can say the accuracy of the temperature measurements in the area with Amerada-gauge in either 1959-1961 or 1979-1980 is about $\pm 2^\circ\text{C}$ including some fluctuations and disturbance in these wells.

b. Disturbances and fluctuations

Like in Mosfellssveit the main disturbance effects in the area is the cooling during drilling. The warming up in the shallow part during discharge in these wells is also very clear in the temperature profiles.

The recovery time for warming up from cooling during drilling is different in the various wells. Usually the recovery time in most of the wells in the area is few months. A few examples will be cited.

G-7. After drilling temperature measurements were carried out four times in the well within a month after drilling. The results of these measurements are shown in Fig. 62. From the diagram we can see that the speed for warming up in the well is rather high. Compared with the temperature profile in Fig. 61 the curve measured on January 24, 1961 and the curve measured on March 25, 1961 are almost the same. So we can consider that the recovery time in the well is about one month.

G-6. The completion time of the well is November 29, 1960. From Fig. 63 we can see that the measurement on March 28, 1961 and the measurement on September 17, 1979 are very close except at shallow depths above 300 meters.

G-2. The completion time of the well is May 14, 1960. The differences between the curve measured on July 27, 1960 and the curve measured on July 18, 1961 are mostly within the error of the temperature measurement.

But the warming up in G-5 is rather slow. The well was completed May 10, 1960, the results of temperature measurement are shown in Fig. 65. Large differences have been obtained in measurements at different times during the first 14 months. From the diagram in Fig. 65 we can see that differences between the data measured on August 10, 1960, April 5, 1961 and on July 12, 1961 are much larger than the assumed errors of the measurements. The recovery time seems to be at least about one year.

From the diagrams in Fig. 59, Fig 61, Fig. 63 and Fig. 64 we can see that largest differences were obtained between the data measured in 1959-1960 and the data measured in 1979-1980. There may be some reasons. We do not exactly know the conditions of measurements and about the calibration of instruments used in 1959-1961. So it is hard to state the reason exactly.

We can see that the temperature values measured in 1959-1961 are usually much higher than the values measured in 1979-1980 in the shallow part of the wells. And the differences are larger in the deep parts of G-3 and G-8, but much less in the deep parts of G-6 and G-7.

The main reason for the large differences in the shallow parts of the wells appears to be the warming up in the shallow parts during discharge and then

cooling during the period when the wells are closed. The difference in the deep part may also be caused by temperature fluctuations in the reservoir. In the main channel of water flow the temperature is stable, for example in the deep parts of G-7 and G-6. But on both sides of it and at shallow depths the temperature fluctuates and of course the general trend is gradual cooling.

4 INTERPRETATION

As previously mentioned there are 8 wells of 300-1000 m depth in the area. The completion time of the wells is during 1958-1961. Temperature measurements were carried out in the wells after drilling and they were measured again during 1979-1980. These results of measurements are shown in Fig. 59 to Fig. 67. Fortunately, these wells lie almost on a line. Temperature profile of the wells are arranged from NW-SE, and isotherm profiles can be drawn in the direction of NW-SE (Fig. 68). The main points that arise from analyses of the temperature data are:

- a. From the diagrams in Fig. 59 to Fig. 64 we can see that a negative temperature gradient is observed in the lower part of all the wells of the area. In the upper part of the wells the temperature increases with depth and comes up to a maximum, below which the temperature decreases again. Thus it is also rather clear that the thermal area is characterized by a horizontal component of water flow.
- b. The maximum temperature in G-1 is 233°C at a depth of about 600 m. This is also the maximum temperature in the area and largest depth of maximum temperature in these wells. From G-1 towards the south-east the maximum temperature decreases and its depth also decreases. The maximum temperature in well G-7 is 224°C at a depth of about 550 m, in G-6 the maximum temperature is 218°C at a depth of about 450 m. We do not know exactly the maximum temperature in G-3 and G-8 because they are too shallow. The maximum temperature in G-5, G-2 and G-4 is below 200°C at a depth of 100-200 meters. The hot water flow in the cross section thus appears to be coming from the place of well G-1 and G-7 and then spreads southeastwards and upwards. It is at a deeper level in G-1 and G-7 and comes up gradually to a shallower level in G-5, G-2 and G-4, but the flow is still nearly horizontal.

- c. According to the main circulation losses during drilling of well G-7 the main aquifers are at a depth of 400-500 meters, which corresponds with the maximum temperature interval. The second main aquifers are at about 800 m depth. The temperature of the geothermal water in the second aquifers is less than in the first aquifers but it is more homogeneous in the deeper levels of the area.
- d. The horizontal temperature gradient in the cross section in Fig. 68 (NW-SE) is so high (coming up to $40^{\circ}\text{C}/\text{km}$), that I do not think this cross section can present the main flow channel of the thermal water. Geological mapping suggests the main channel to be in the N-S direction passing through the center region between G-8 and G-3 close to G-1 and G-7. Unfortunately well G-8 is too shallow for the maximum temperature to be obtained. However, the shape of the temperature curve in G-8 is more similar to that of well G-3 than G-1 or G-7. There seems to be a fissure or a fault near G-1 and G-7 which makes the main flow channel. Another evidence is that there are several hot springs to the north of G-1 aligned in the direction N-S in the valley Grensdalur. Saemundsson et al. (1972) considered that the distribution of the springs is most likely controlled by faults, which have been active until recently.

5 CONCLUSION AND DISCUSSION

Ölfusdalur is a high temperature field. The maximum temperature of geothermal water in the eight wells studied is 180°C - 230°C . The maximum temperature measured in the field is 233°C . It is still below the boiling temperature. The whole field is a single phase reservoir (no steam in the formation).

Some of the measurement conditions in 1959-1961 in the field are not known. Some of the wells are too shallow and some wells can not be measured again, so some features about the field could not be understood in detail. But a preliminary temperature model of the field is presented here based on the available data.

The geothermal water flow appears to come from the north along faults that pass near G-1 and G-7. The faults may be the main channel of

the hot water flow. There may be an up-flow zone in the north, but in the drilled part of the field the flow is near horizontal. The temperature measurements suggest up-flow somewhere near G-1 and G-7, then the water flows towards the east, and from depth upwards. It may also flow symmetrically towards the west. But unfortunately there is no deep well in the western part of the field to substantiate this. Fig. 69 shows the preliminary model of thermal water flow in an east-west cross section of the field.

The main aquifers are at 400-500 m in G-1 and G-7 and at 100-200 m in G-5 to G-4. In G-7 a deeper aquifer seems to be present at about 800 meters. However, the main aquifers seem to follow the maximum temperature measured in each well.

According to this temperature model, the next drilling should be suggested on both sides of G-1 (or G-7) along the direction of N-S.

ACKNOWLEDGEMENTS

I would first like to thank the organizers of the UNU Geothermal Training Programme in Iceland under the direction of Dr. Ingvar Birgir Fridleifsson for creating good conditions for my study. Dr. Valgardur Stefansson was my main supervisor in learning the techniques of bore-hole geophysics and in the research work leading to this report. Dr. Ingvar Birgir Fridleifsson read and reviewed the whole report with suggestions and recommendations. Further, Mr. Jens Tomasson reviewed the first part of the report and Dr. Kristjan Saemundsson the second part of the report. Their support is very much appreciated.

I would also like to thank Mr. Benedikt Steingrimsson, Mr. Hilmar Sigvaldason, Mr. Gudjon Gudmundsson and Mr. Gudni Gudmundsson for their guidance in the application and instrumentation of well logging methods in Iceland. I would like to thank Ms. Ingunn Sigurdardottir, Ms. Sylvia Johannsdottir and Ms. Erna Birna Forberg for drawing the figures, and Ms. Erla Sigthorsdottir for typing the manuscript.

REFERENCES

Fridleifsson, I.B., 1973: Petrology and structure of the Esja Quaternary volcanic region, South-west Iceland. (D. Phil thesis), Oxford University, 208 pp.

Fridleifsson, I.B., 1977: Distribution of large basaltic intrusions in the Icelandic crust and the nature of the layer 2 - layer 3 boundary. Geol. Soc. Amer. Bull., 88, 1689-1693.

Fridleifsson, I.B., 1979: Geothermal activity in Iceland. Jökull 29, 45-54.

Palmason, G., S. Arnorsson, I.B. Fridleifsson, H. Kristmannsdottir, K. Saemundsson, V. Stefansson, B. Steingrímsson, J. Tomasson, and L. Kristjansson, 1979: The Iceland crust: Evidence from drillhole data on structure and processes. In: Deep Drilling Results in the Atlantic Ocean: Ocean Crust (ed: M. Talwani, C.G. Harrison and D.E. Hayes), Maurice Ewing Series, pp. 43-65, Am. Geophys. Union.

Saemundsson, K., 1967: Vulkanismus und Tektonik des Hengils-Gebietes in Südwest-Island. Acta Naturalia Islandica, Vol. II no.7.

Saemundsson, K., S. Arnorsson, and S. Benediktsson, 1972: Greinargerð um borun í Sogni. Orkustofnun report.

Stefansson, V. and B. Steingrímsson, 1980: Geothermal logging I., Orkustofnun report OS80017/JHD09.

Thorsteinsson, Th., 1975: Redevelopment of the Reykir hydrothermal system in southwestern Iceland. Second U.N. Geothermal Proceedings: 2173-2184.

Tómasson, J., 1975: Jarðhitasvæði í Mosfellssveit. Orkustofnun report OSJHD 7508.

Tómasson, J. 1977: Framvinduskýrsla um borholur Mg-27 til Mg-35 í Mosfells-sveit. Orkustofnun report OSJHD 7711.

Tómasson, J., 1978: Framvinduskýrsla um borholur Mg-36 til Mg-39 í Mosfells-sveit. Orkustofnun report OSJHD 7838.

Tomasson, J. and H. Kristmannsdottir, 1974: Reykir-Reykjavik Investigation of three low-temperature areas in Reykjavik and its neighborhood. Proceedings Int. Symp. on Water-Rock interaction. Praha, 243-249.

Tomasson, J., I.B. Fridleifsson, and V. Stefansson, 1975: A hydrological model for the flow of thermal water in southwestern Iceland with special reference to the Reykir and Reykjavik thermal areas. Proceedings of the Second U.N. Symp. on Development and Use of Geothermal Resources, San Francisco 1975, 643-648.

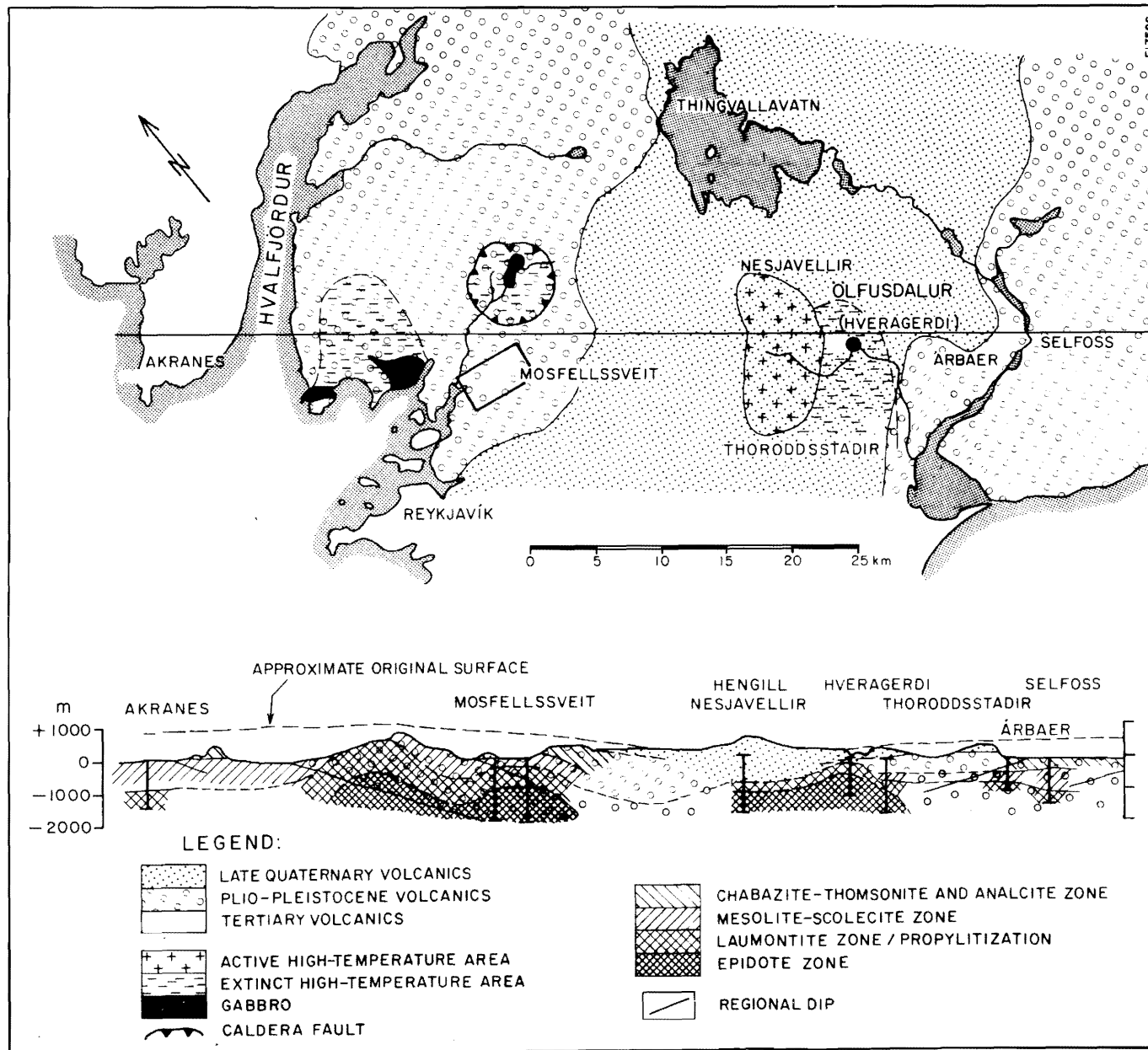


Fig.1. Geological situation of Mosfellssveit and Ölfusdalur geothermal field. (from Palmason et al 1979).

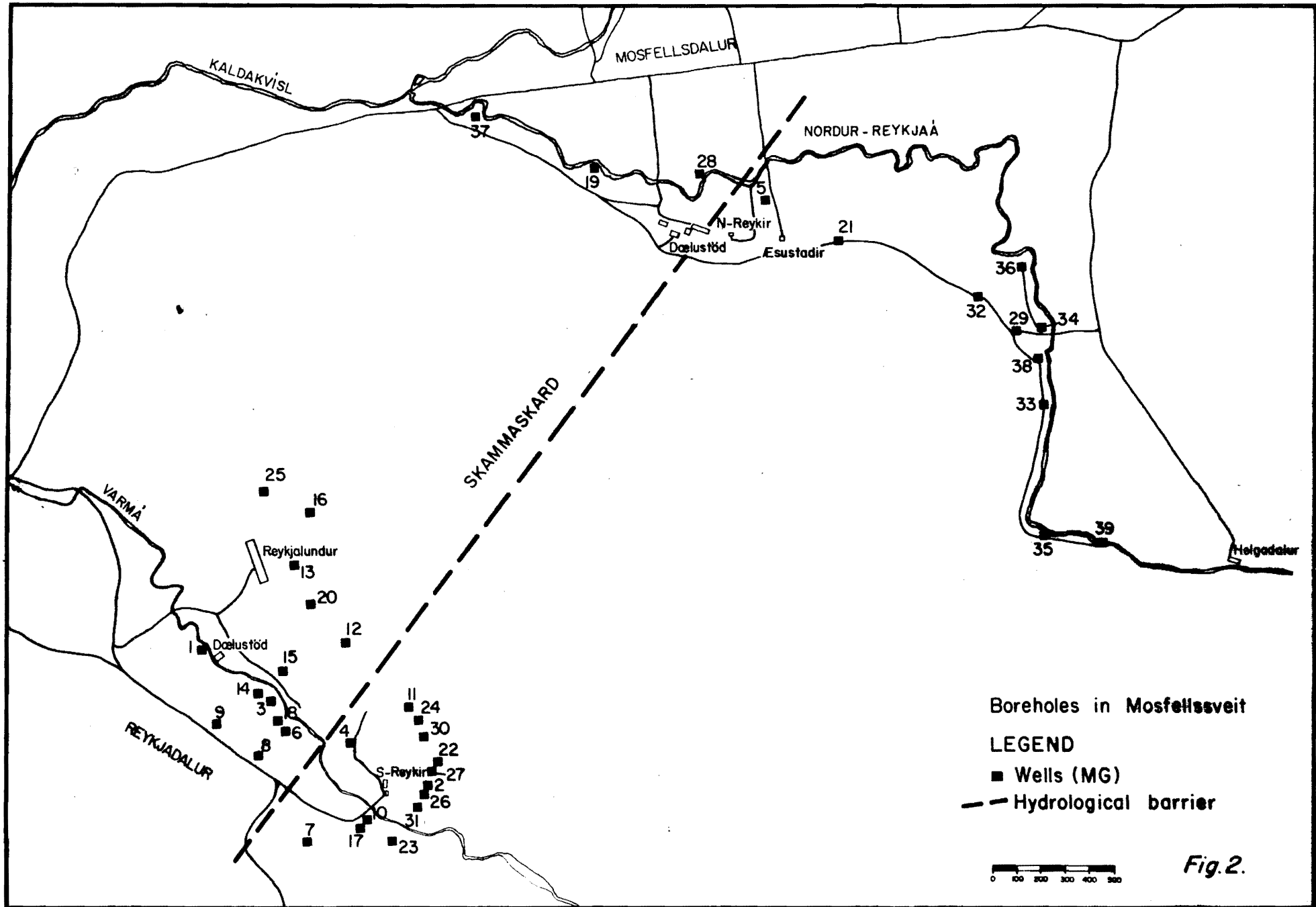
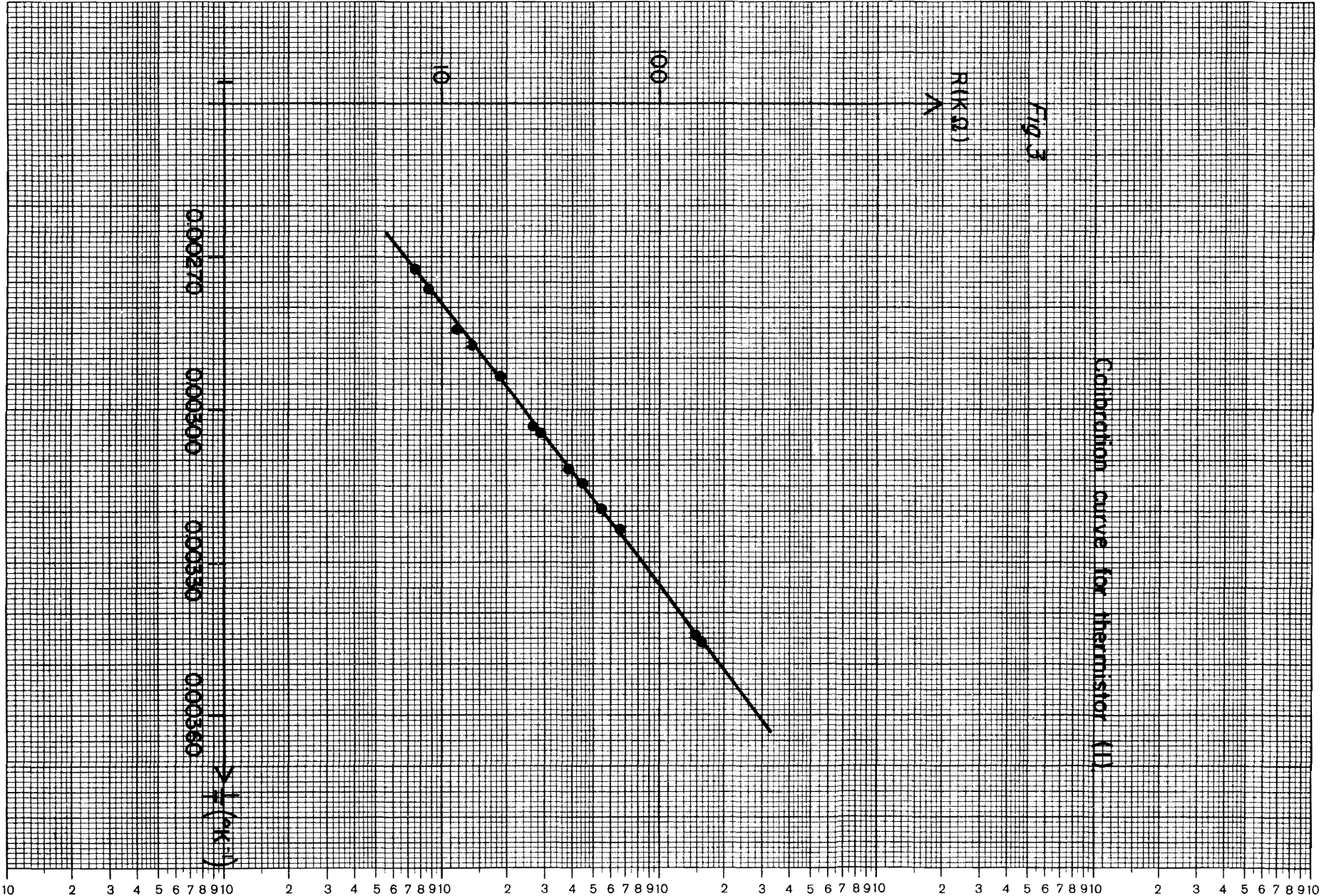


Fig.2.

Calibration curve for thermistor (II)

Fig. 3



800909. ZHOU/EBF HSP F-20014.



COPYRIGHT CARL SCHLEICHER & SCHÜLL-EINBECK WAN.

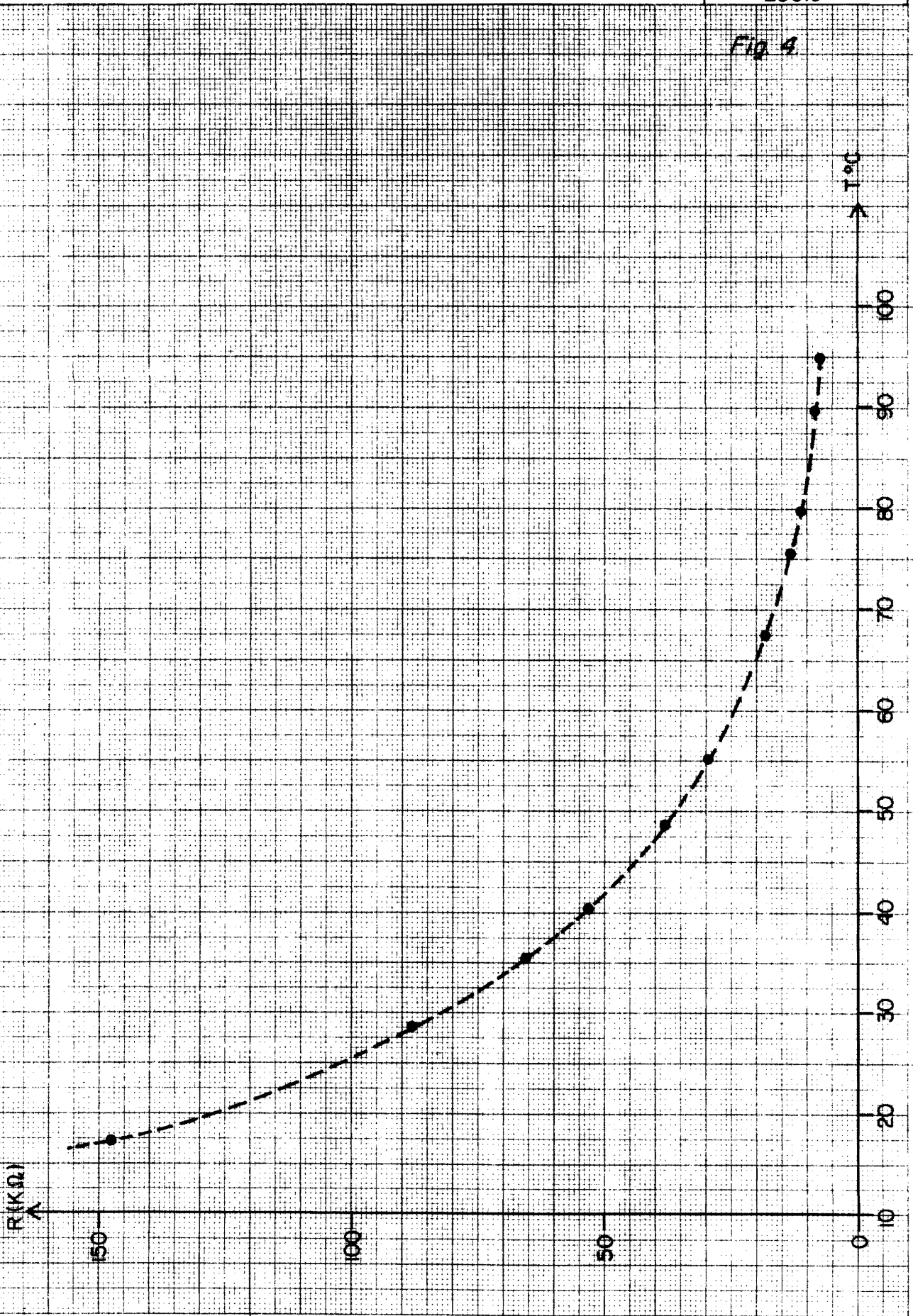


Nr. 442 1/2 A 4 P MADE IN GERMANY

Eine Achse logar. geteilt von 1 bis 1000000, Einheit 42,5 mm, die andere in mm

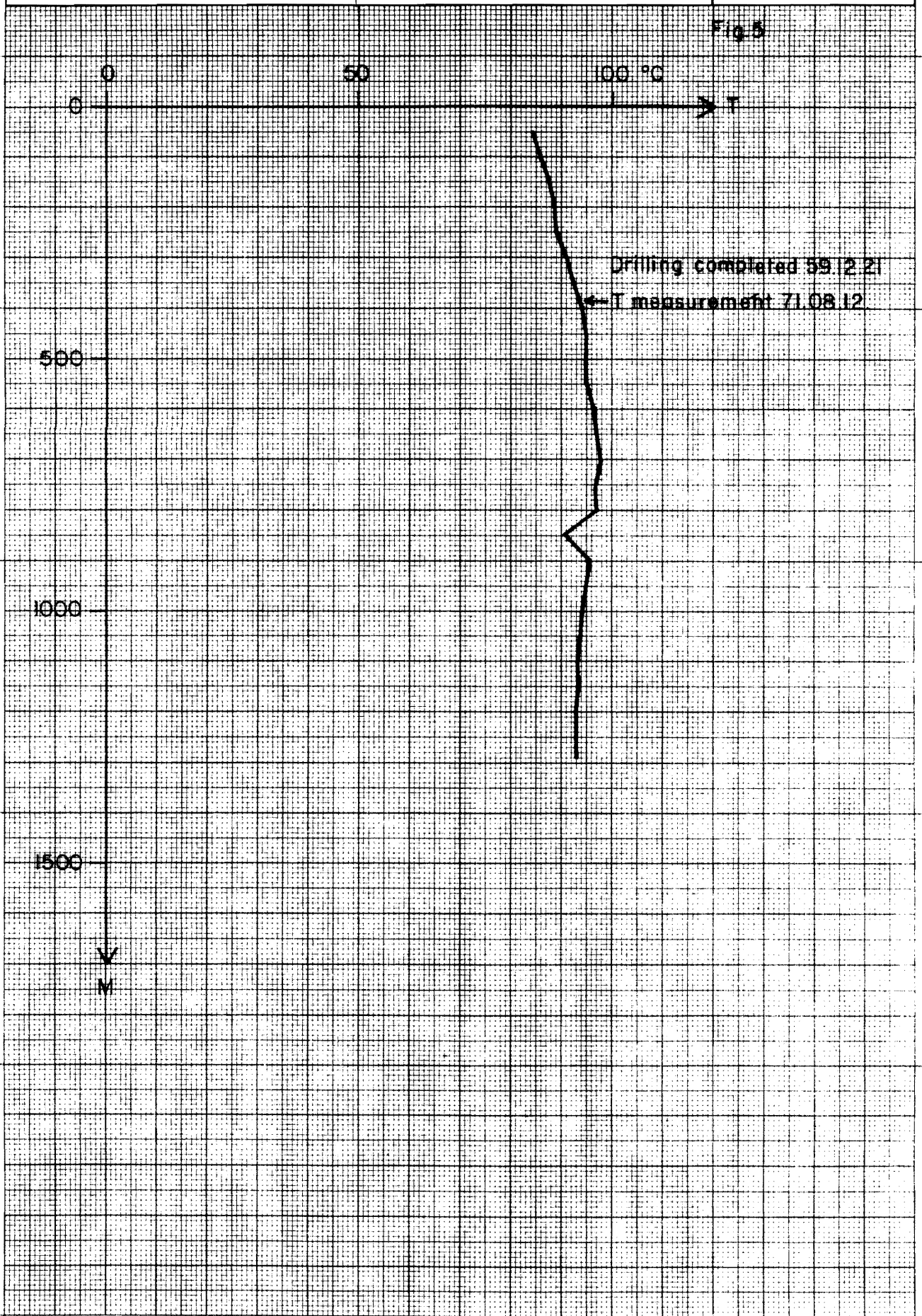
Calibration curve for thermistor (2).

Fig. 4





Temperature profile of well MG-1





80-08-25

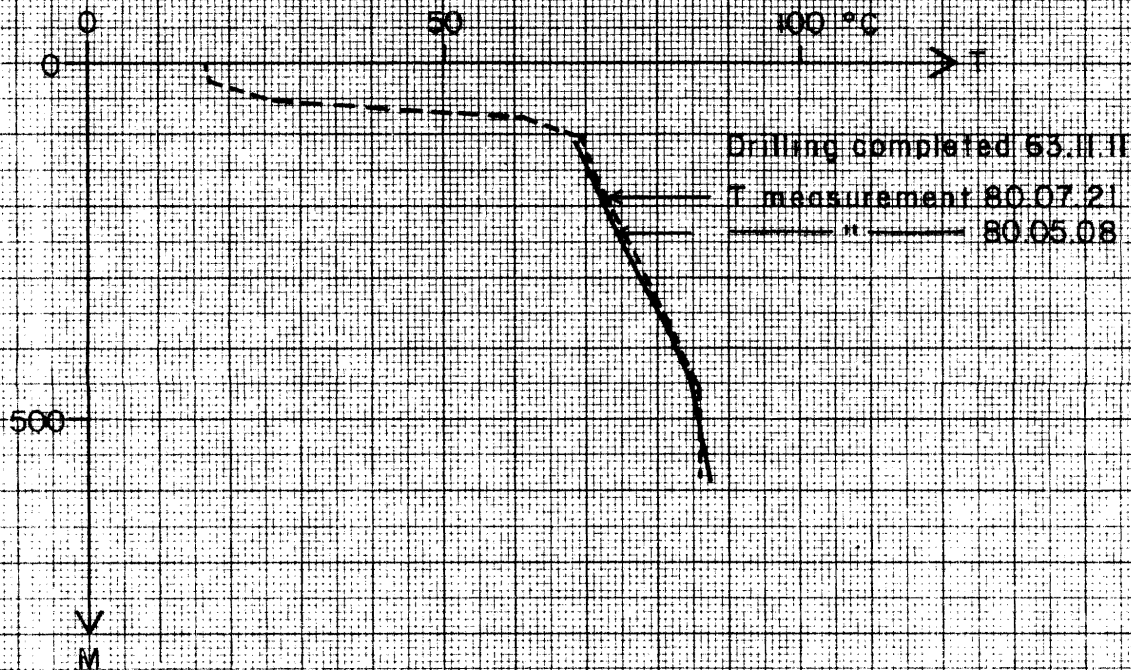
ZHOU/Sy.J.

JHD/HSD Mosfs.

F 19890

Temperature profile of well MG-2

Fig 6





ORKUSTOFNUN

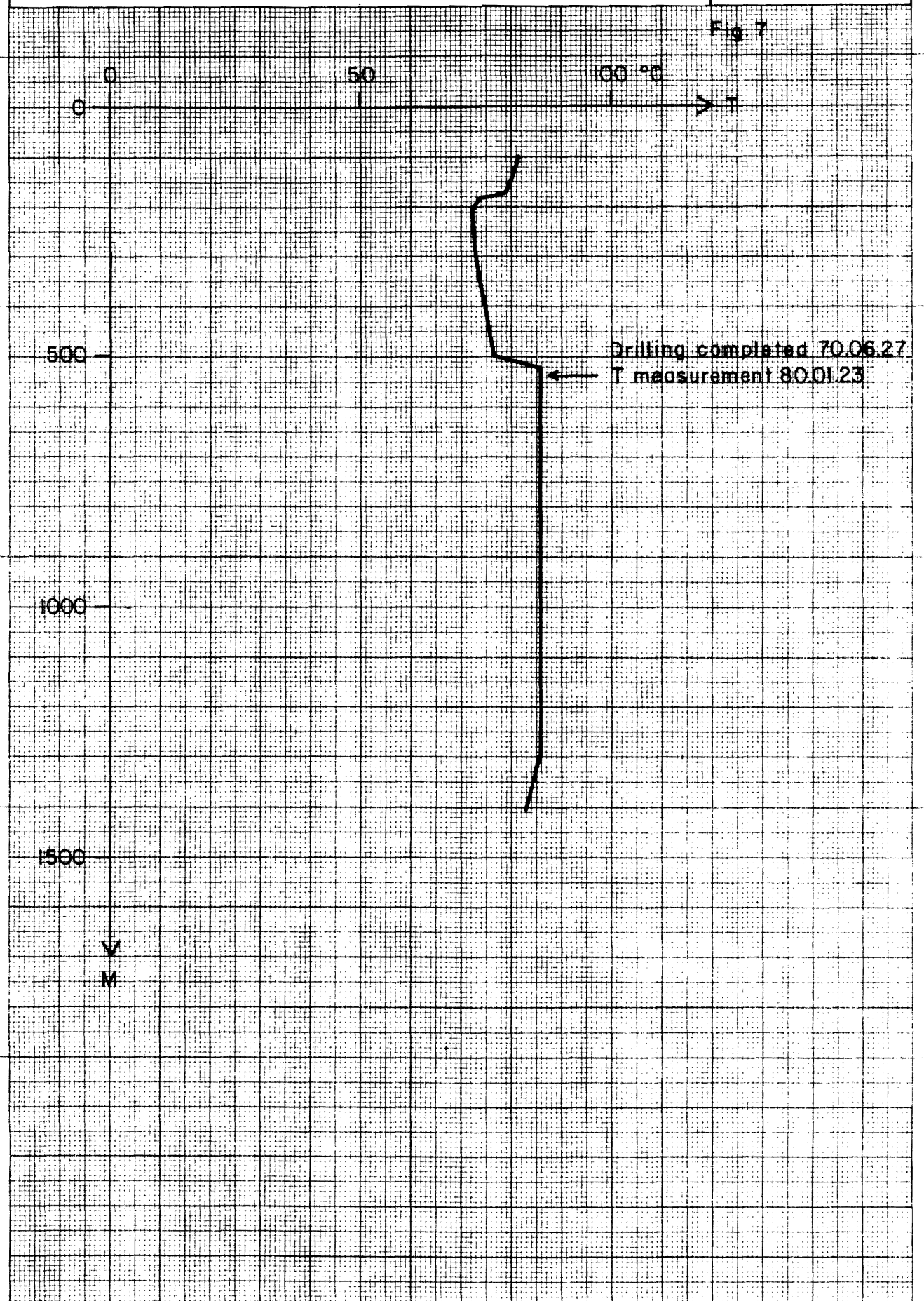
80-08-25

ZHOU/Sy.J.

JHD/HSP Mosf.

F. 1989I

Temperature profile of well MG-3





80-08-25

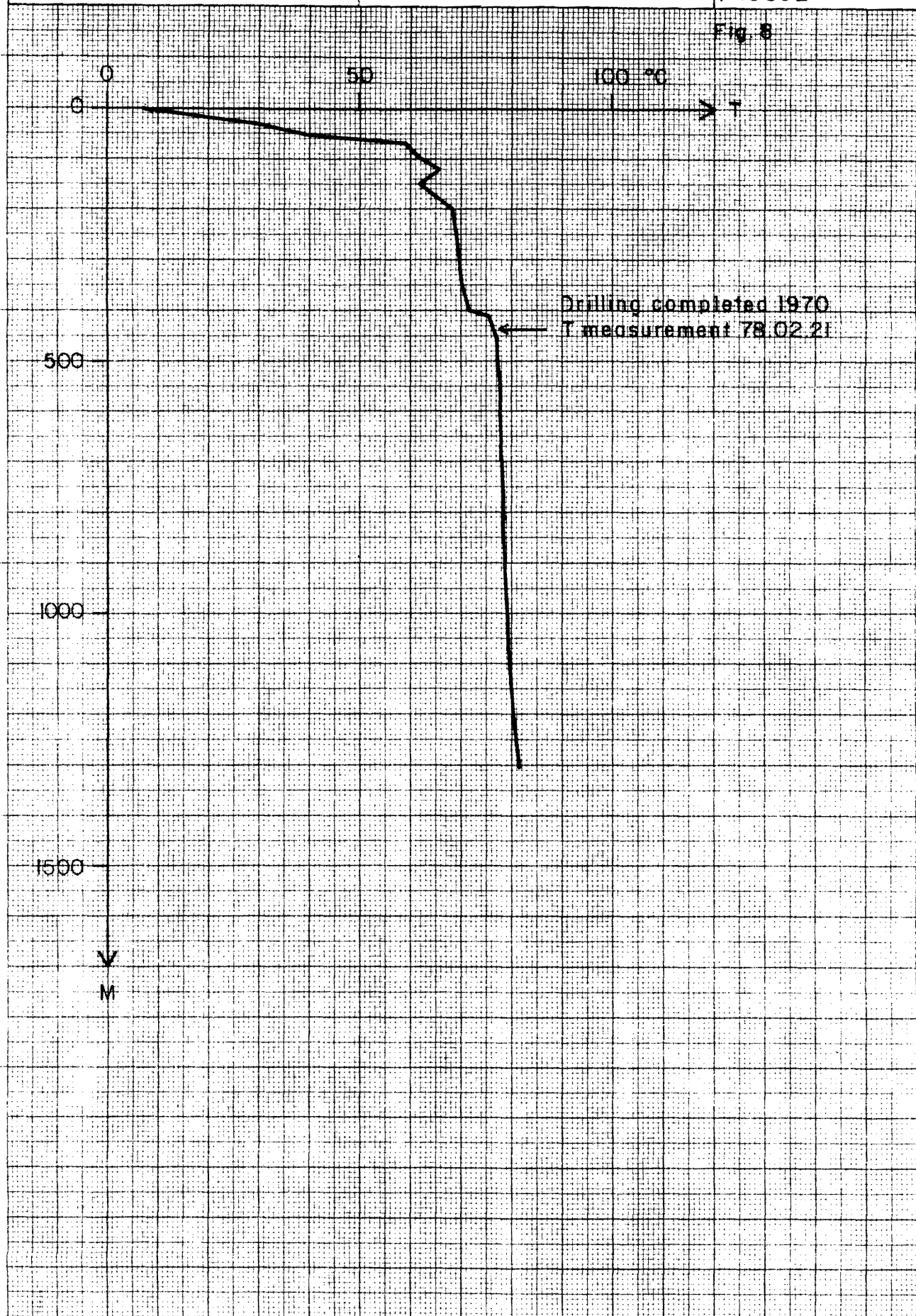
ZHOU/Sy.J.

JHD/HSP Mosf.

F 19892

Temperature profile of well MG-4

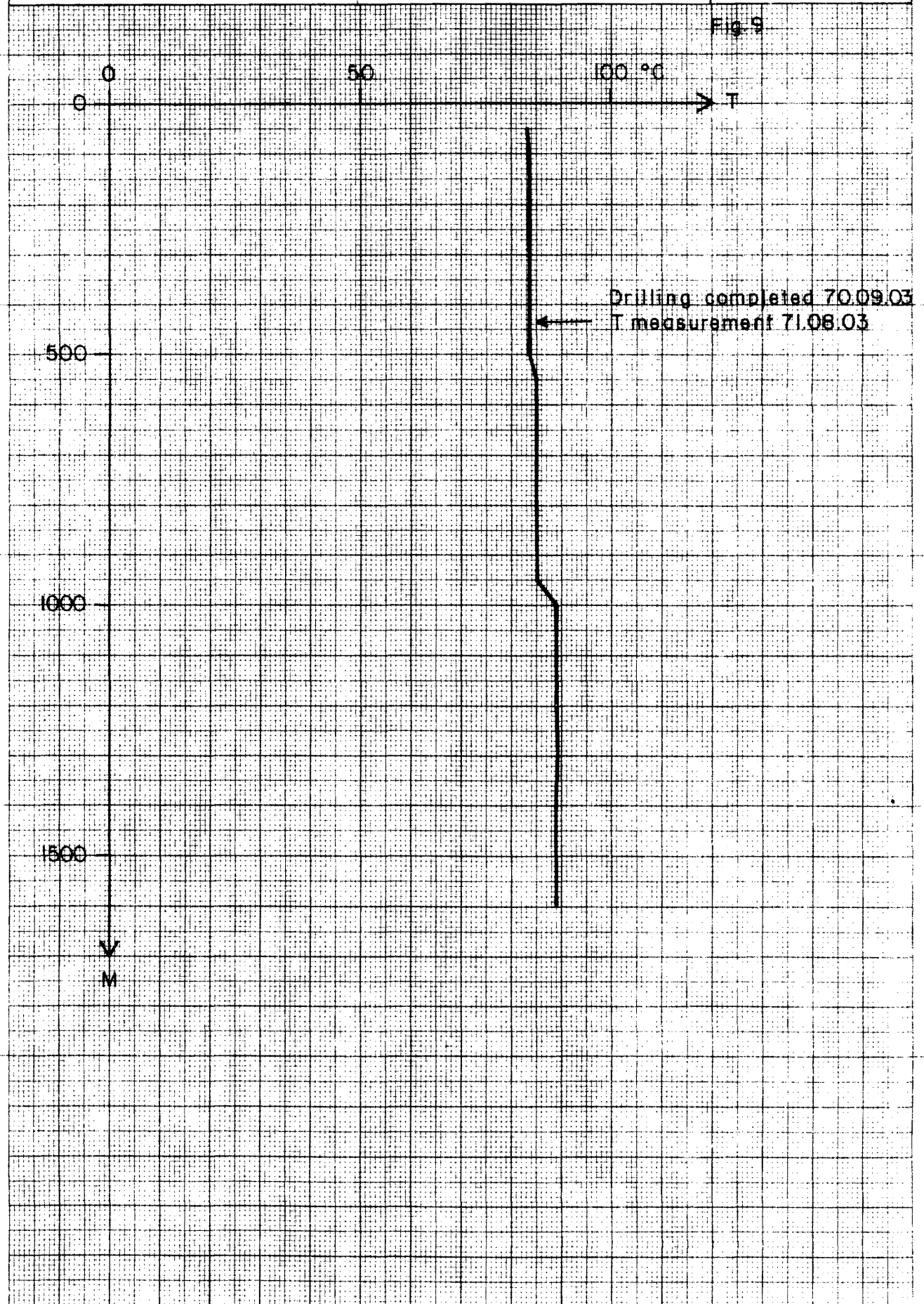
Fig. 8





Temperature profile of well MG-5

Fig. 9





80-08-25

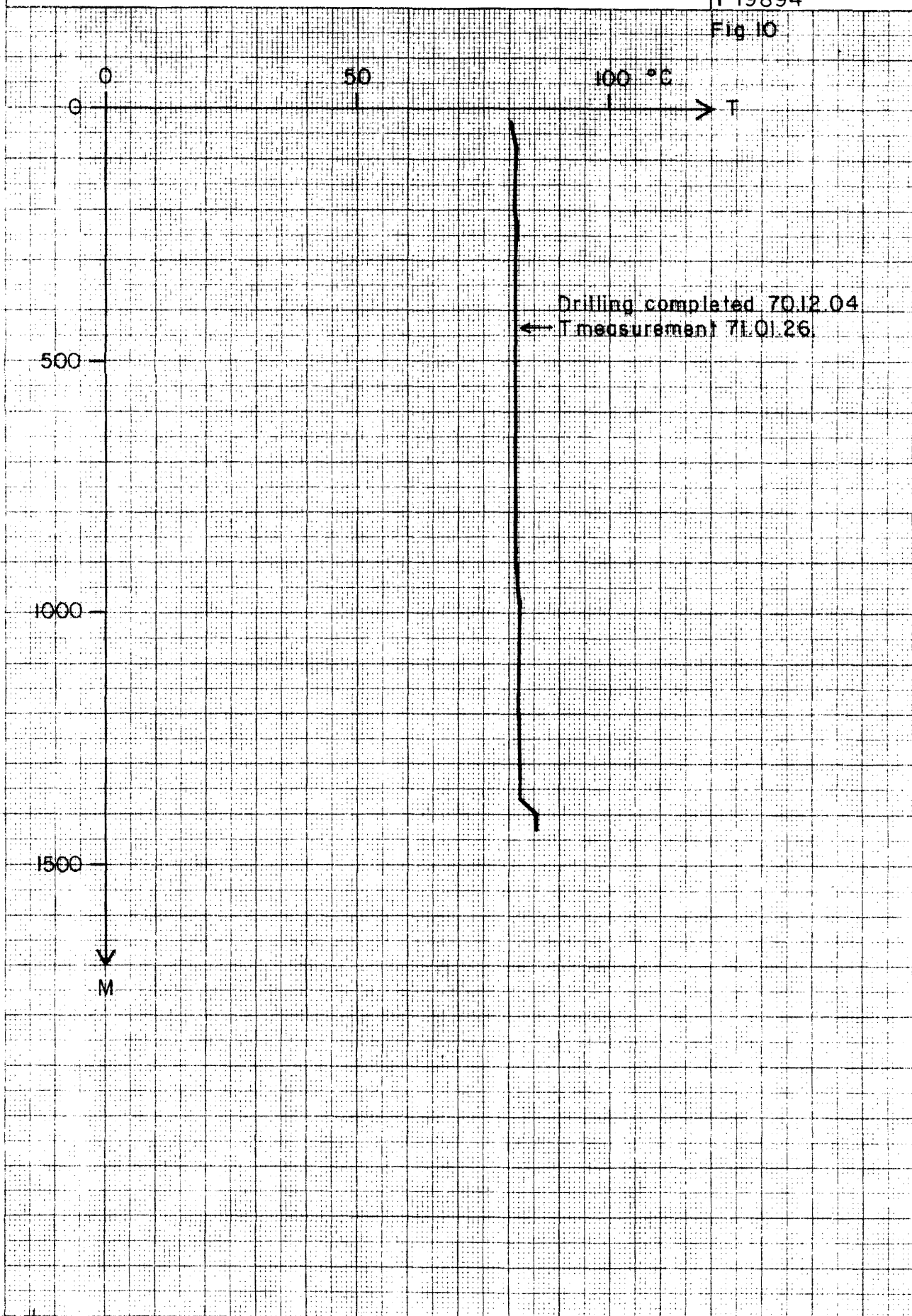
ZHOU/Sy.J.

JHD/HSP. Mosf.

F 19894

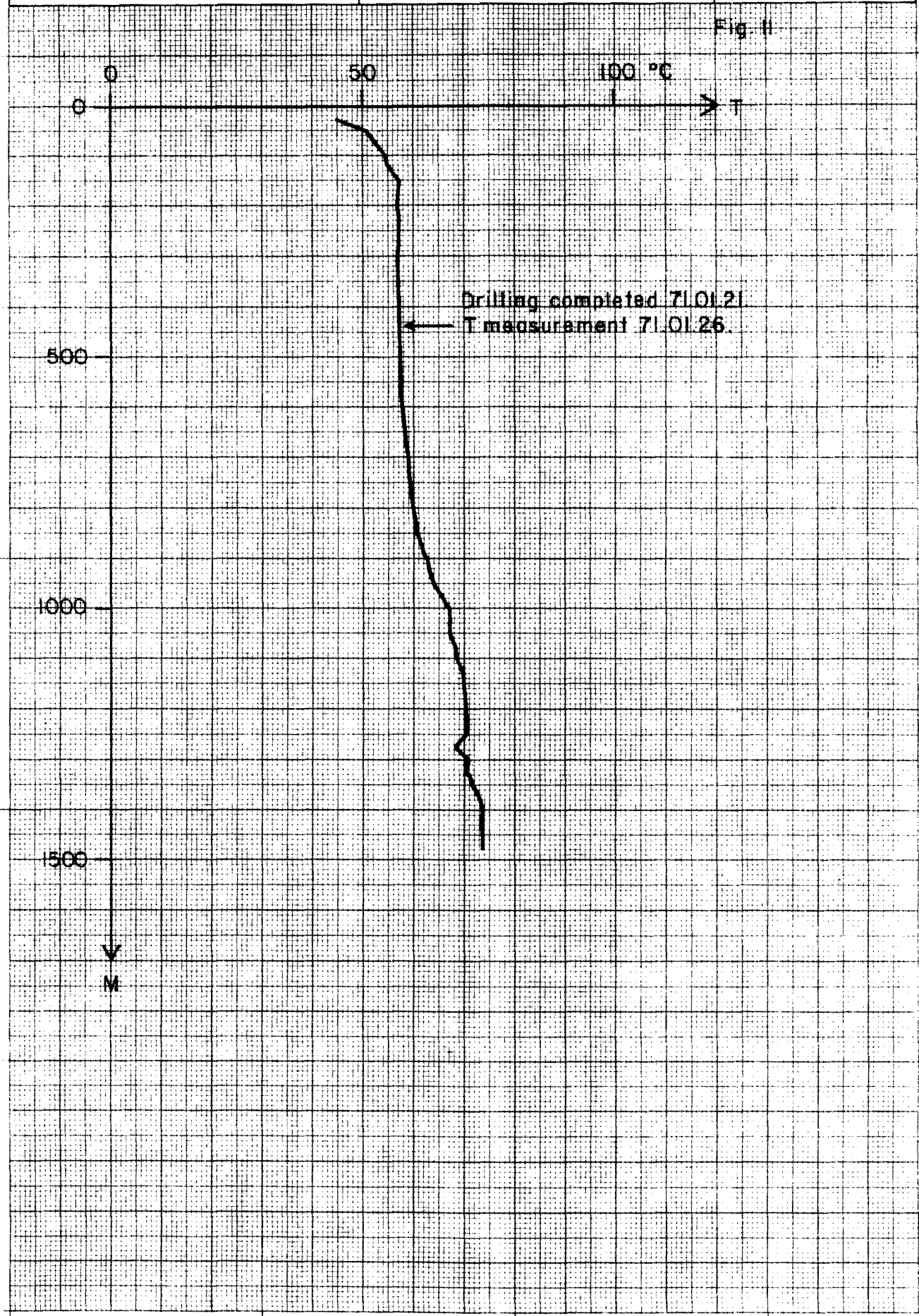
Temperature profile of well MG-6

Fig 10



Temperature profile of well MG-7

Fig. II





80-08-25

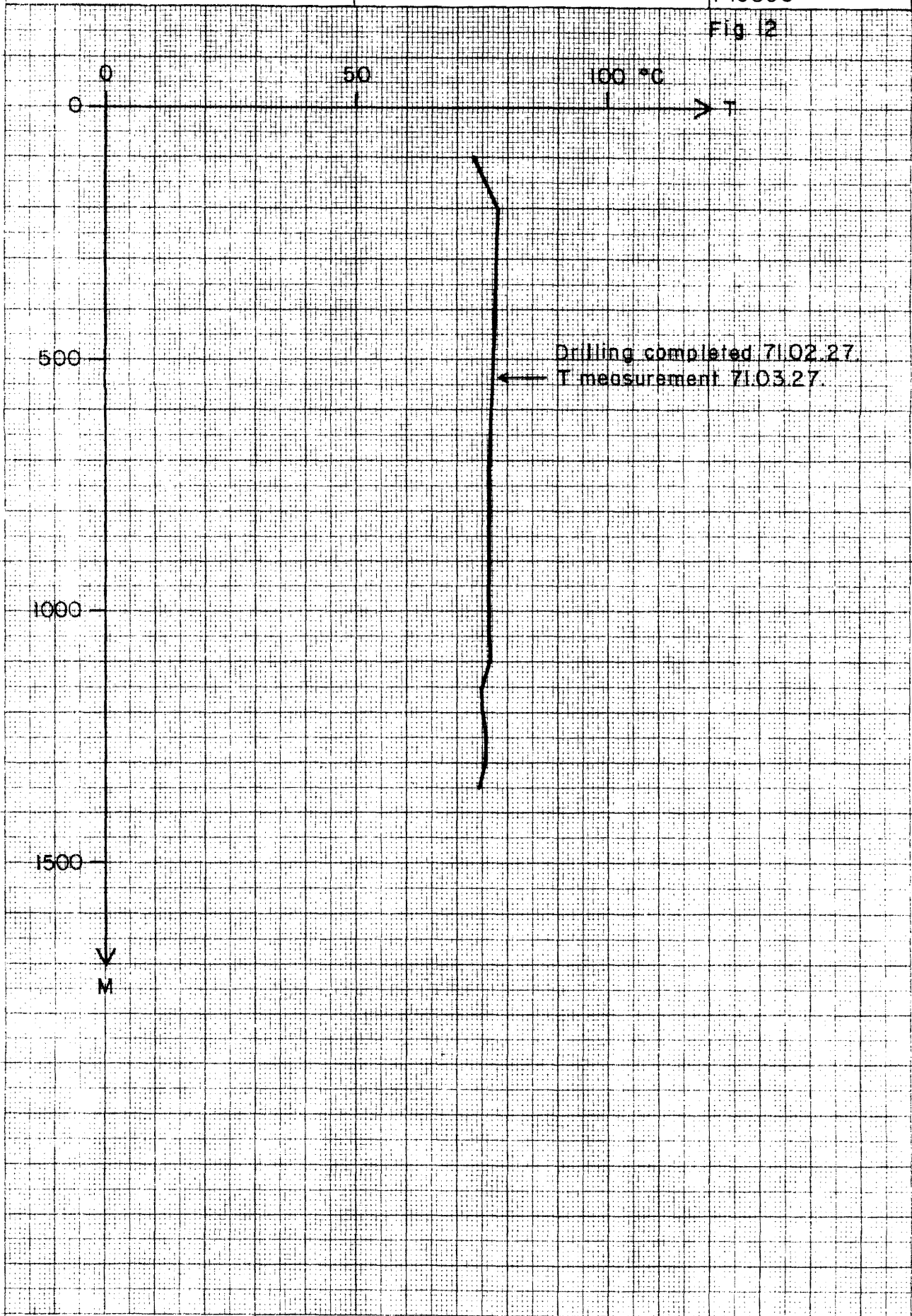
ZHOU/Sy.J.

JHD/HSP Mosf.

FI9896

Temperature profile of well MG-8

Fig 2

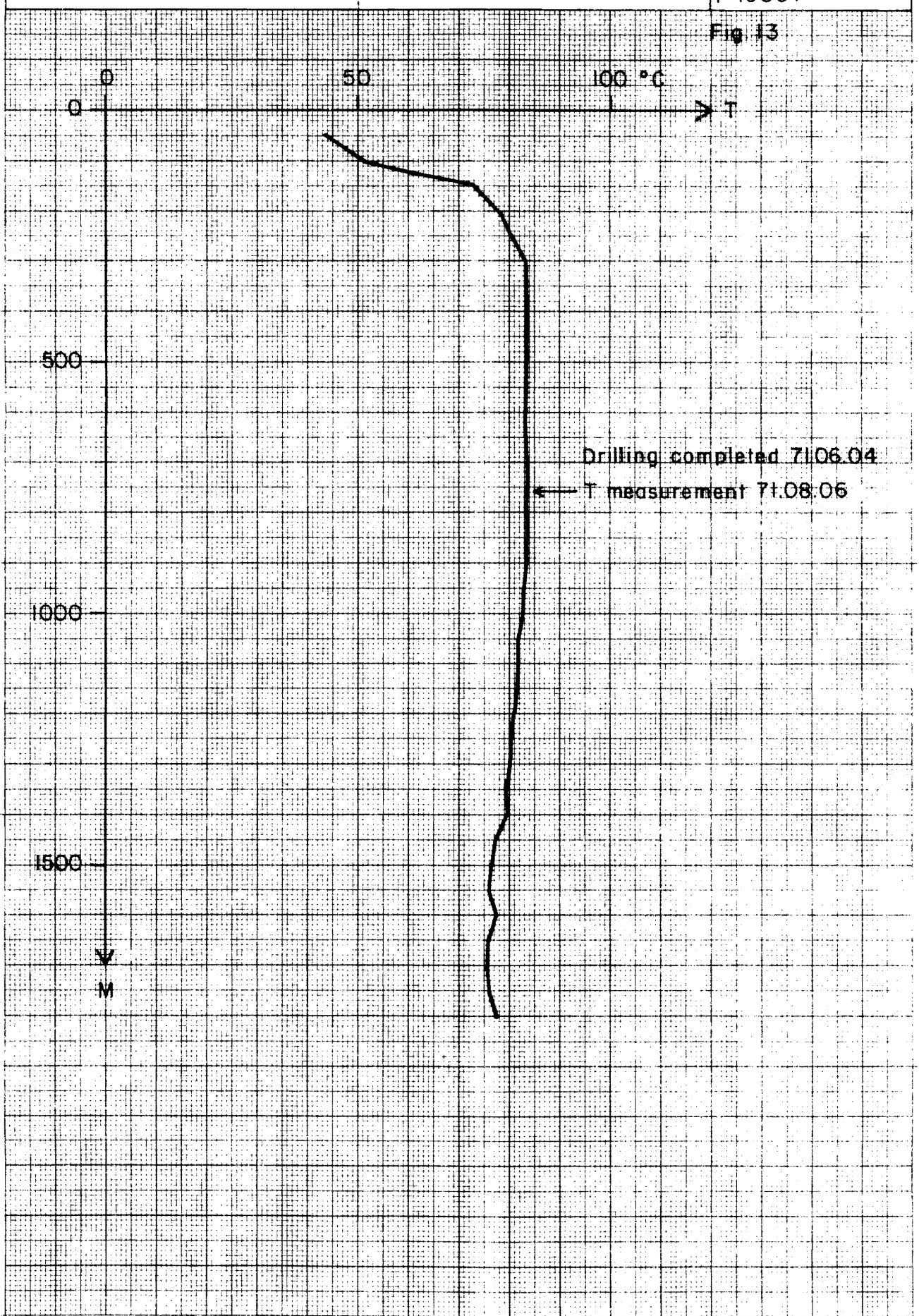




80-08-25
ZHOU/Sy.J
JHD/HSB Mosf.
F 19897

Temperature profile of well MG-9

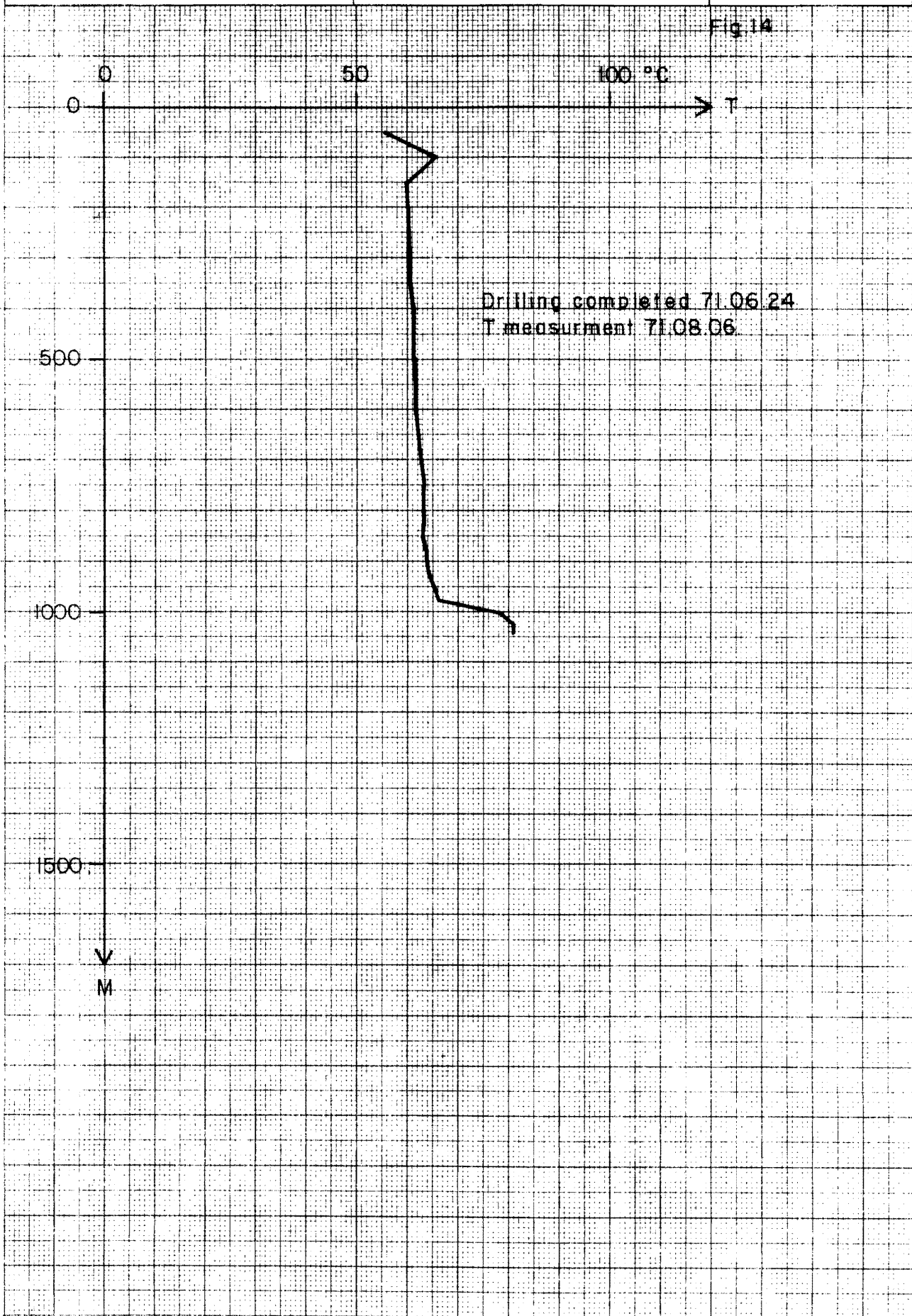
Fig. 13





Temperature profile of well MG-10

Fig. 14





80-08-25

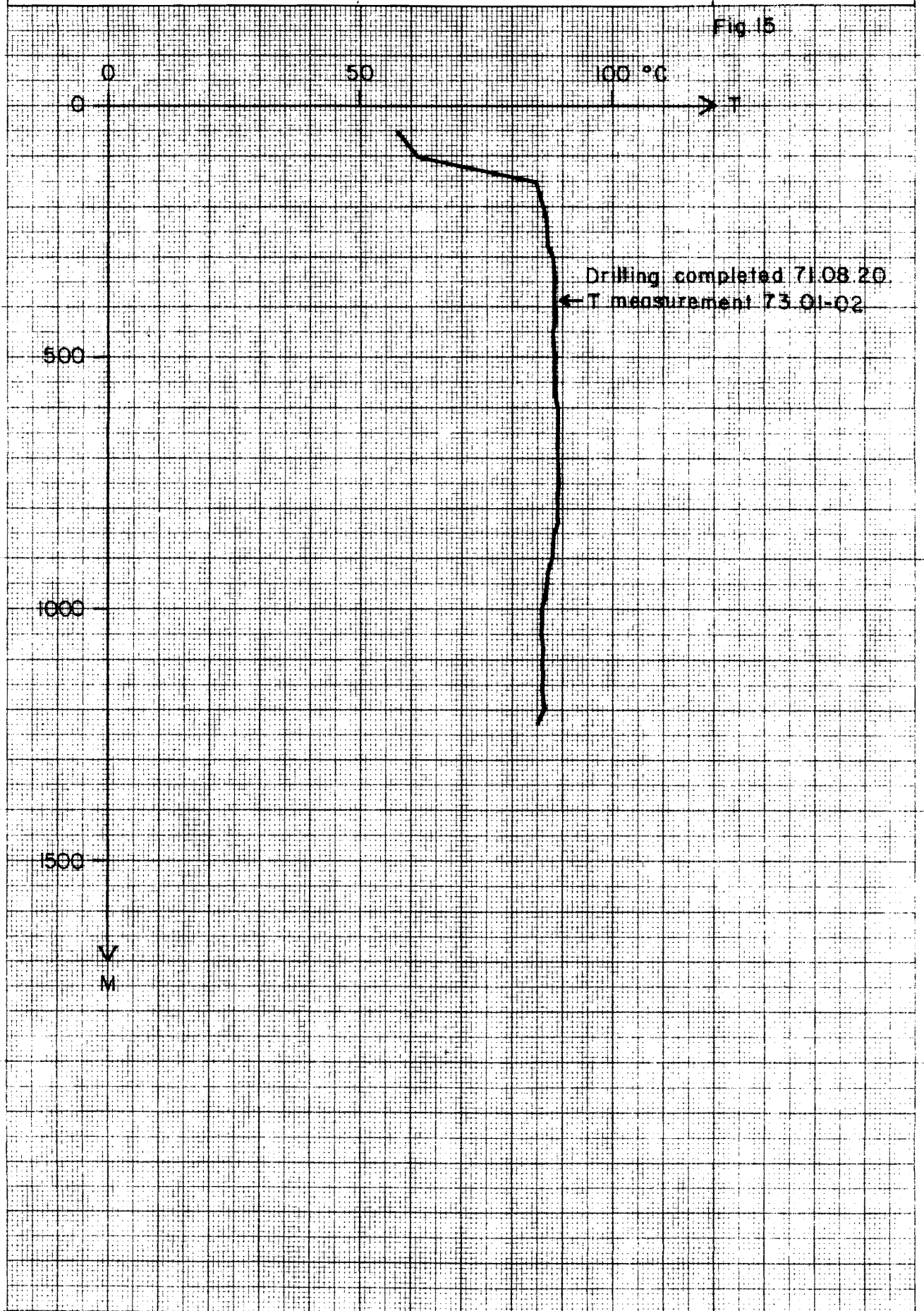
ZHOU/Sy.J.

JHD/HSP Mosf.

F 19899

Temperature profile of well MG-11

Fig. 15





ORKUSTOFNUN

80-08-25

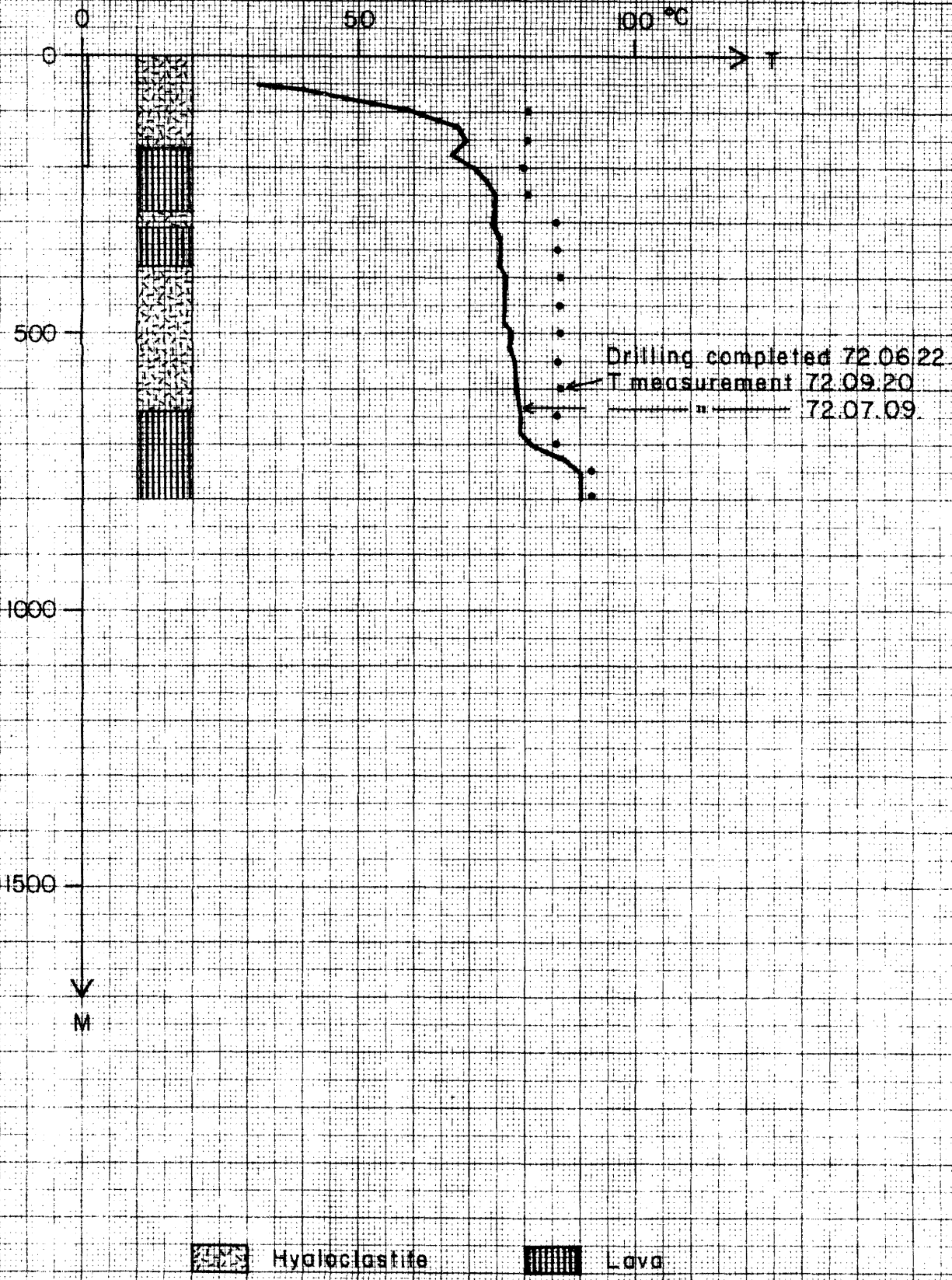
ZHOU/Sy.J

JHD/HSP Mosf

F 1990

Temperature profile and simplified geological section of well MG-12

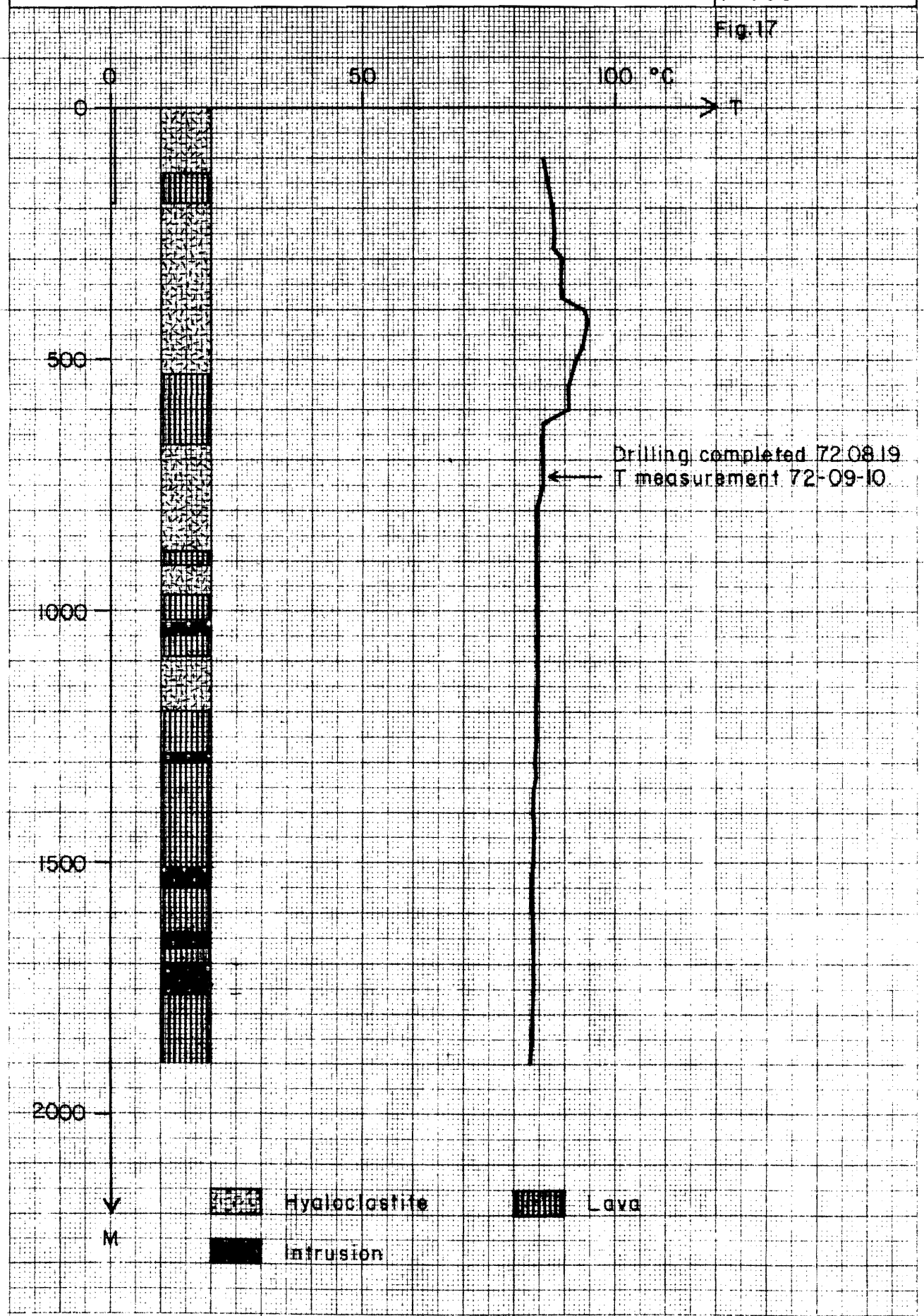
Fig. 15



80-08-25
ZHOU/Sy.J.
JHD/HSP Most.
F 19901

Temperature profile and simplified geological section of well MG-13

Fig. 17





ORKUSTOFNUN

Temperature profile and simplified geological section of well MG-14

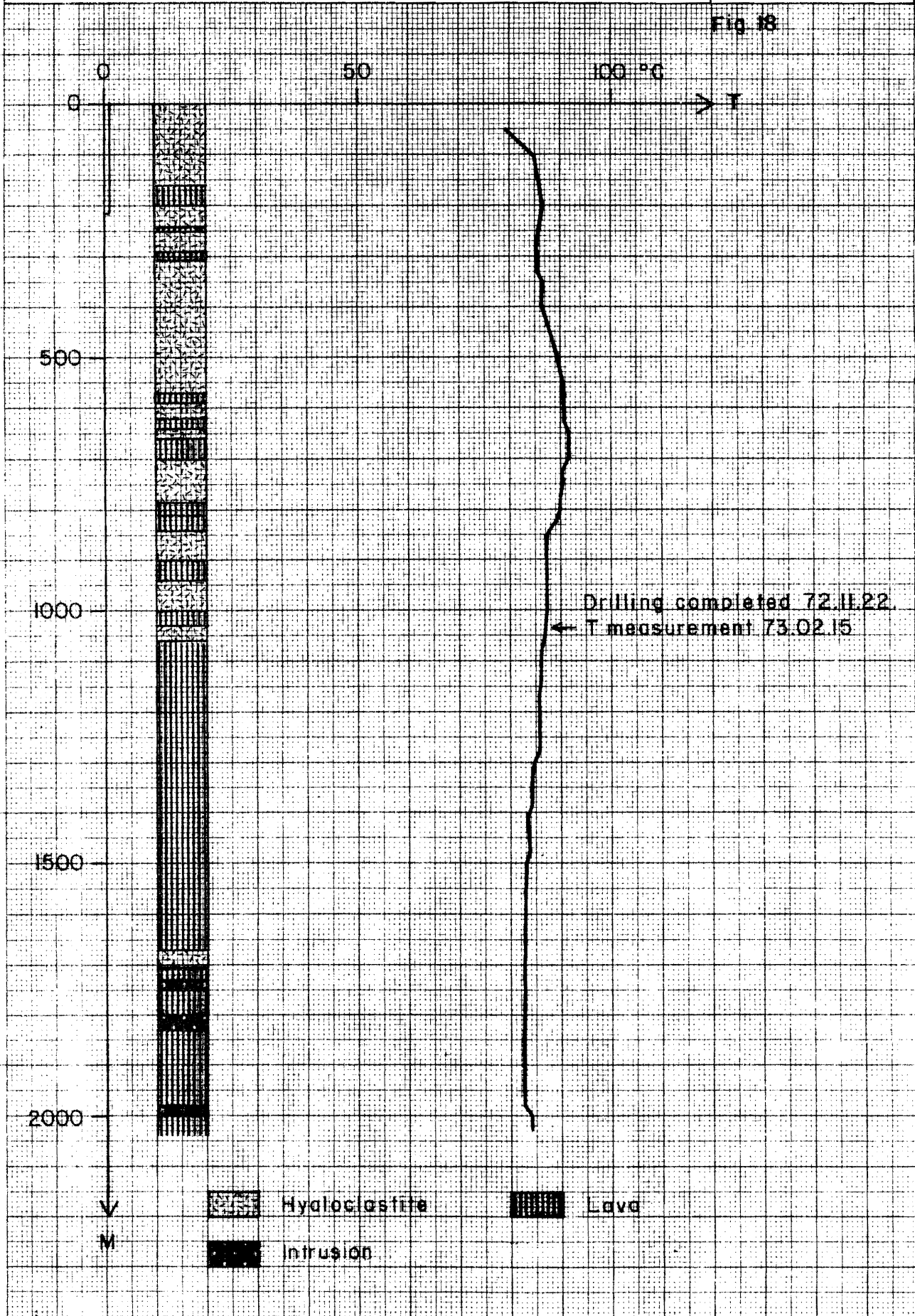
80-08-25

ZHOU/Sy.J

JHD/HS P Mosf.

F 19902

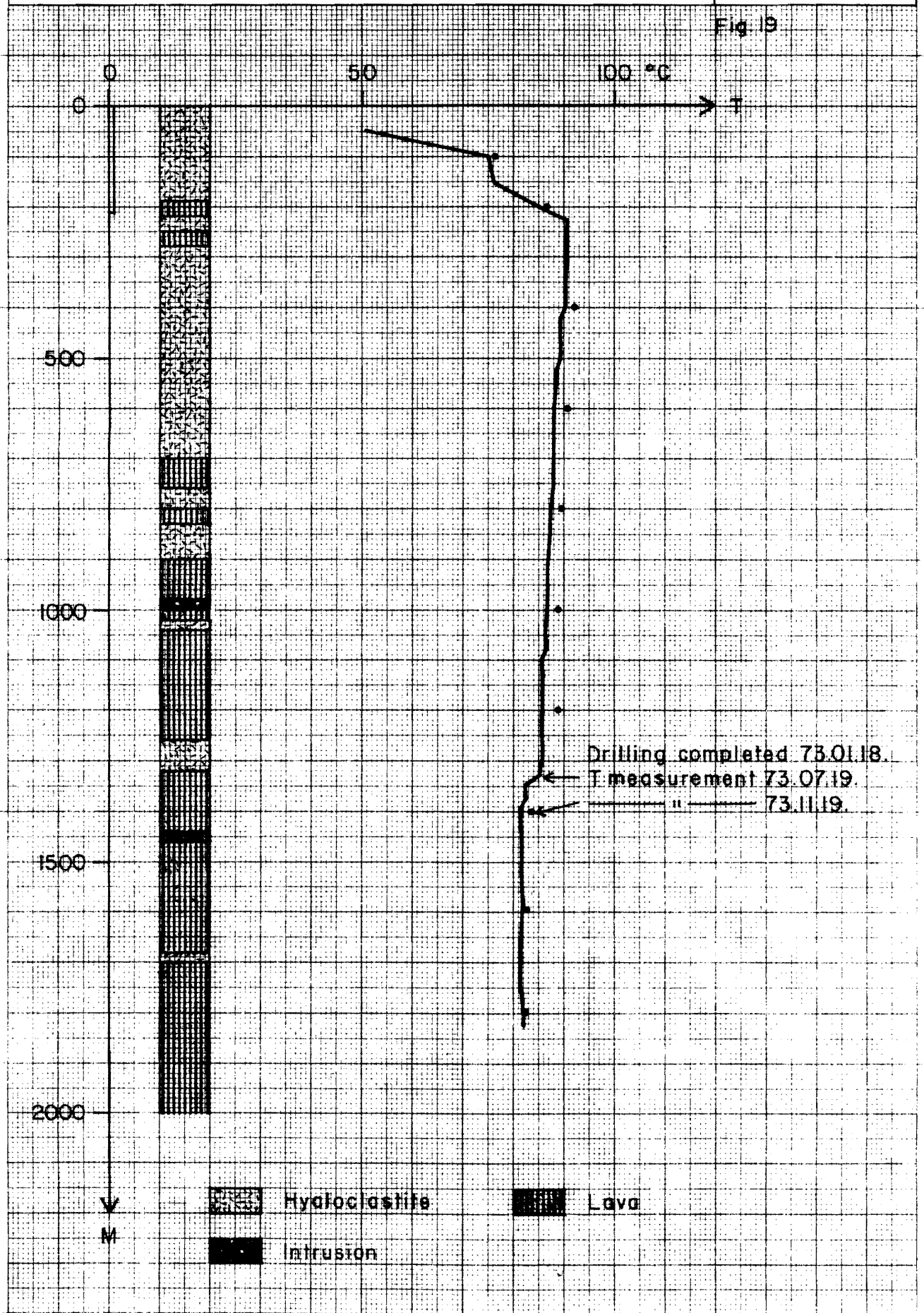
Fig. 18





Temperature profile and simplified geological section of well MG-15

Fig. 19





80-08-25

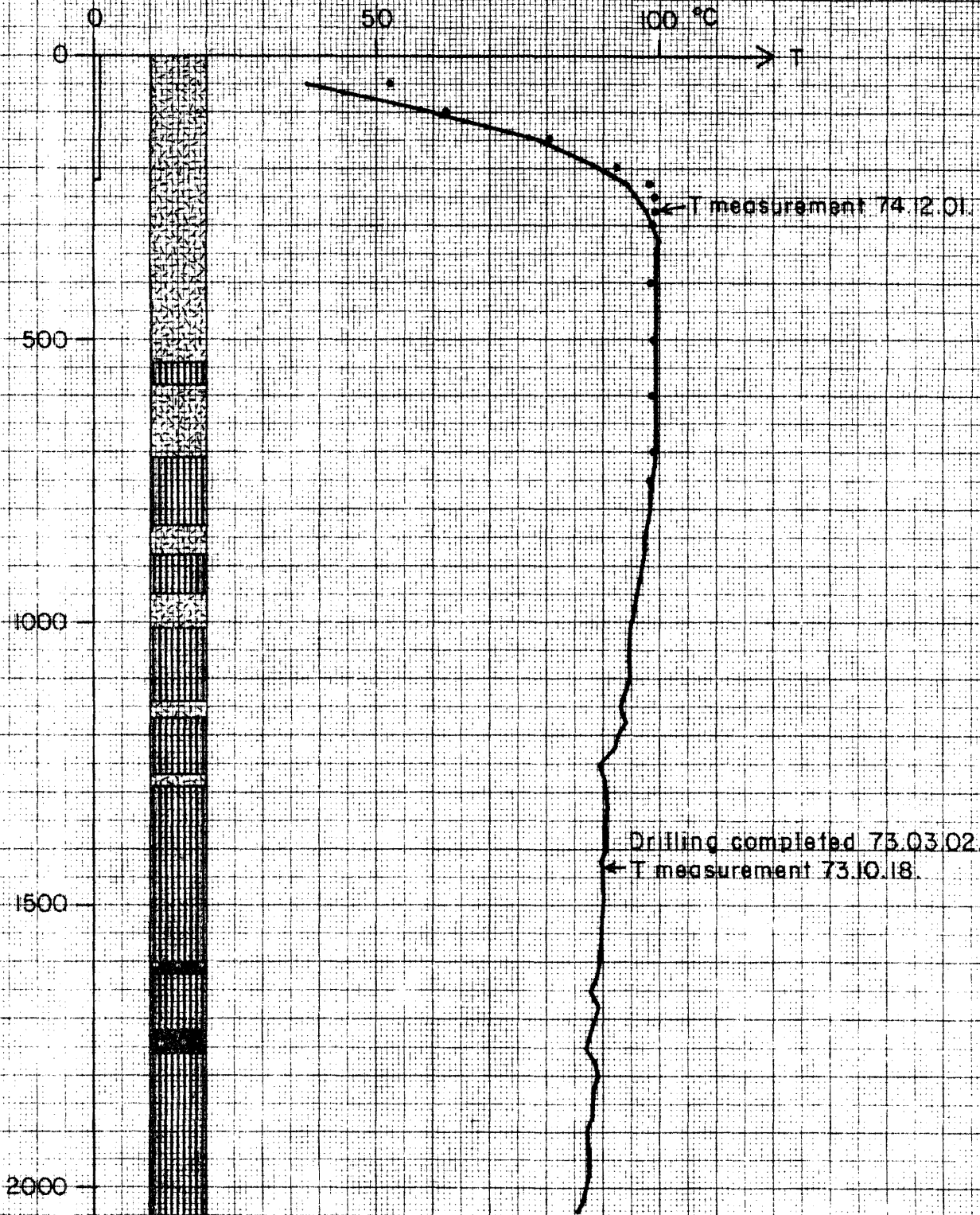
ZHOU/Sy.J.

JHD/HSP Mosf.

F 19904

Temperature profile and simplified geological section of well MG-16

Fig. 20



V
M



Hyaloclastite



Lava



Intrusion



ORKUSTOFNUN

Temperature profile and simplified geological section of well MG-17

80-08-25

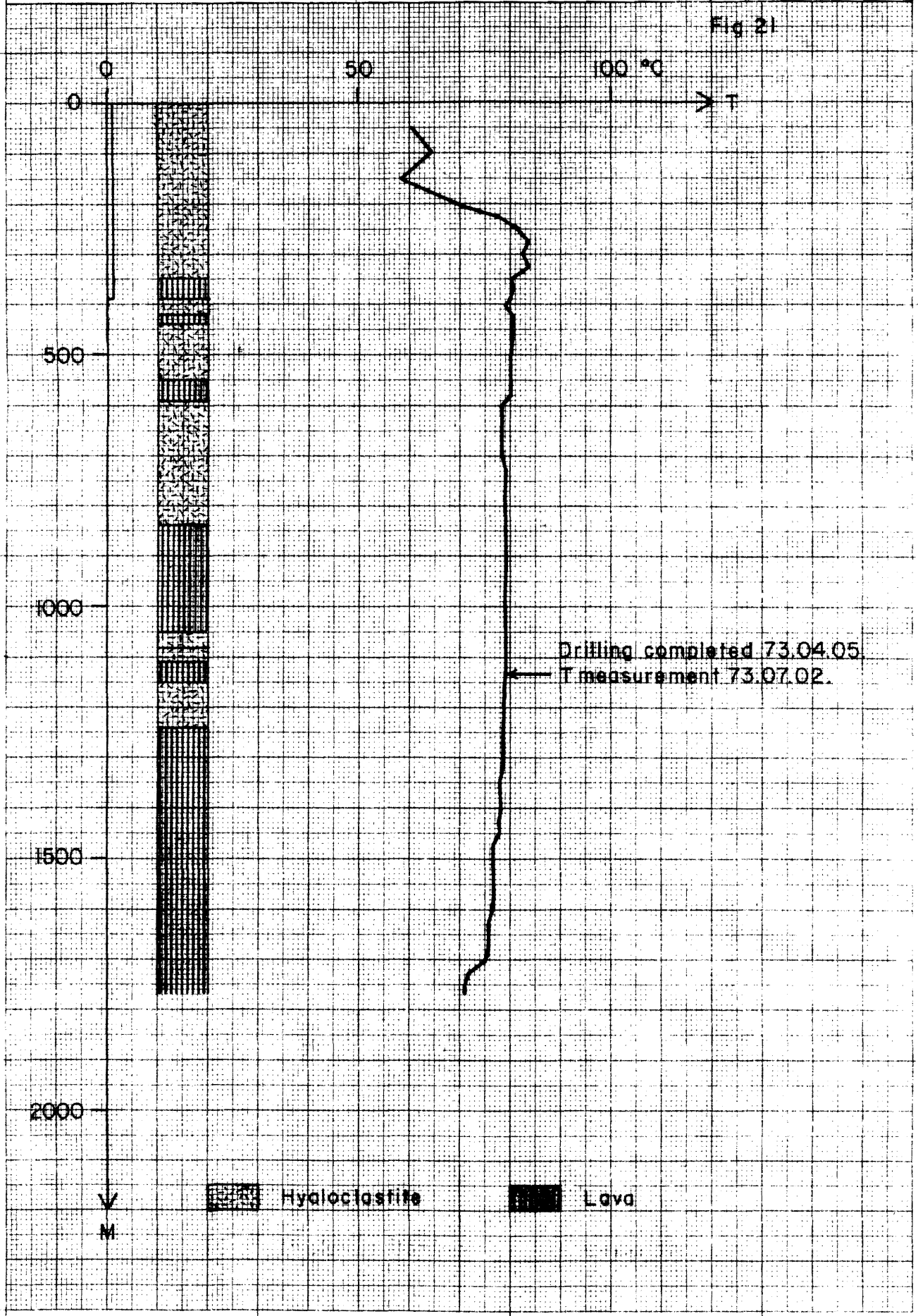
ZHOU/Sy.J.

JHD/HSP

Mosf.

F 19905

Fig 21



V
M



Hyaloclastite



Lava



ORKUSTOFNUN

80-08-25

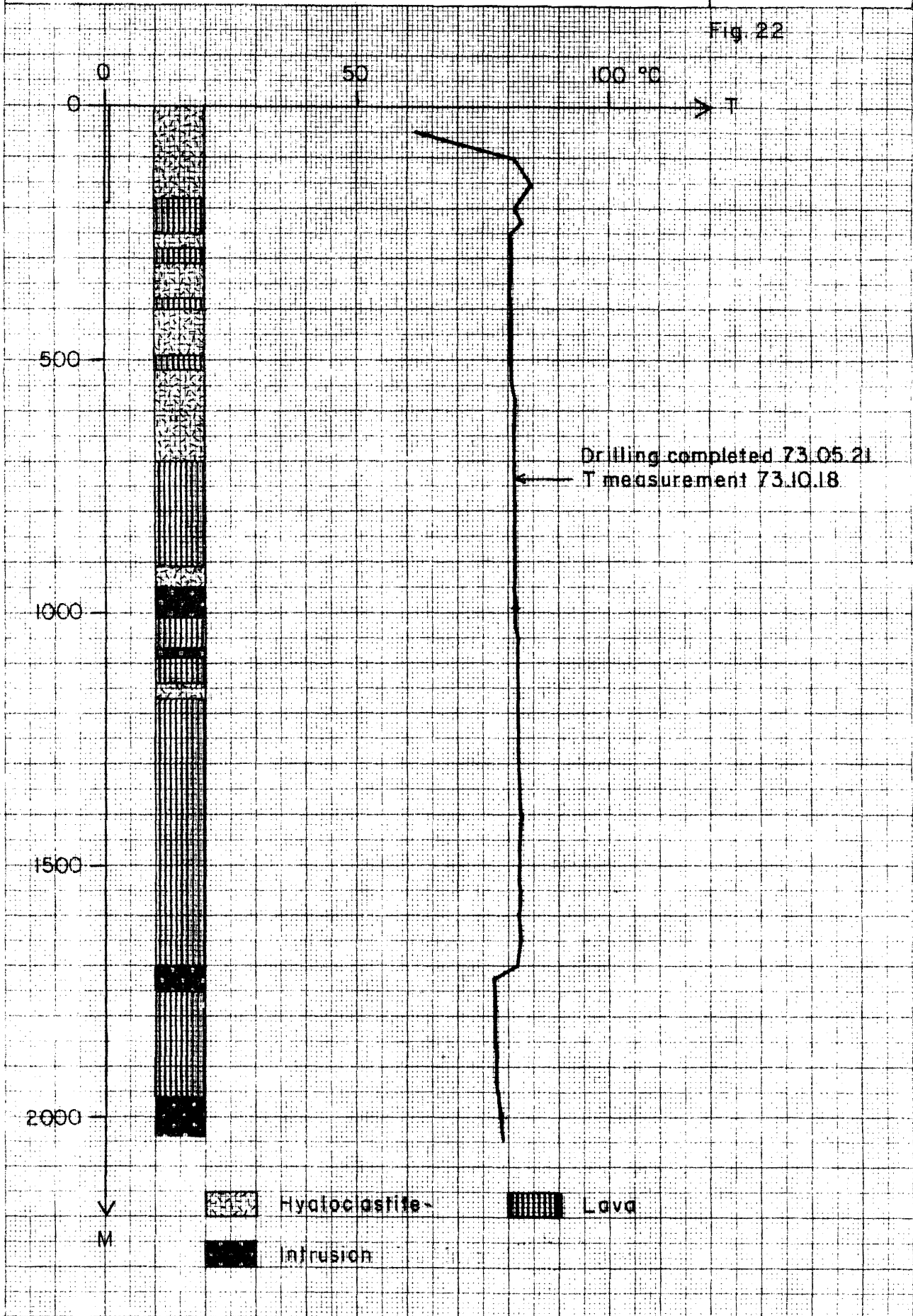
ZHOU/Sy.J.

JHD/HSP Mosf.

F 19906

Temperature profile and simplified geological section of well MG-18

Fig. 22





ORKUSTOFNUN

80-08-25

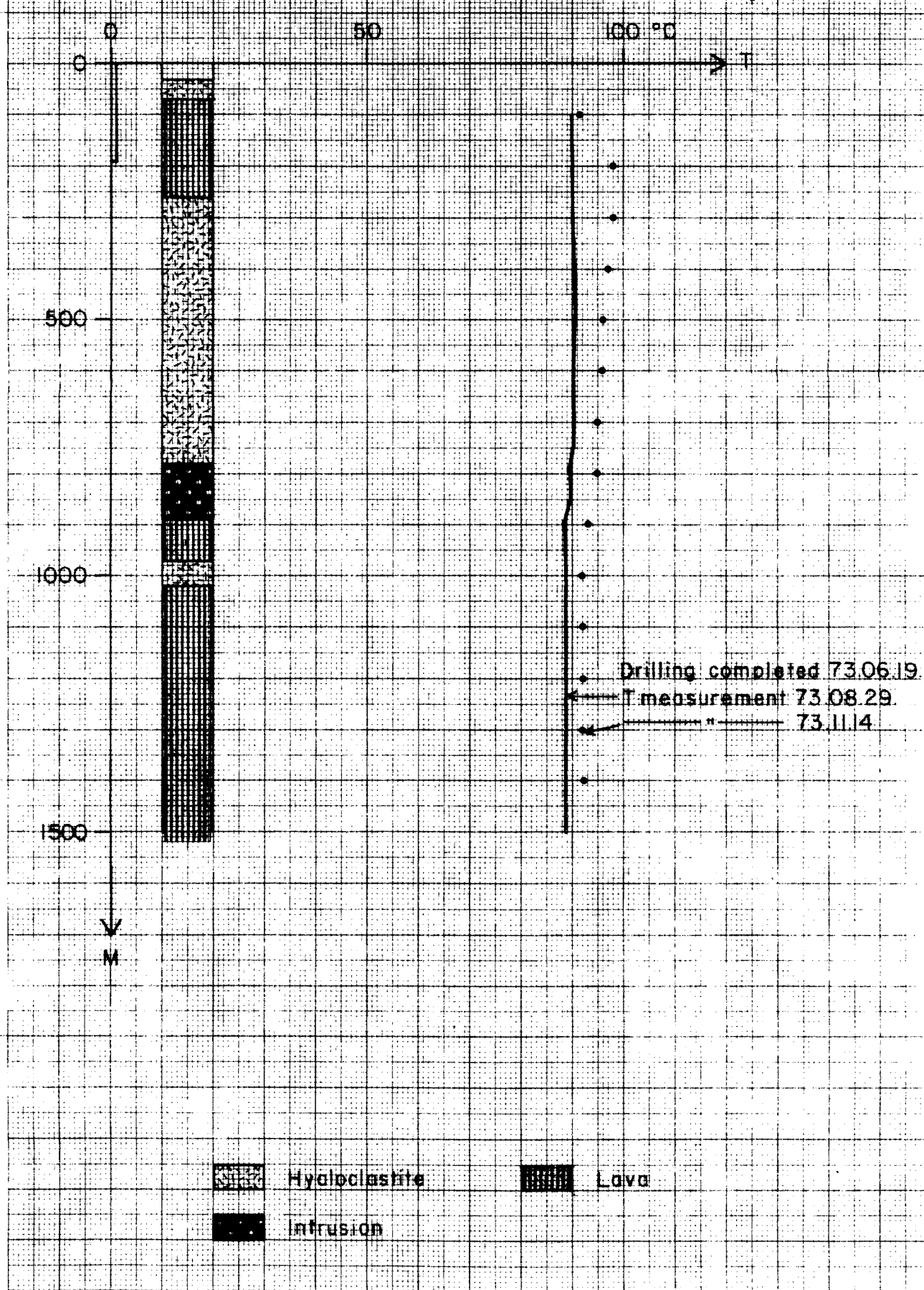
ZHOU/Sy.J

JHD/HSP

F 19907

Temperature profile and simplified geological section of well MG-19

Fig 23





ORKUSTOFNUN

Temperature profile and simplified geological section of well MG-20

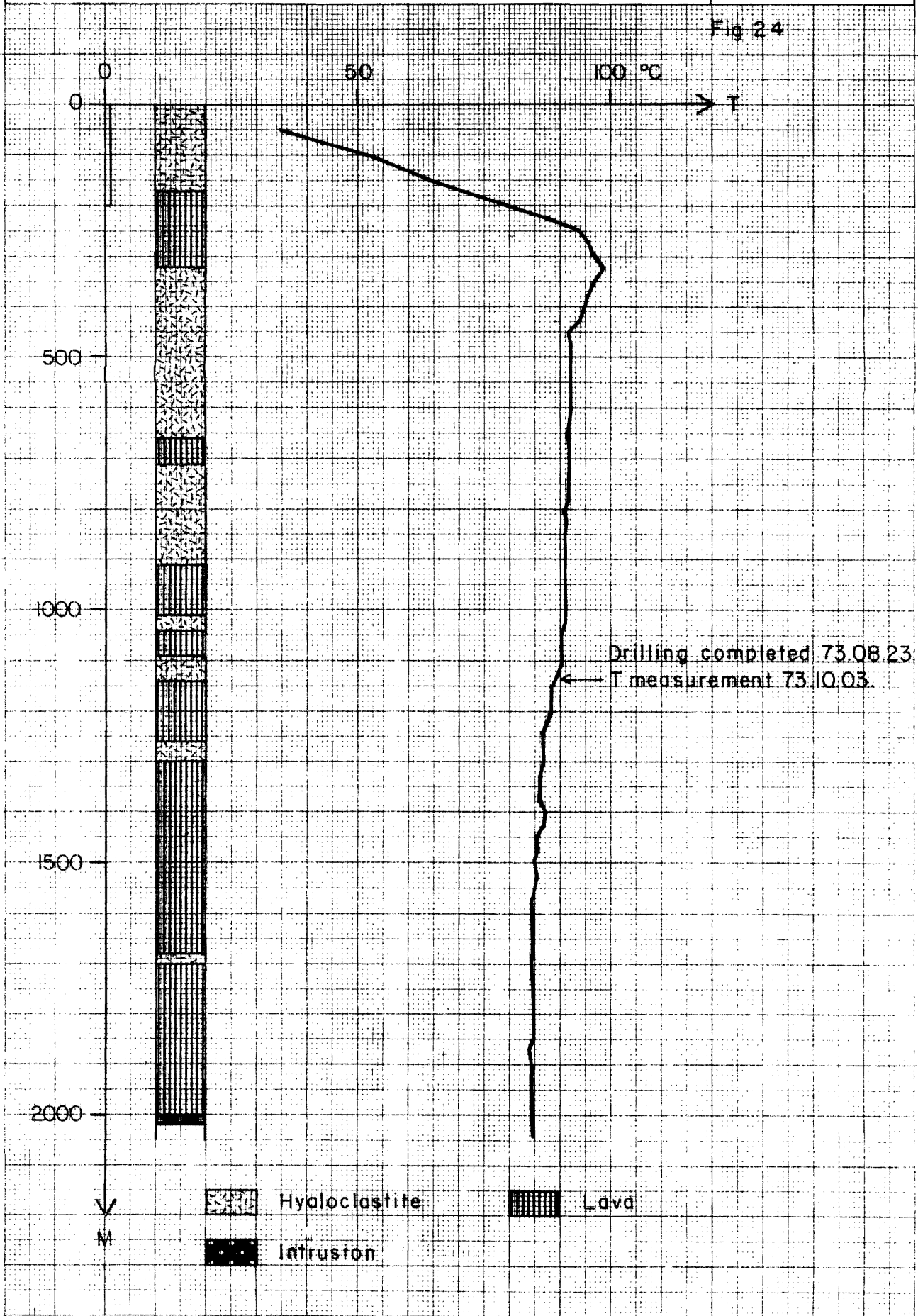
80-08-25

ZHOU/Sy.J.

JHD/HSP Mosf.

F 19908

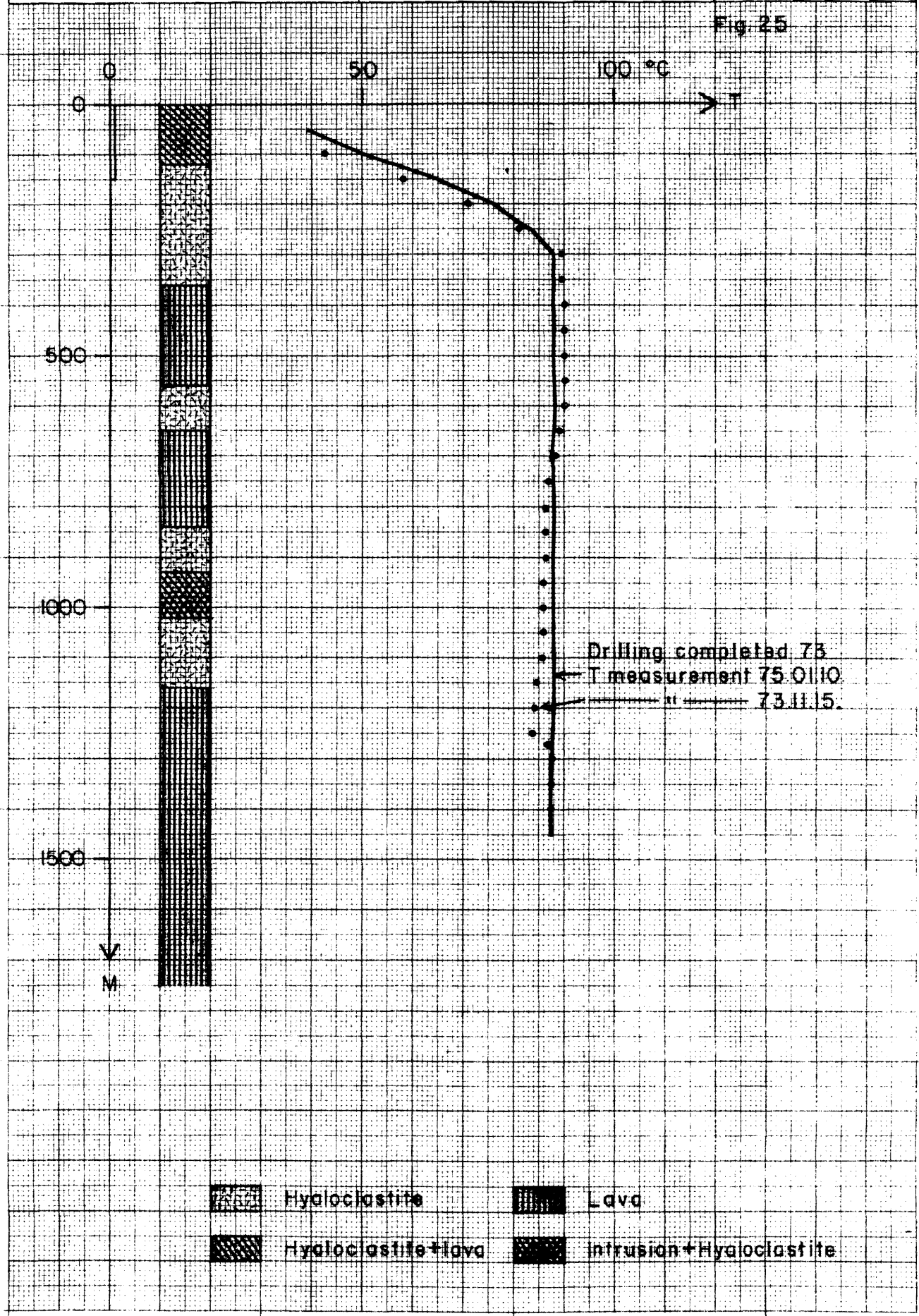
Fig 24



80-08-25
ZHOU/Sy.J.
JHD/HSP Mosf.
F19909

Temperature profile and simplified geological section of well MG-21

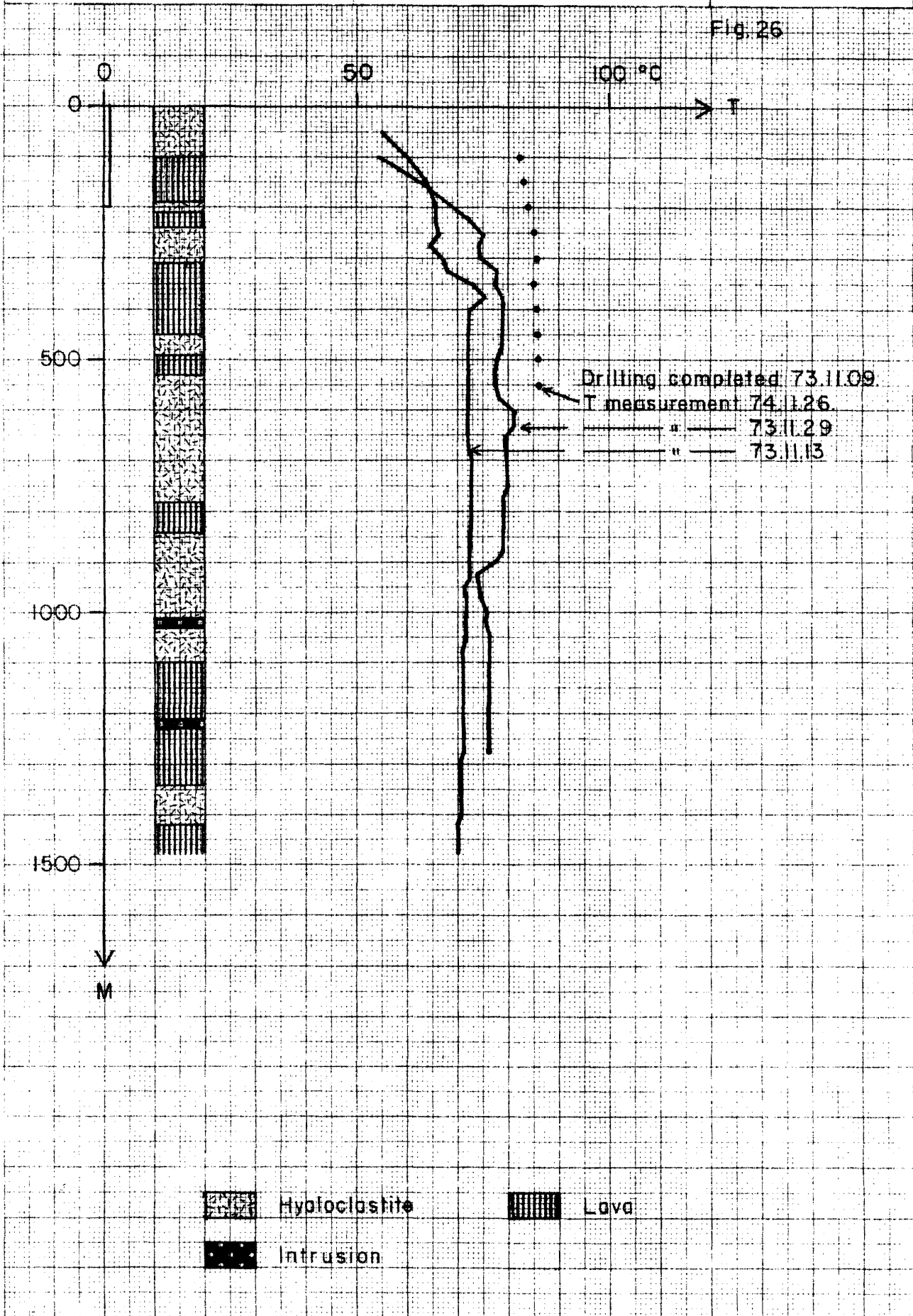
Fig. 25





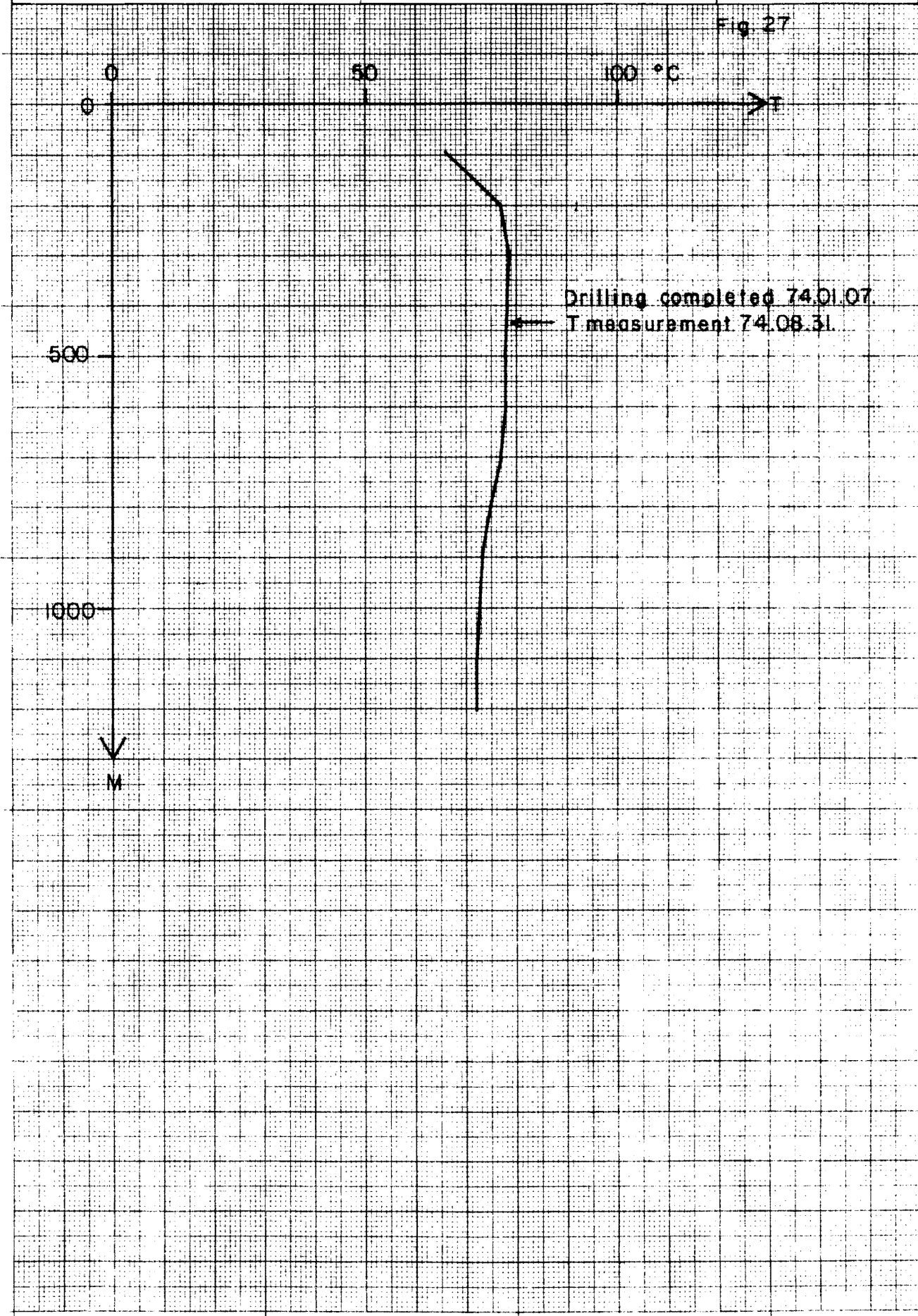
Temperature profile and simplified geological section of well MG-22

Fig. 26



Temperature profile of well MG-23

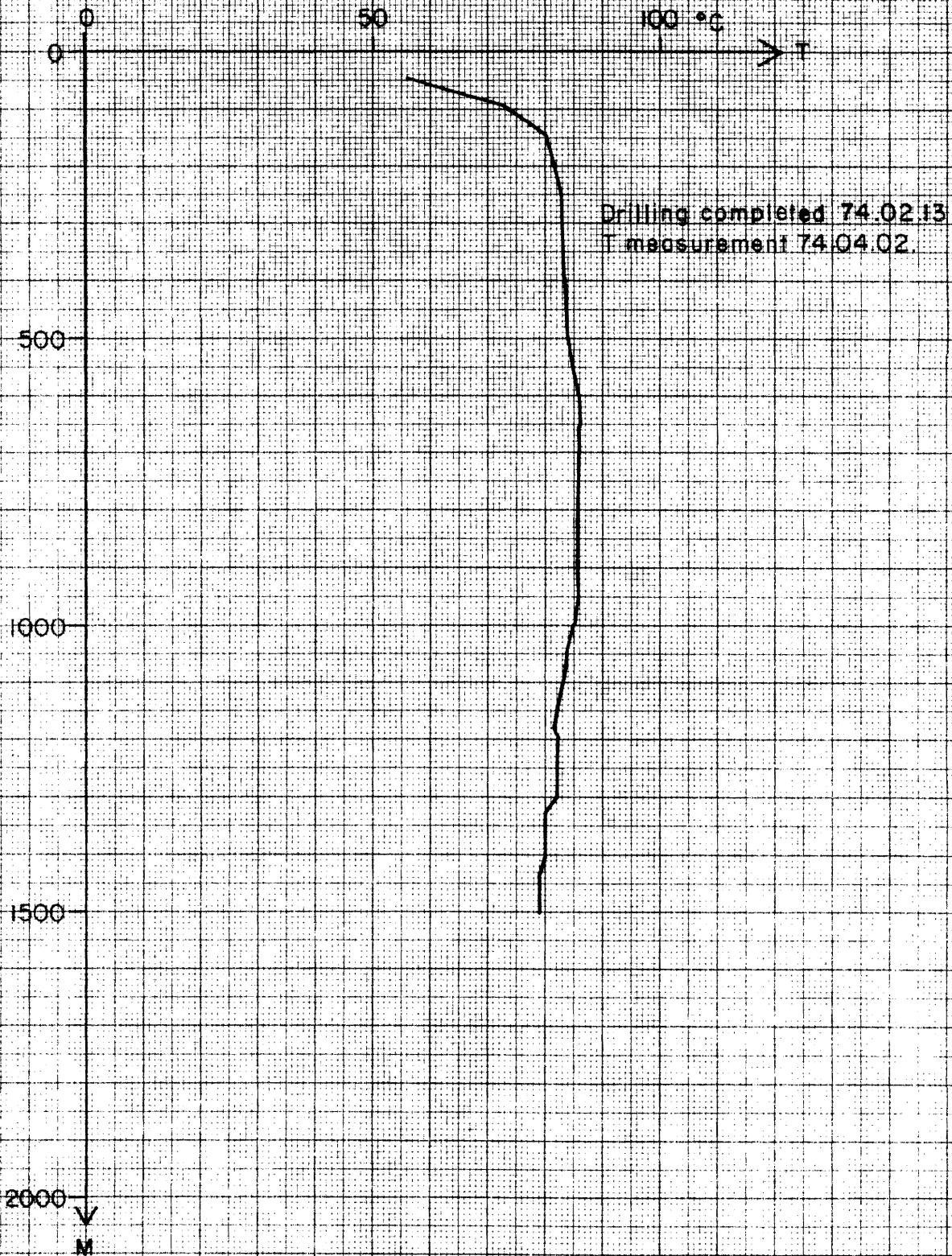
Fig. 27





Temperature profile of well MG-24

Fig. 28





ORKUSTOFNUN

80-08-25

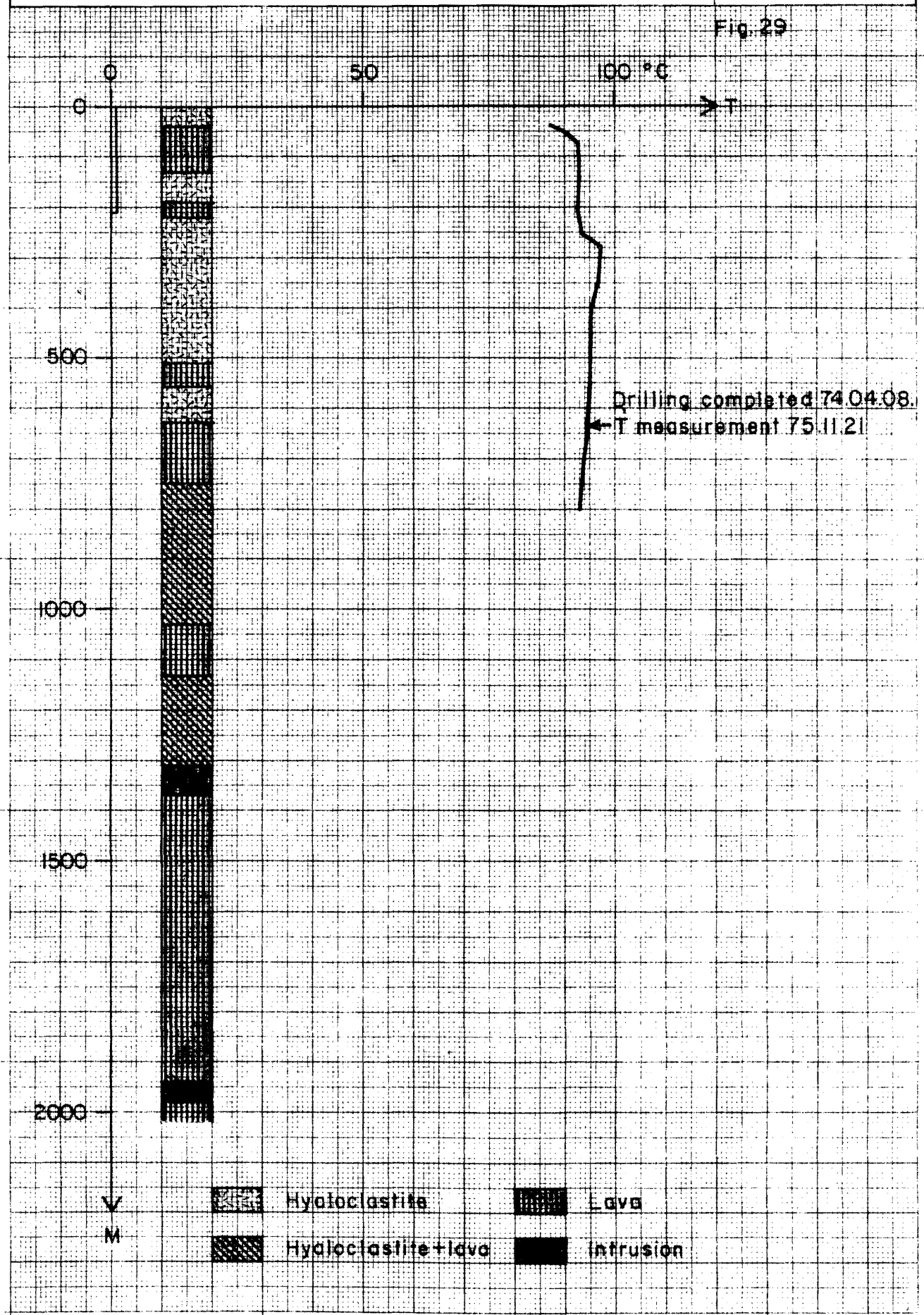
ZHOU/Sy.J.

JHD/HSP Mosf.

F 19913

Temperature profile and simplified geological section of well MG-25

Fig. 29



V
M

	Hyaloclastite		Lava
	Hyaloclastite+lava		Intrusion



Temperature profile and simplified geological section of well MG-27

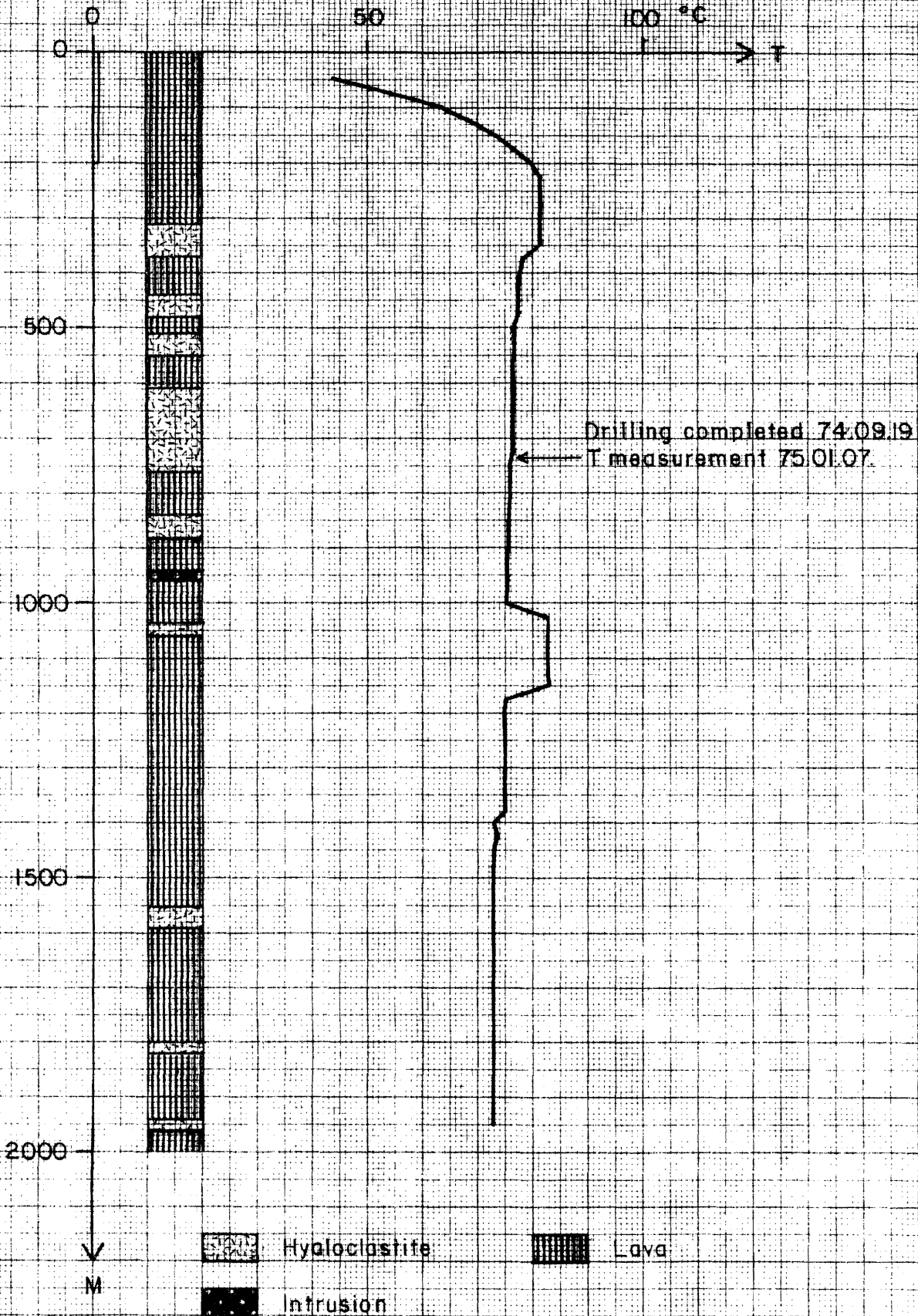
80-08-25

ZHOU/Sy.J.

JHD/HSP Mosf.

F19914

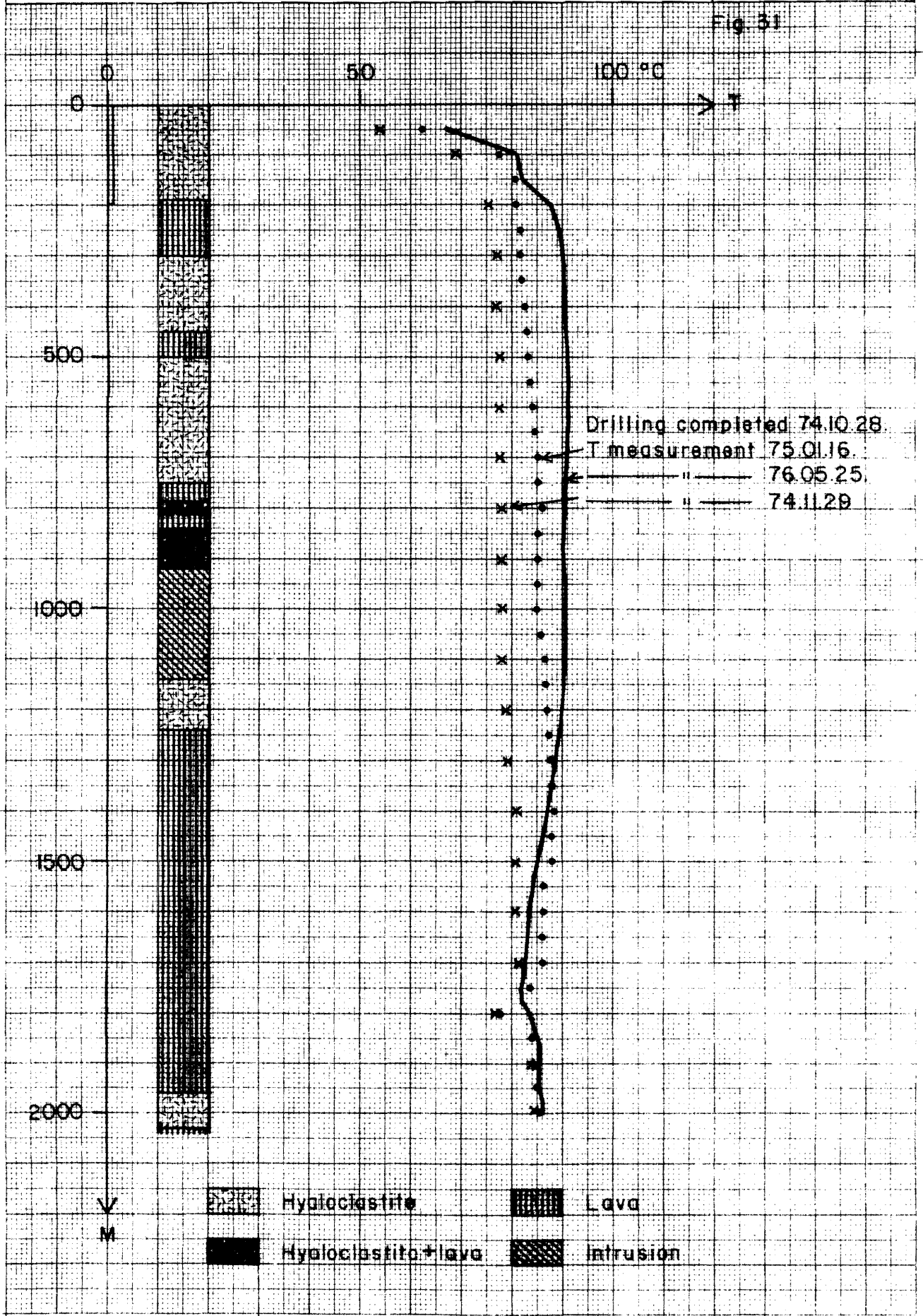
Fig. 30





Temperature profile and simplified geological section of well MG-28

Fig. 51





80-08-25

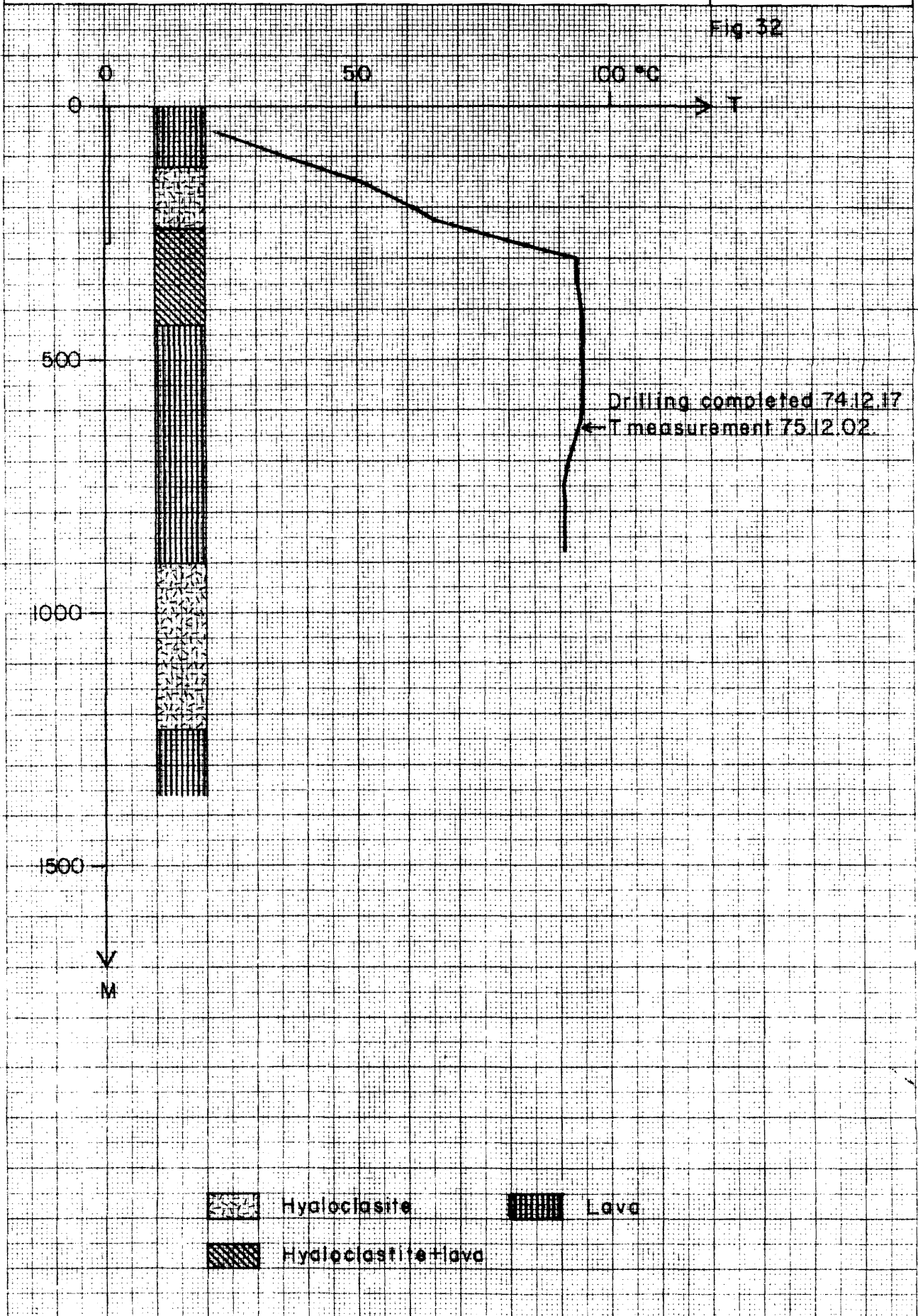
ZHOU/Sy.J.




JHD/HSP Mosf.

F19916

Temperature profile and simplified geological section of well MG-29

Fig. 32



 Hyaloclasite  Lava
 Hyaloclastite+lava



ORKUSTOFNUN

Temperature profile and simplified geological section of well MG-30

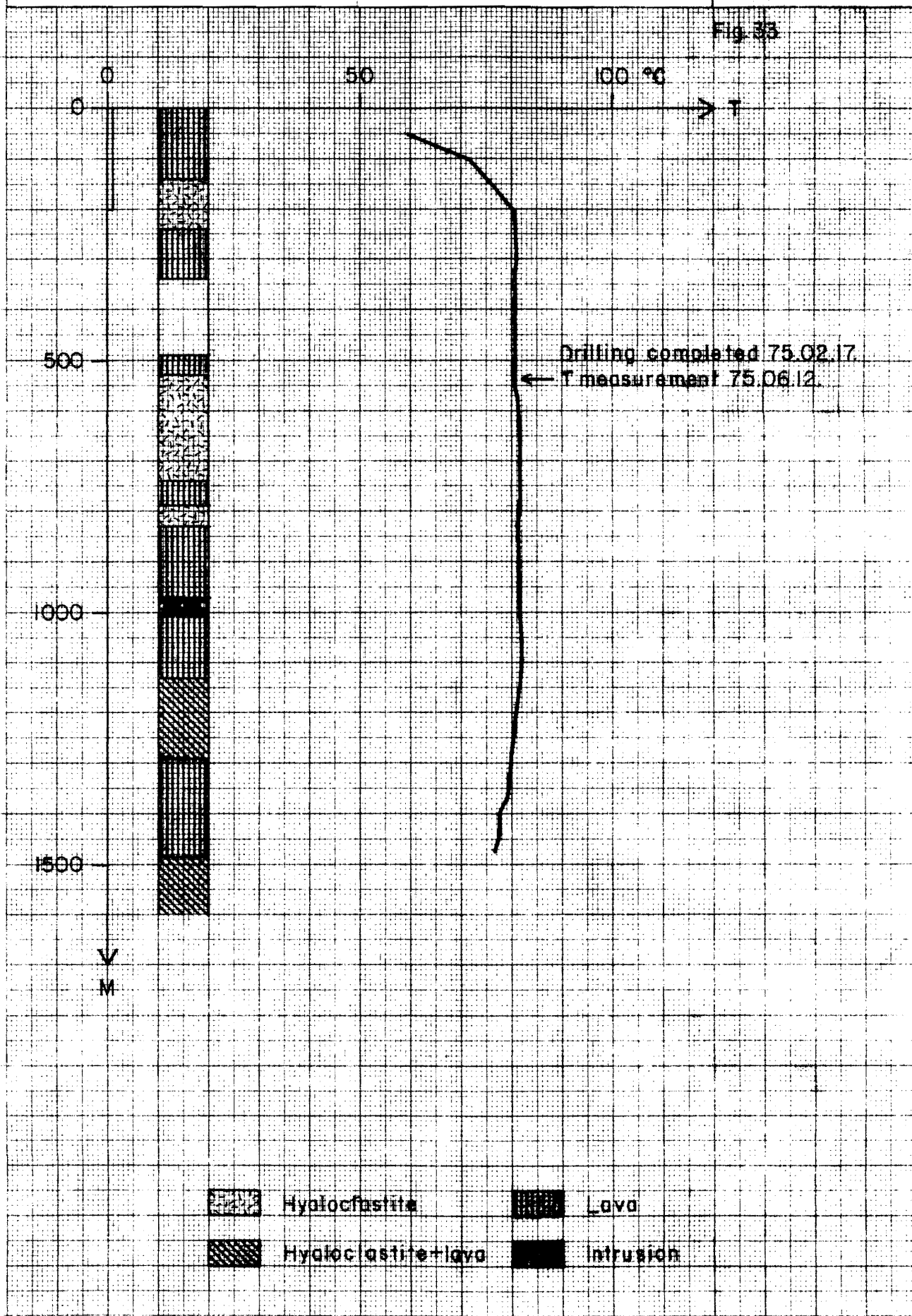
80-08-25

ZHOU/Sy.J.

JHD/HSP Mosf.

F 19917

Fig. 33



	Hyaloclastite		Lava
	Hyaloclastite+lava		Intrusion



ORKUSTOFNUN

80-08-25

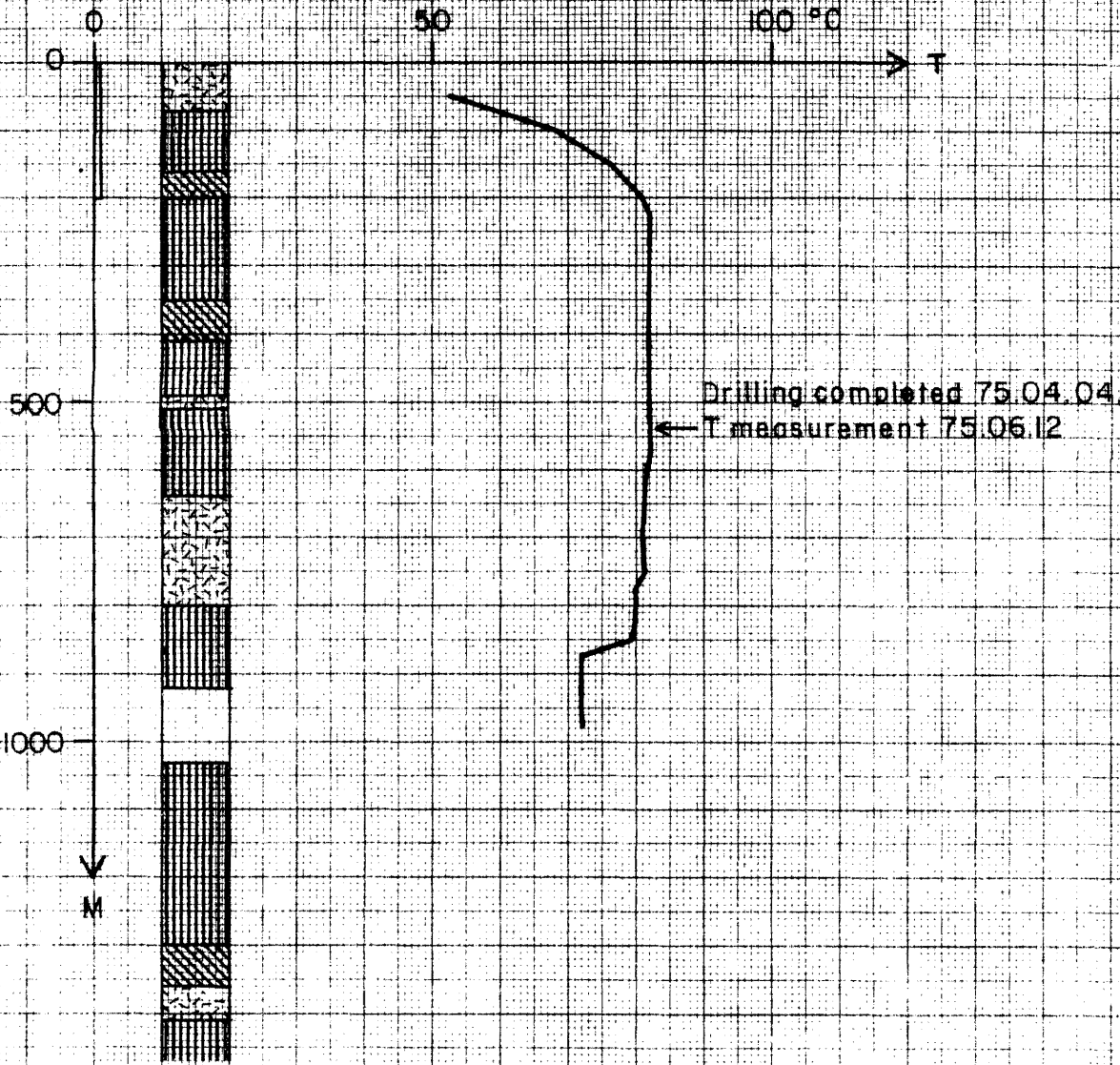
ZHOU/Sy.J.

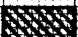
JHD/HSP Mosf.

F 19918

Temperature profile and simplified geological section of well MG-31

Fig. 34



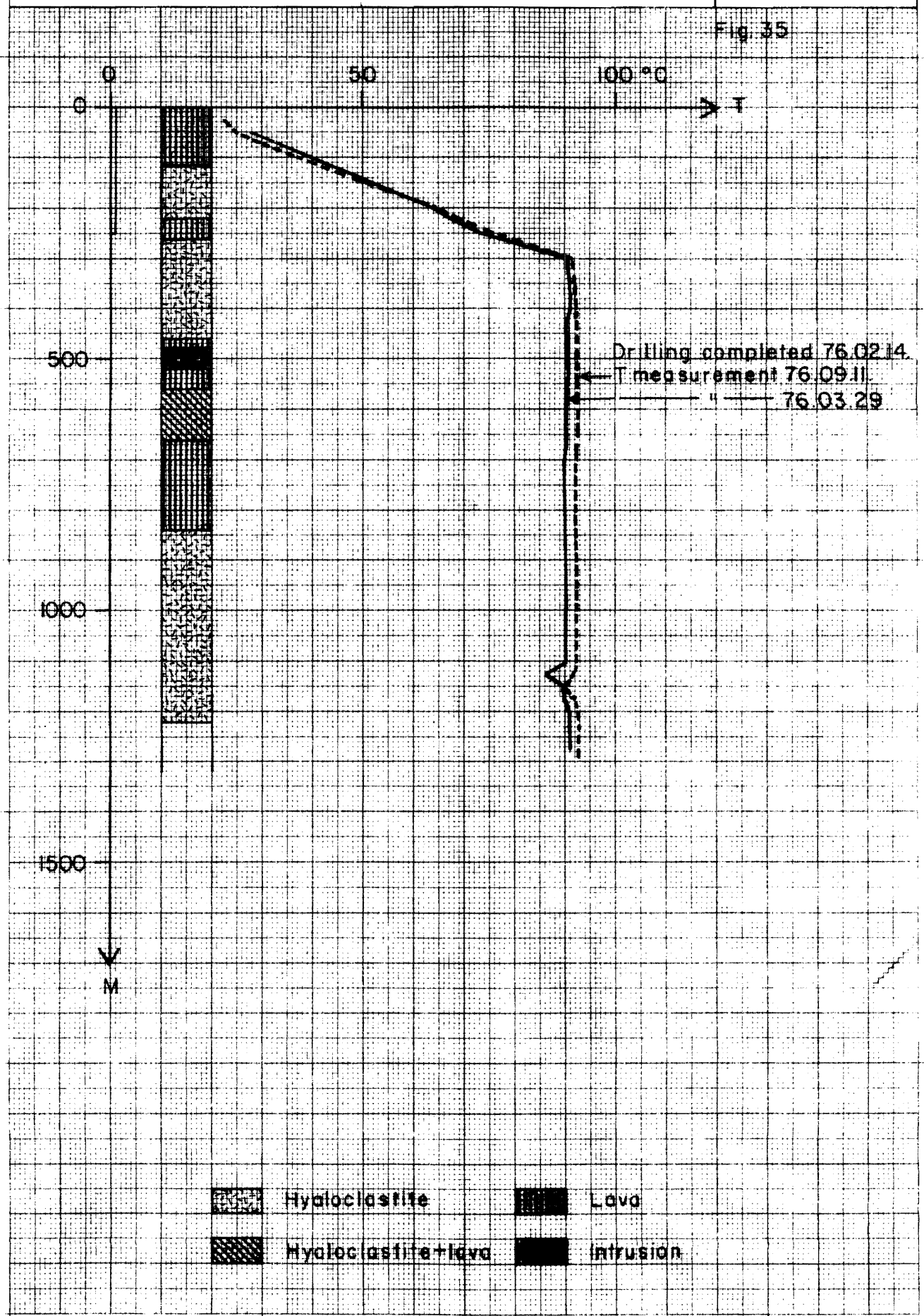
-  Hyaloclastite
-  Hyaloclastite+lava
-  Lava



80-08-25
ZHOU/Sy.J.
JHD/Sy.J.
F.19919

Temperature profile and simplified geological section of well MG-32

Fig. 35





Temperature profile and simplified geological section of well MG-33

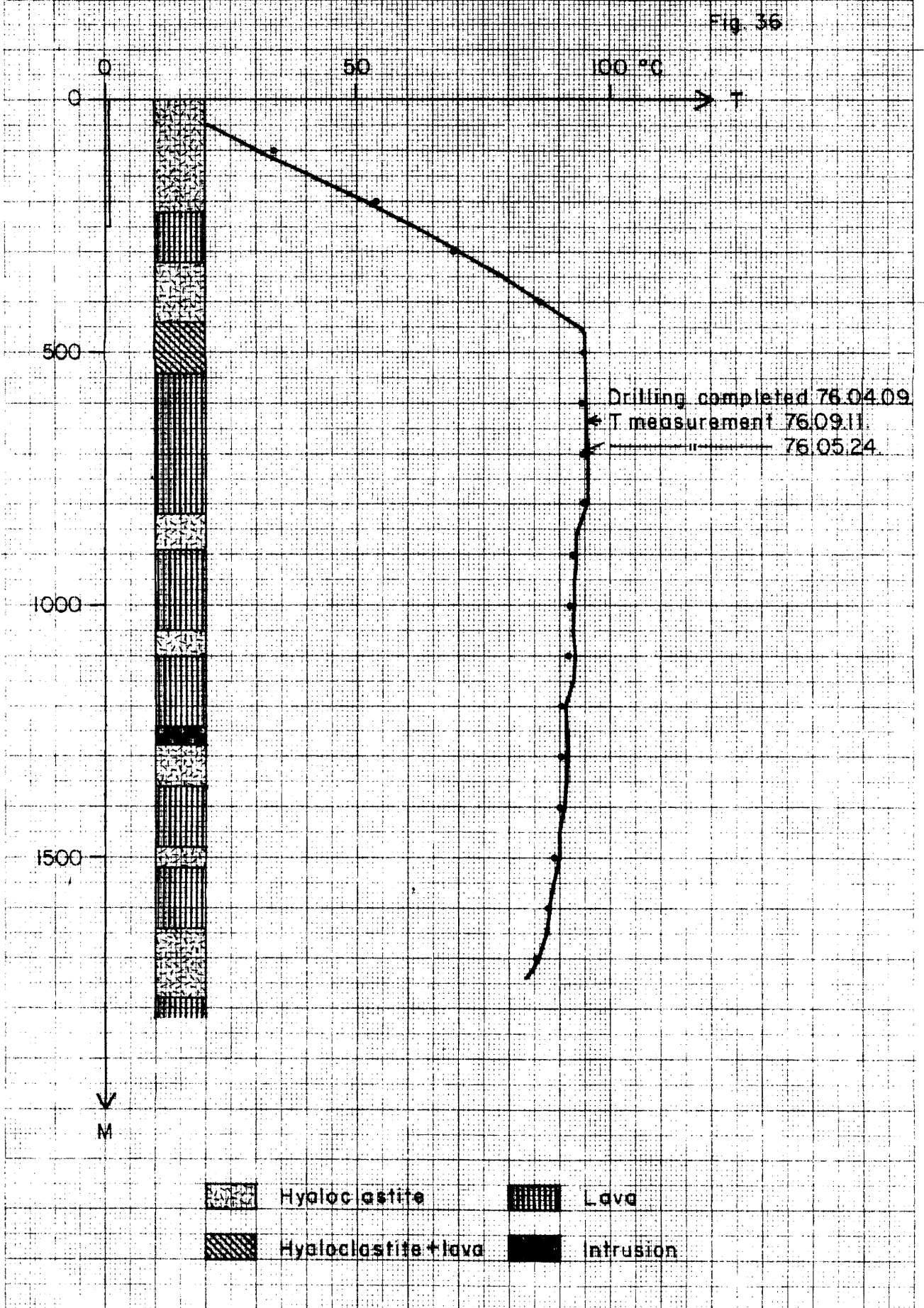
80-08-25

ZHOU/Sy.J.

JHD/HSP Mosf.

F19920

Fig. 36





80-08-25

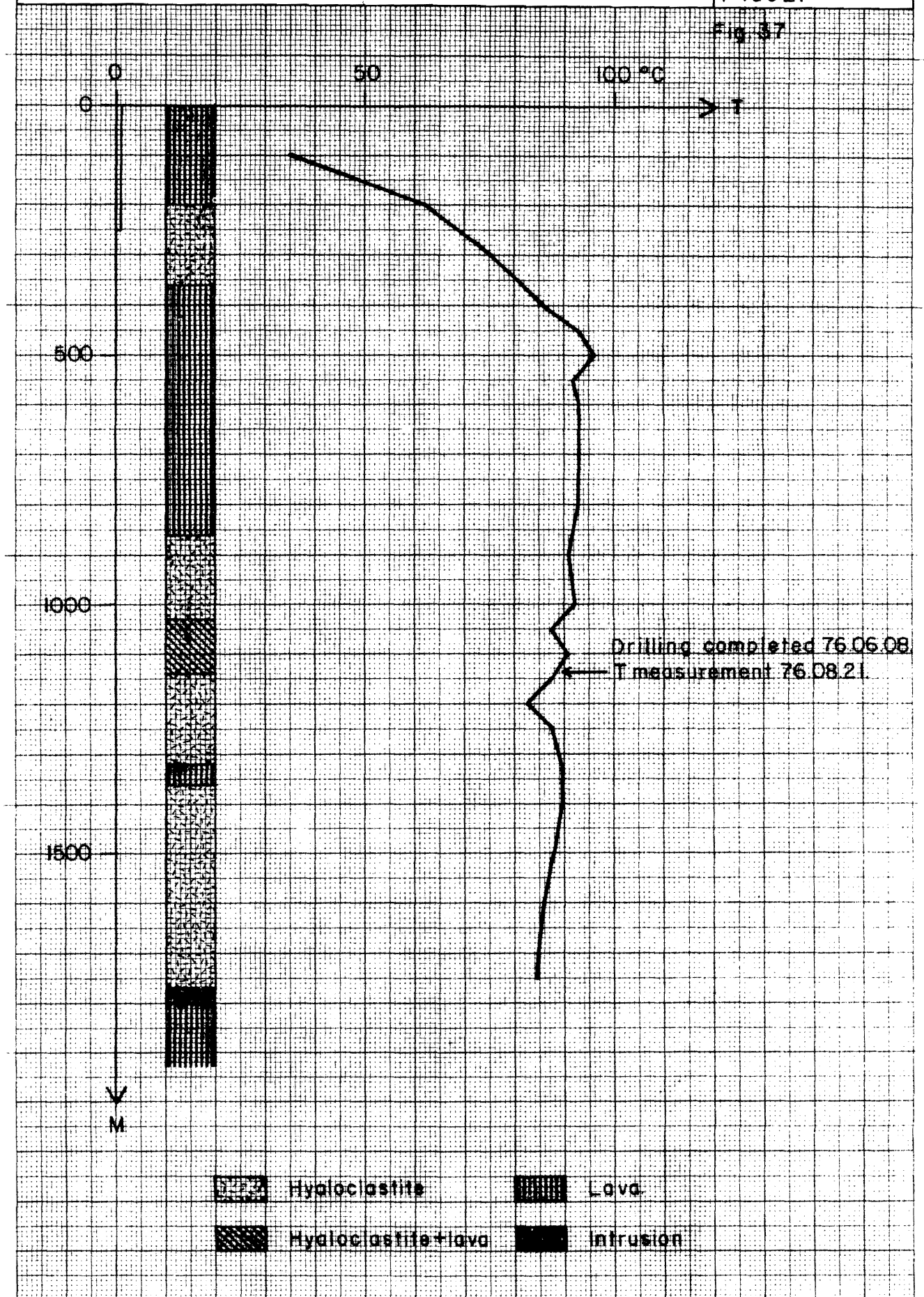
ZHOU/Sy.J.

JHD/HSP Mosf.

F 19921

Temperature profile and simplified geological section of well MG-34

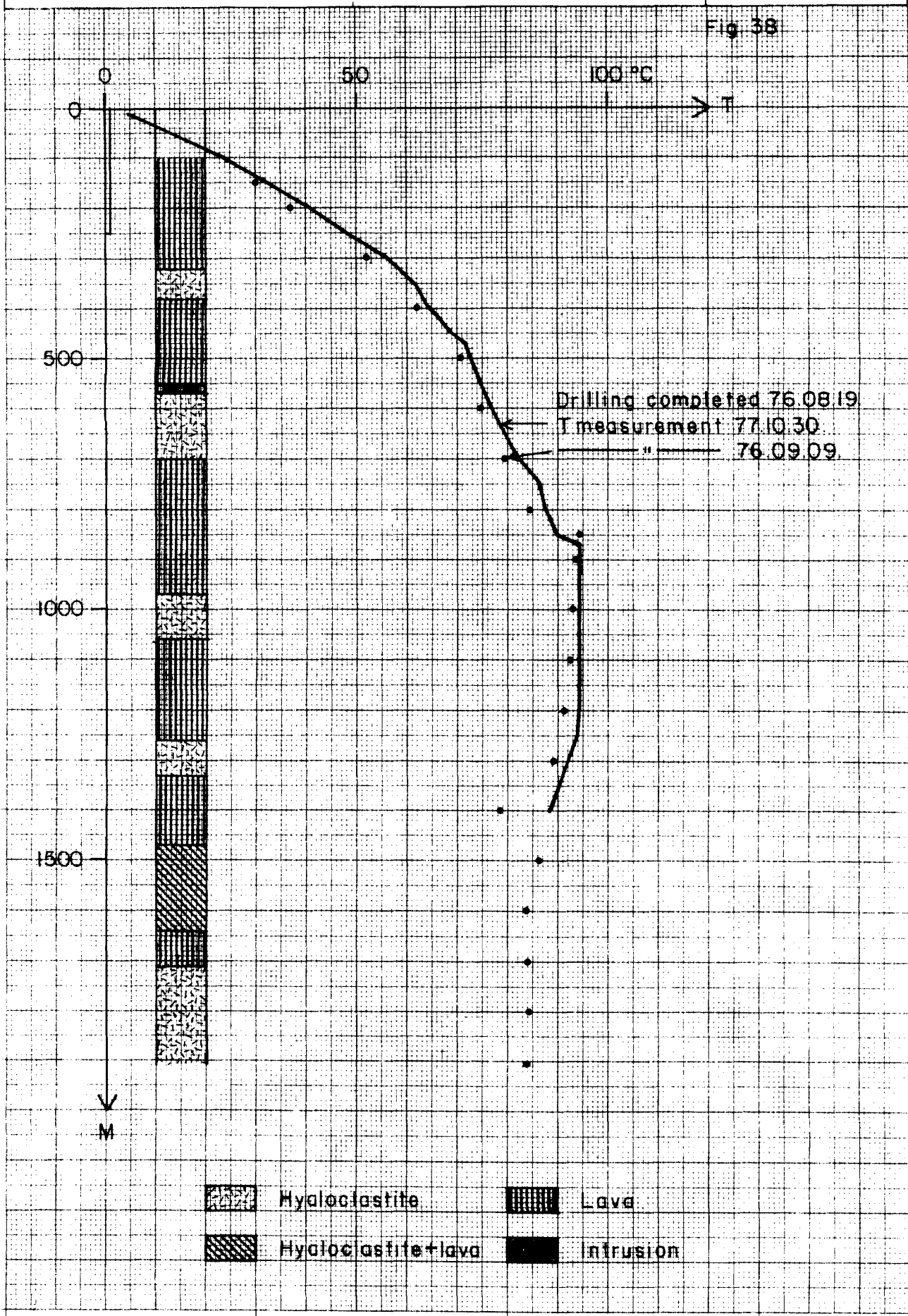
Fig. 37





Temperature profile and simplified geological section of well MG-35

Fig. 38



 Hyaloclastite	 Lava
 Hyaloclastite+lava	 Intrusion



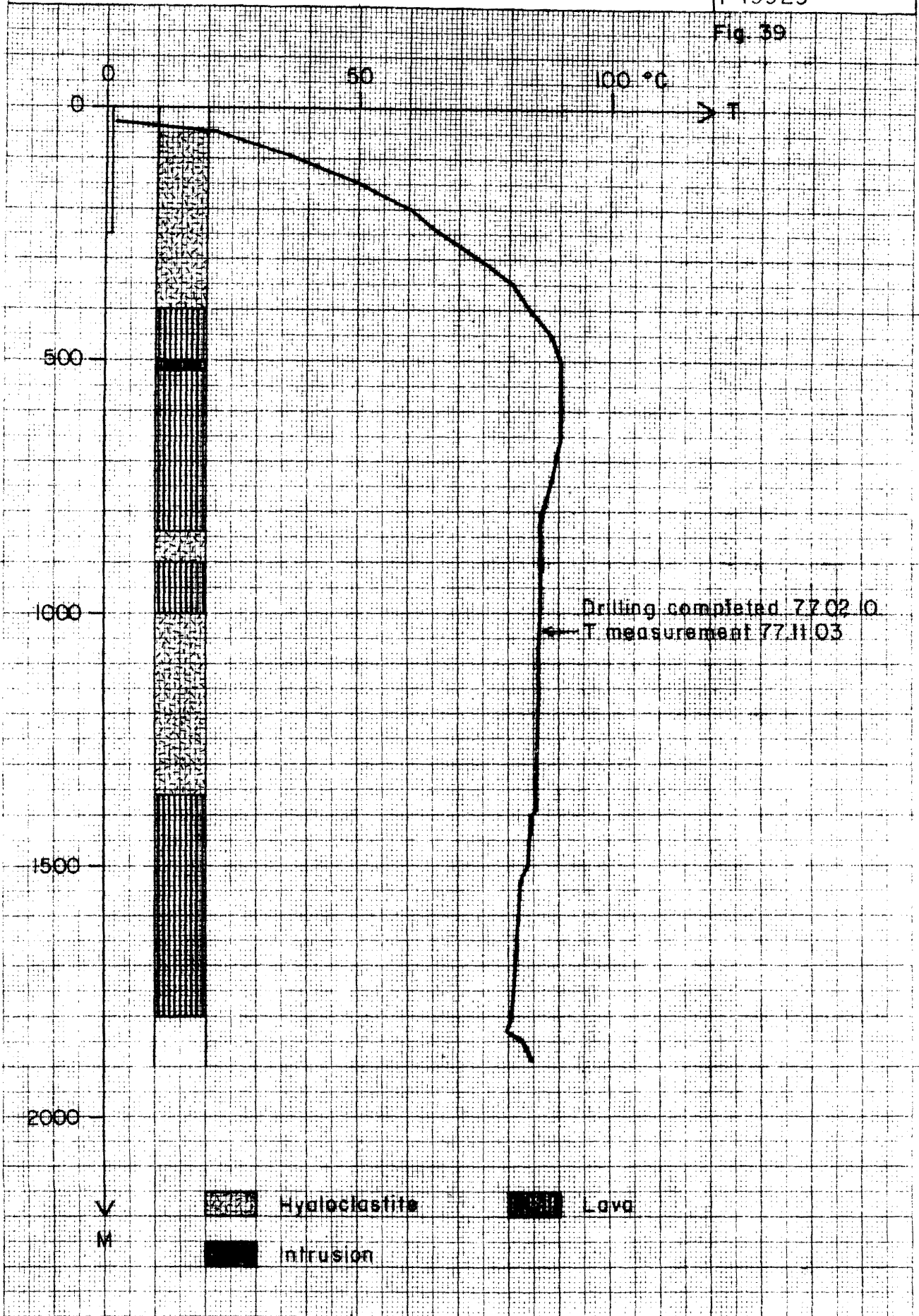
Temperature profile and simplified geological section of well MG-36

ZHOU/Sy.J.

JHD/HSP Mosf.

F 19923

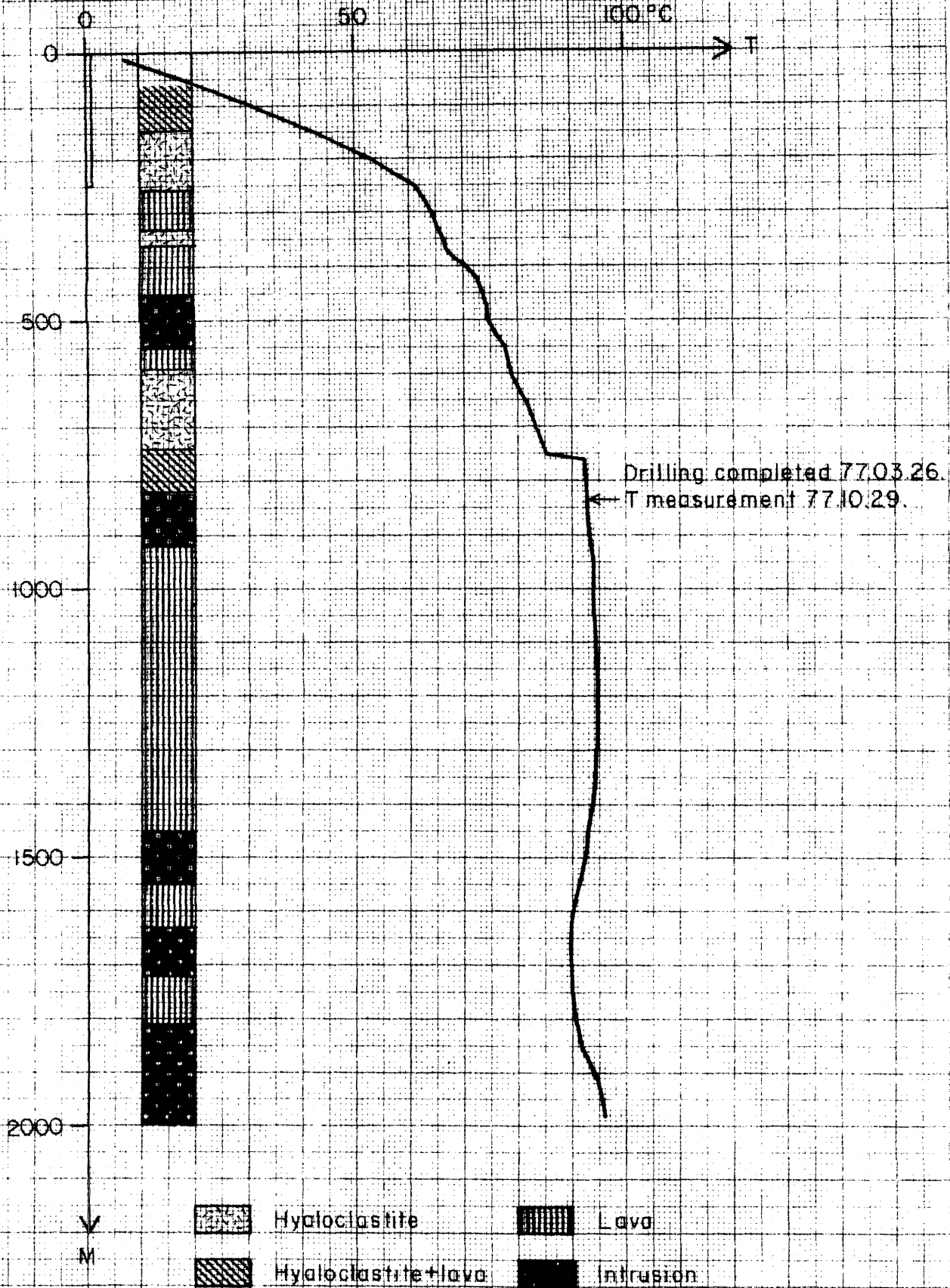
Fig. 39





Temperature profile and simplified geological section of well MG-37

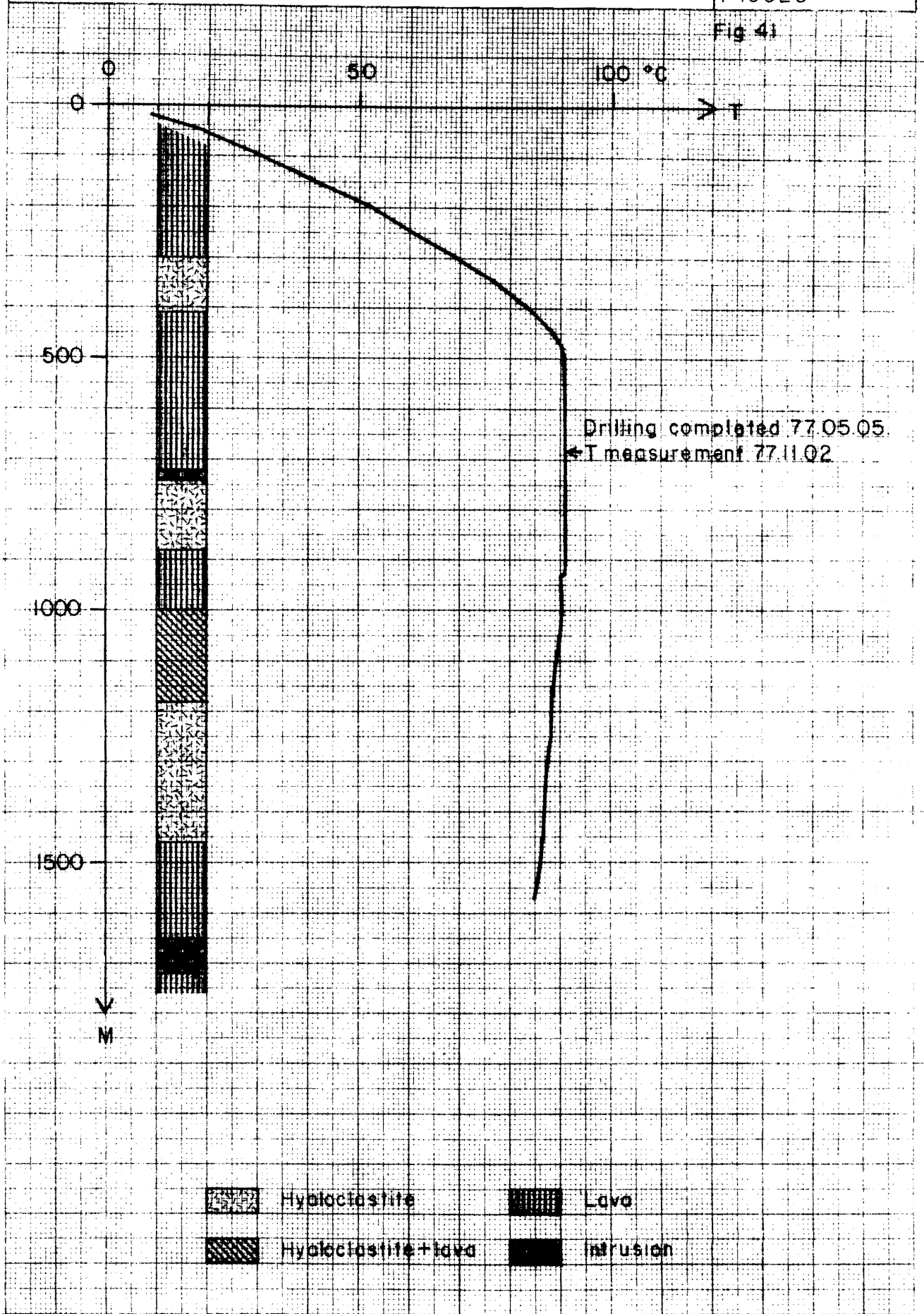
Fig. 40





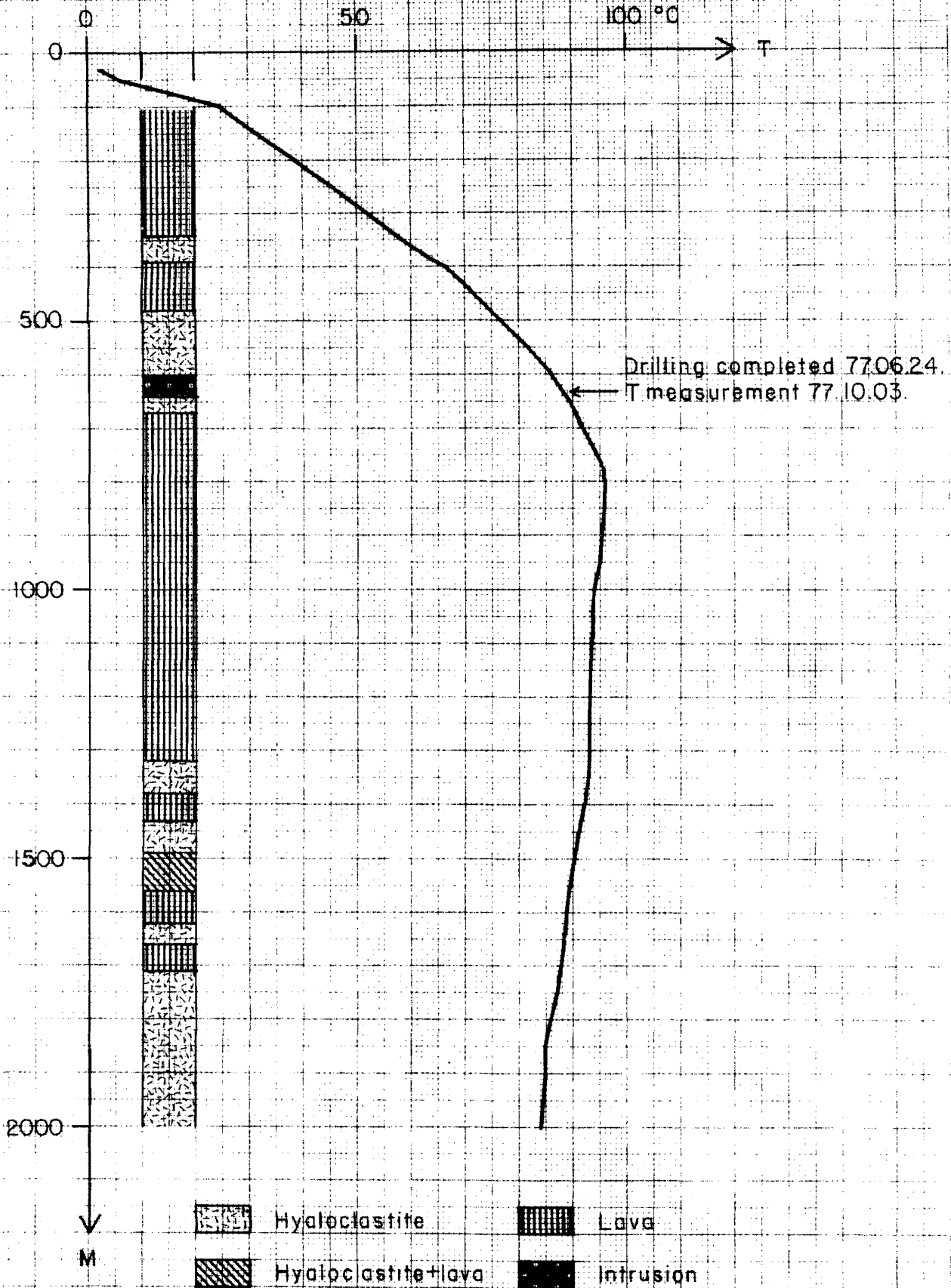
Temperature profile and simplified geological section of well MG-38

Fig 41



Temperature profile and simplified geological section of well MG-39

Fig. 42





Temperature profile NW-SE, S-Reykir, Mosfellssveit

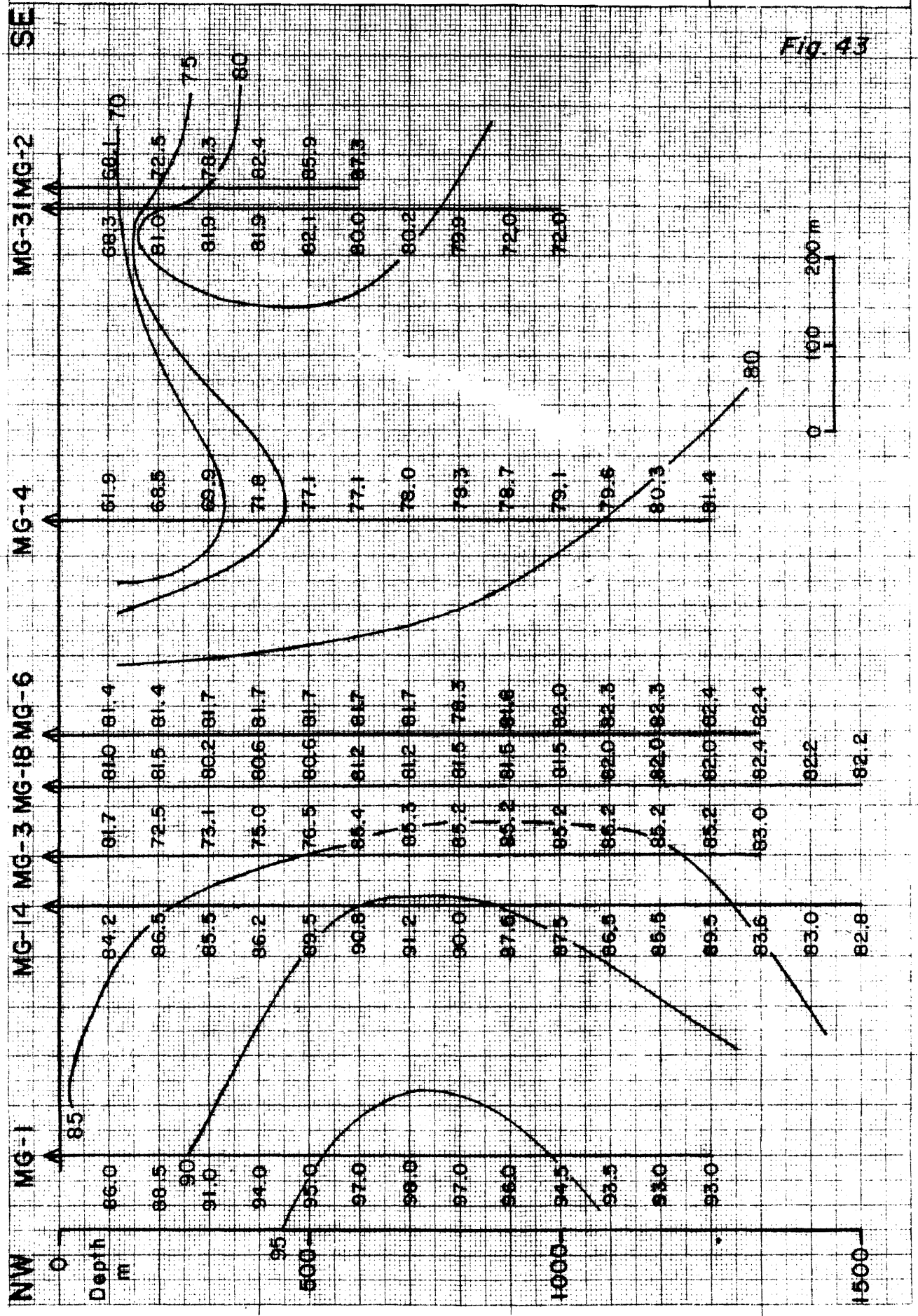


Fig. 43



Temperature profile N-S, S-Reykir, Mosfellssveit

80.08.25
ZHOU / IS
JHD-HSBMosf.sv.
F-19876

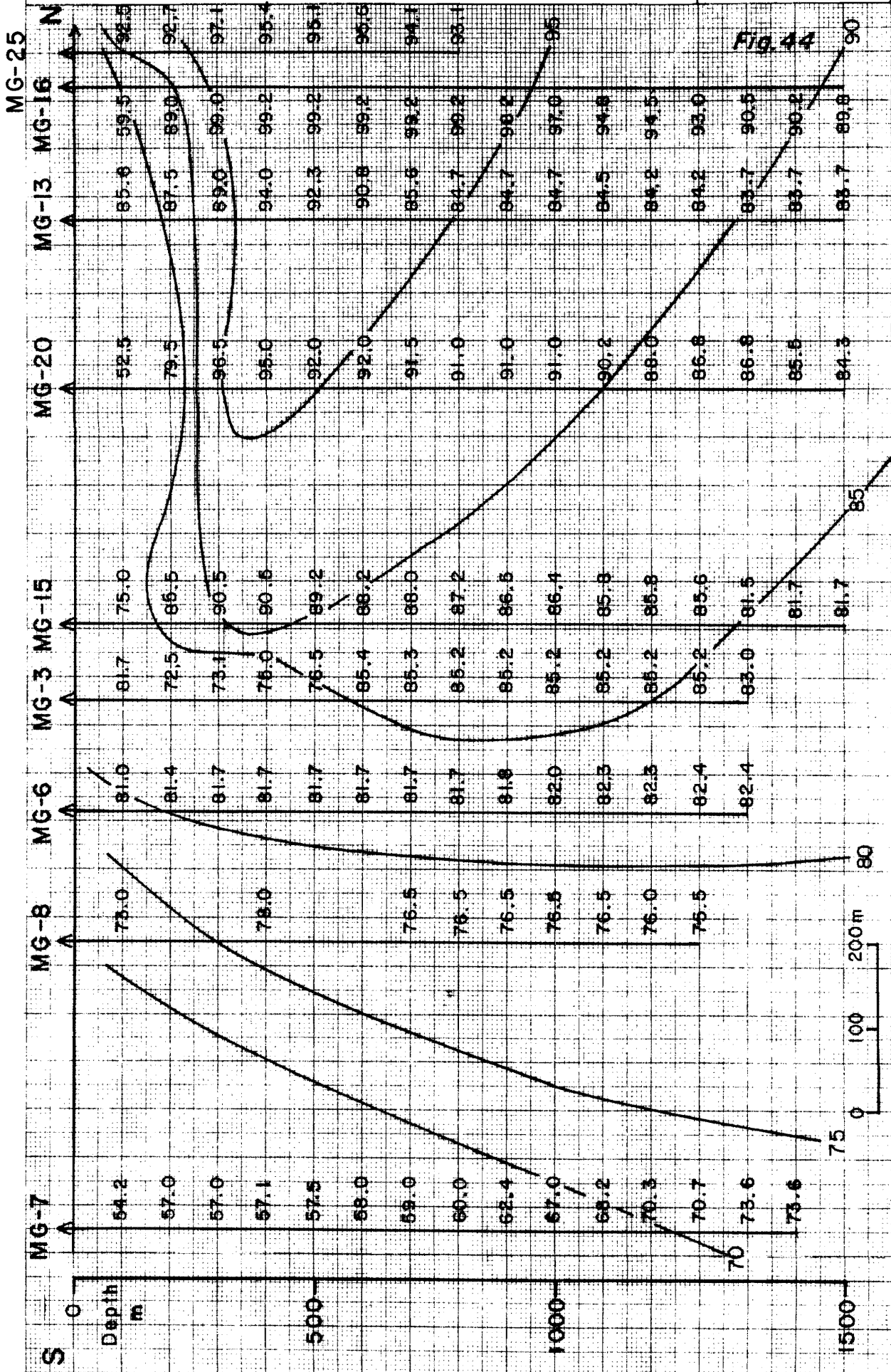


Fig. 44

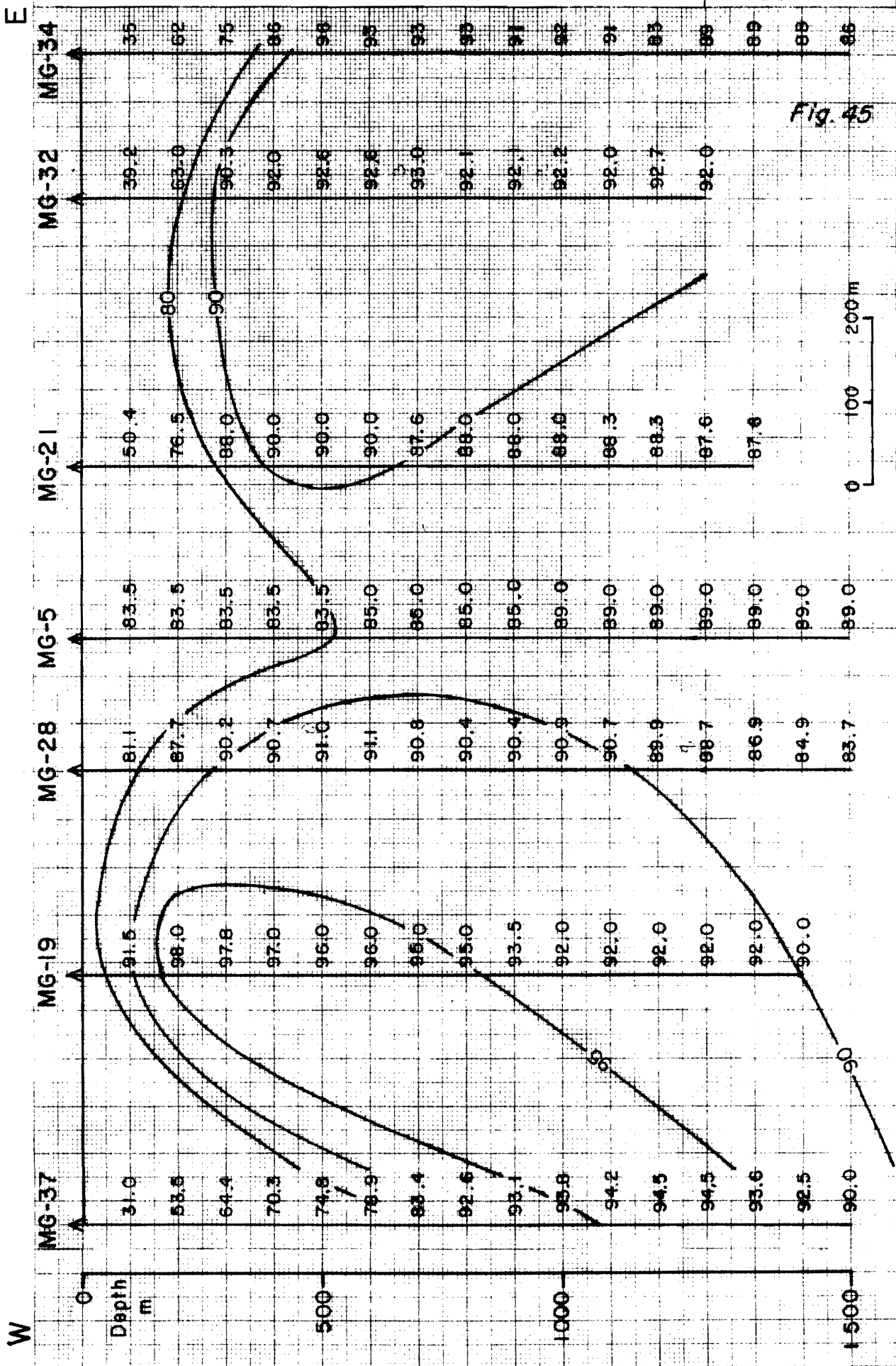


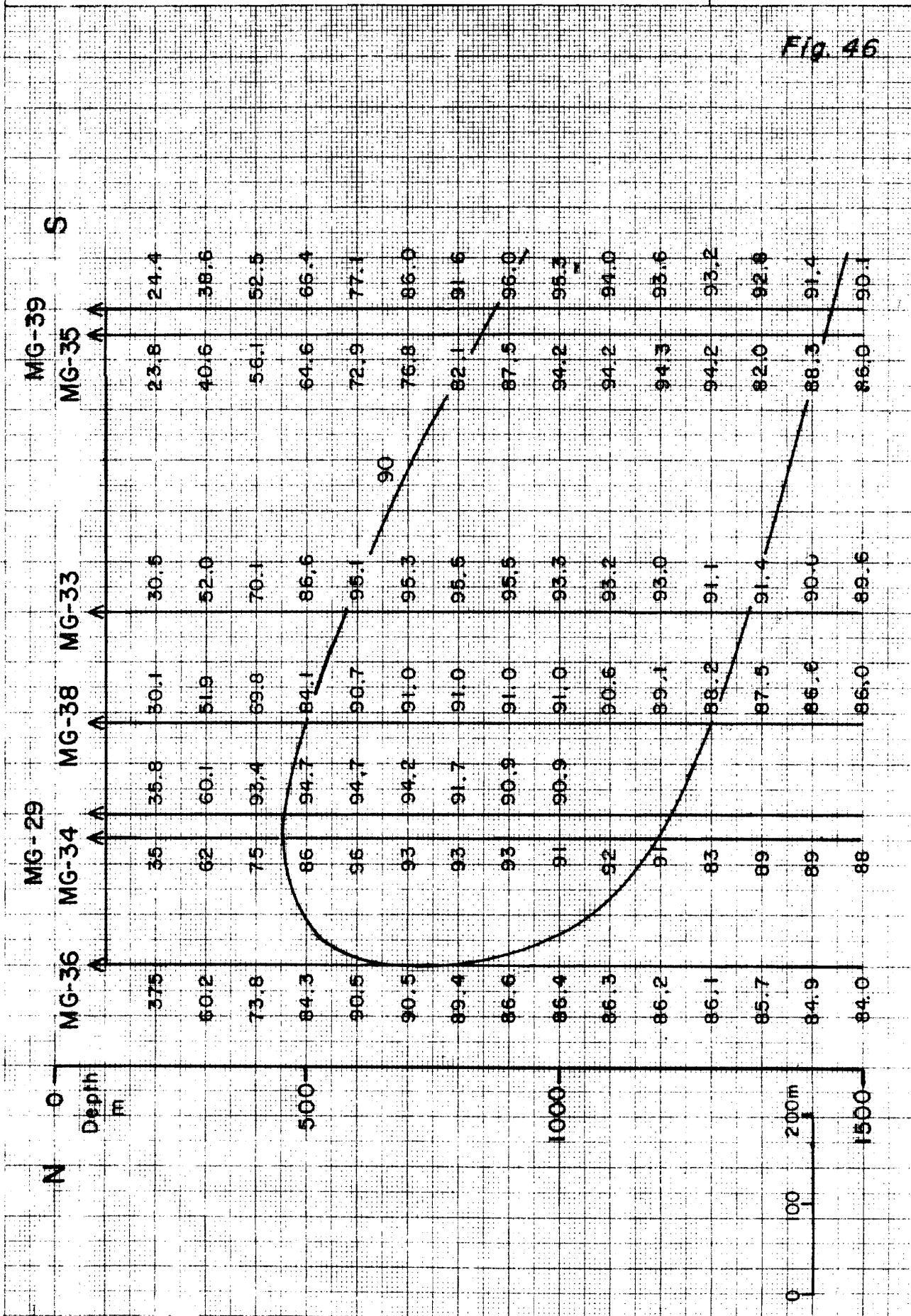
Fig. 45



80.08.25
ZHOU / IS
JHD-HSB Mosf.sv.
F-19877

Temperature profile N-S, N-Reykir, Mosfellssveit

Fig. 46





Map showing depth of maximum temperature at S-Reykir Mosfellssveit

80.08.25

ZHOU / IS

JHD-HSB Mosf. sv.

F-19884

Fig. 47a

MG-1
• 700

• 300

• 325 (-700)

• 425

• 325

• > 800

• 225-400

• 700 (500-800)

MG-3 • 500-1300

• 300-900

• 150

• > 1400

• 600-800
(300-900)

• 600

• > 1300

• 200-1300

• 200 (-1100)

• 300-900

MG-2 • 300
• > 800

• > 300

• 250-700

• > 1000

• 300

• > 1400

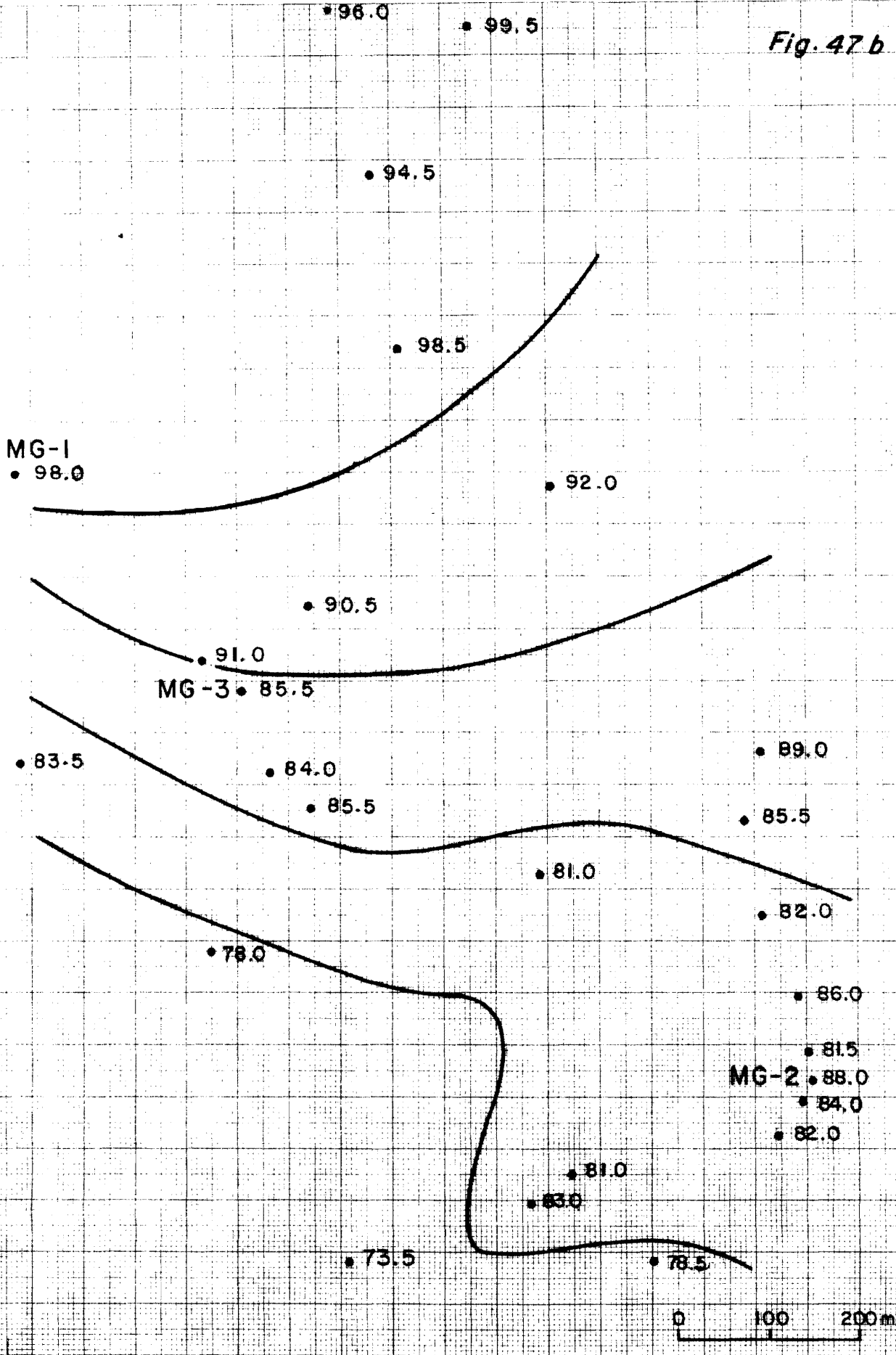
• 300

0 100 200 m



Map showing maximum temperature at S-Reykir Mosfellssveit

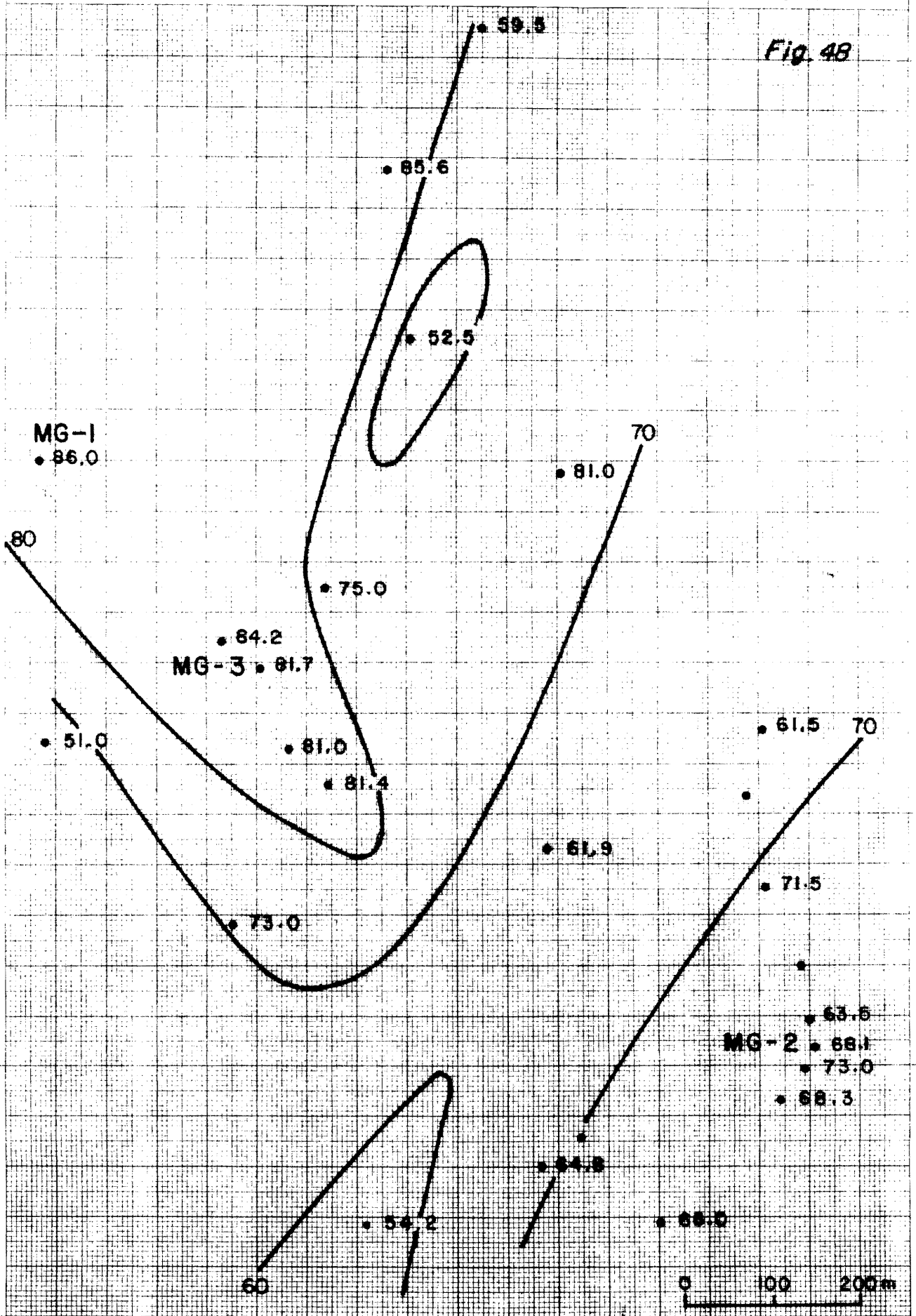
Fig. 47 b





Isotherms at 100 m depth, S-Reykir, Mosfellssveit

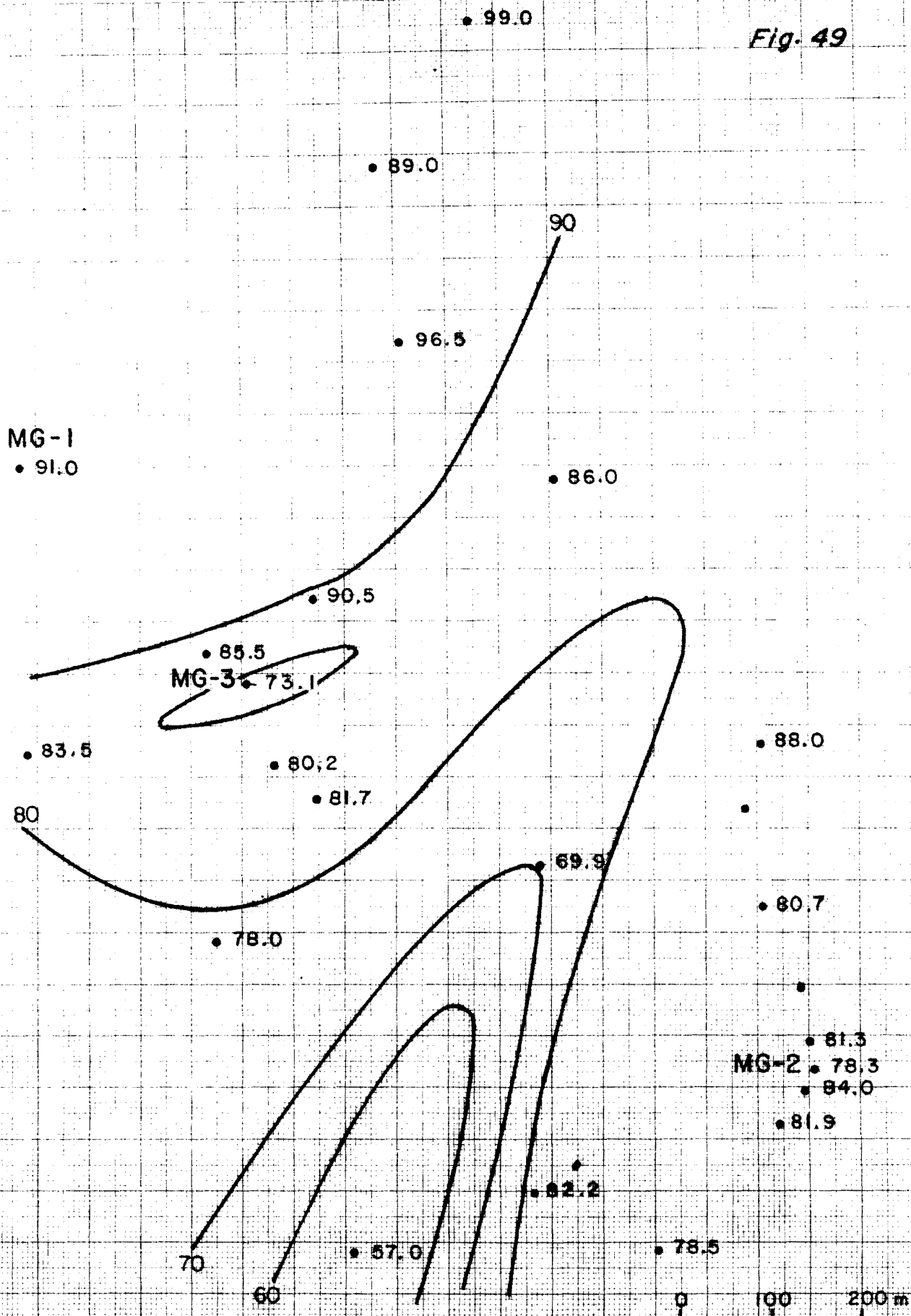
Fig. 48





Isotherms at 300m depth, S-Reykir, Mosfellssveit

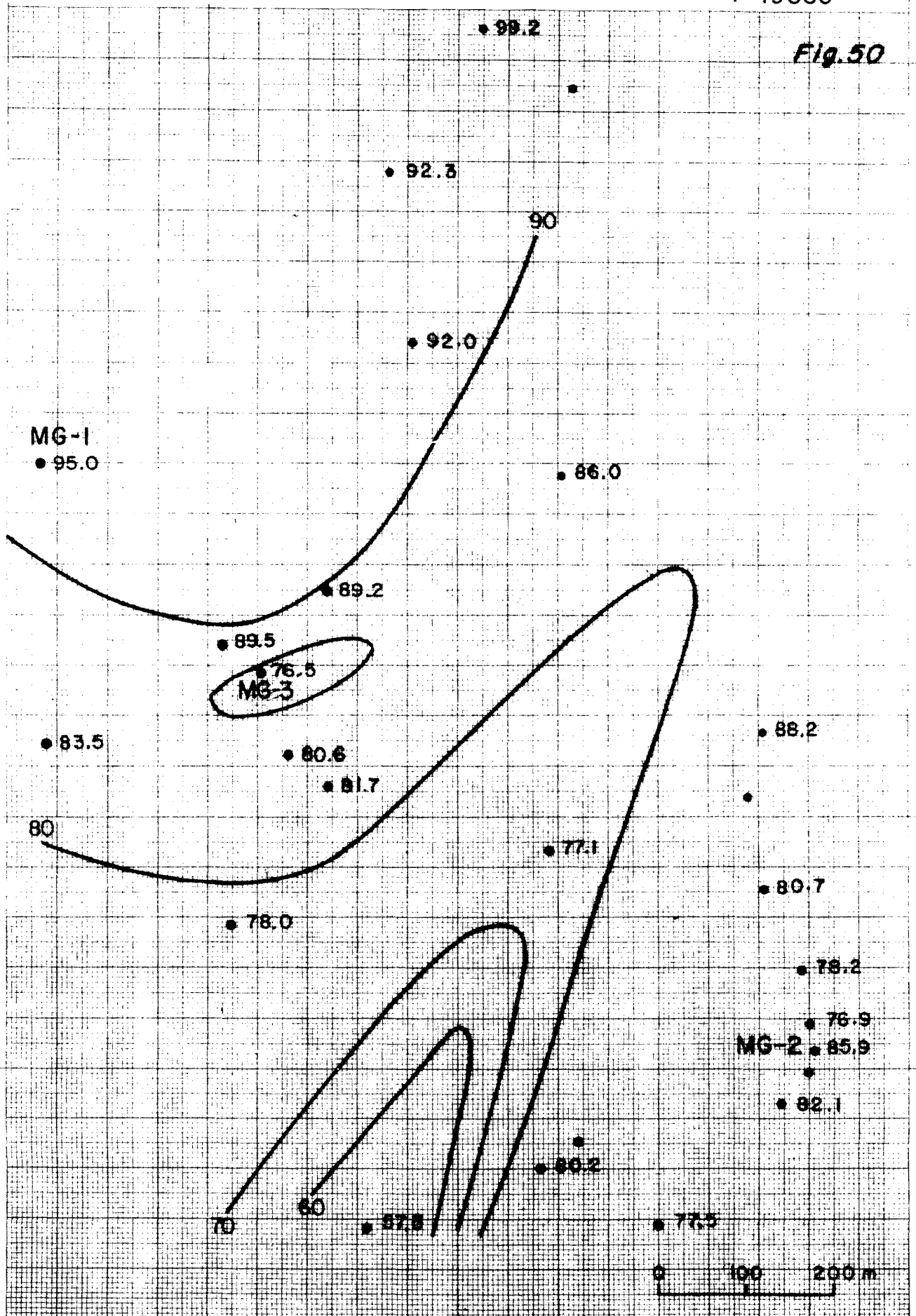
Fig. 49





Isotherms at 500m depth S-Reykir, Mosfellssveit

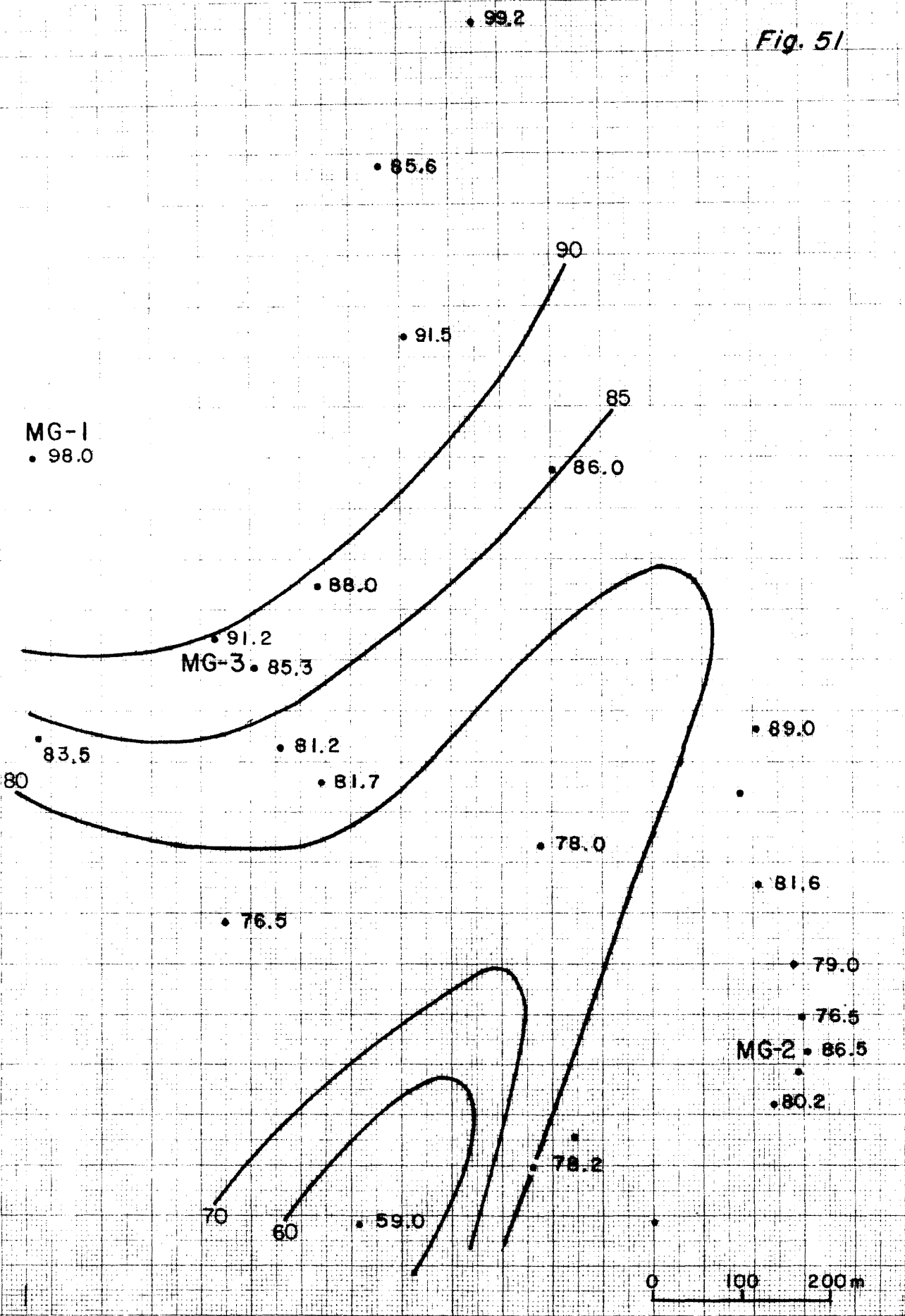
Fig. 50





Isotherms at 700m depth, S-Reykir, Mosfellssveit

Fig. 51





80 08 25

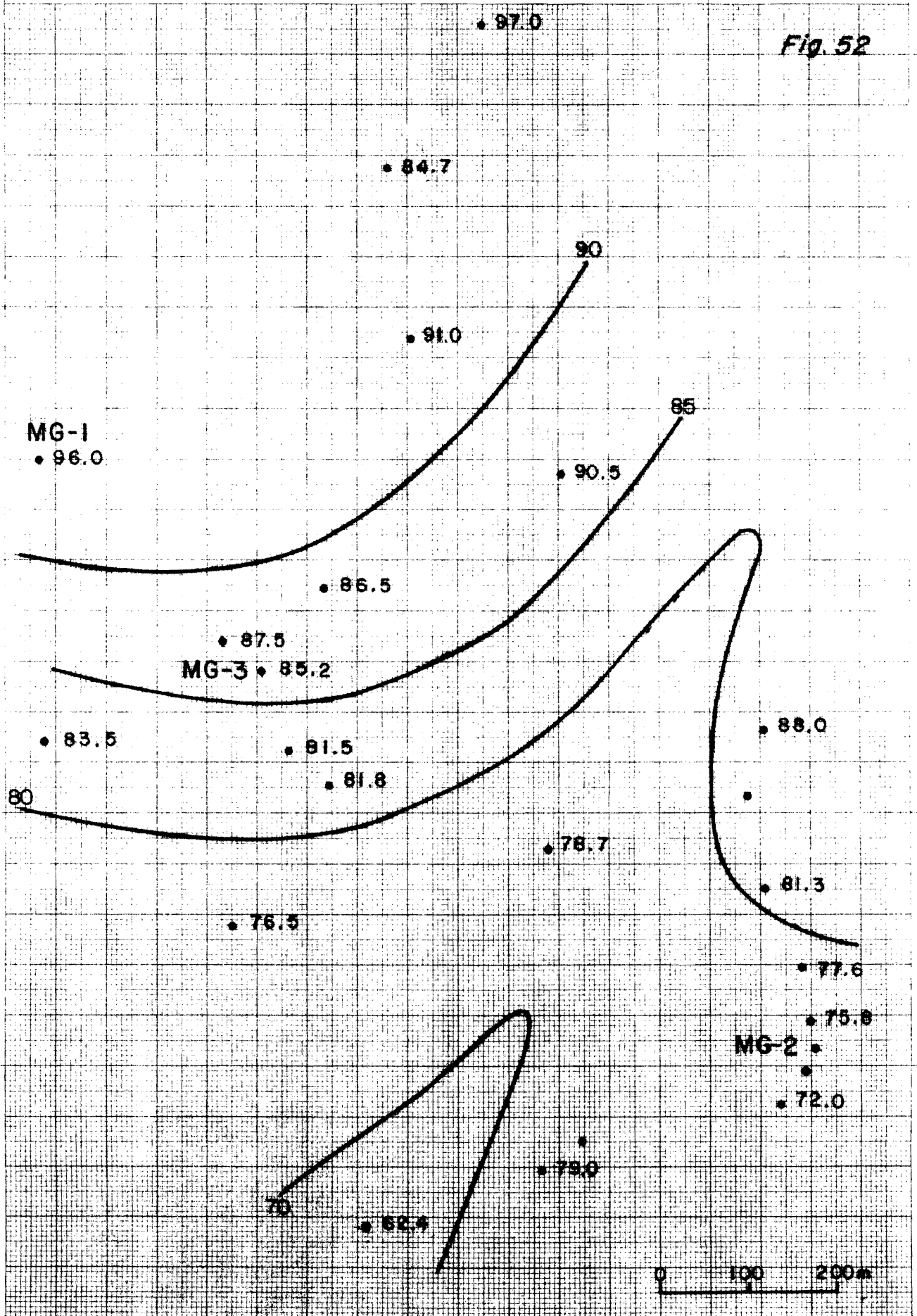
ZHOU / IS

JHD-HSI Mosf.sv.

F-19887

Isotherms at 900m depth, S-Reykir, Mosfellssveit

Fig. 52

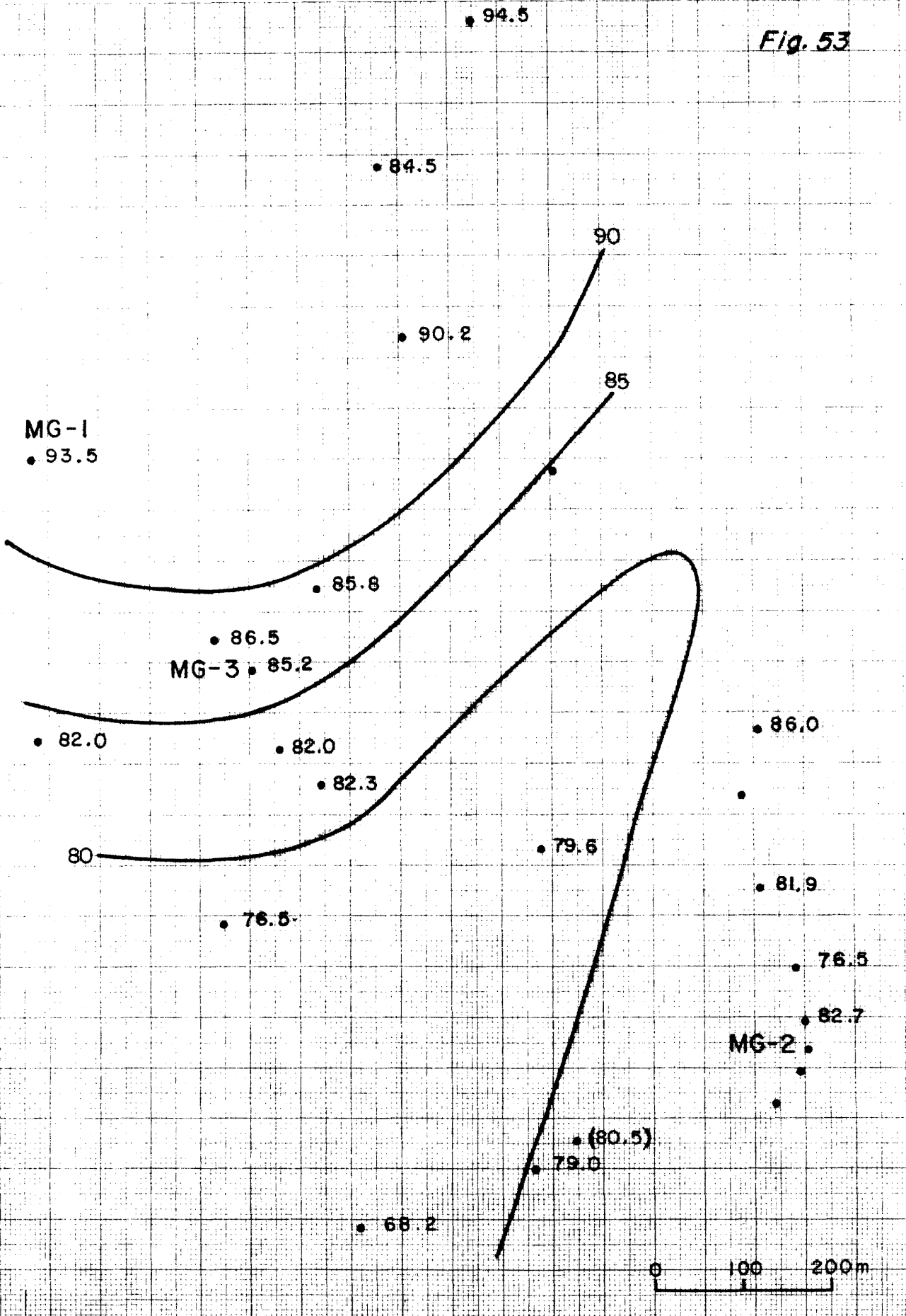


73 25 01 - 523 A4 - 1 x 1 mm



Isotherms at 1100m depth, S-Reykir, Mosfellssvelt

Fig. 53





80 08 25

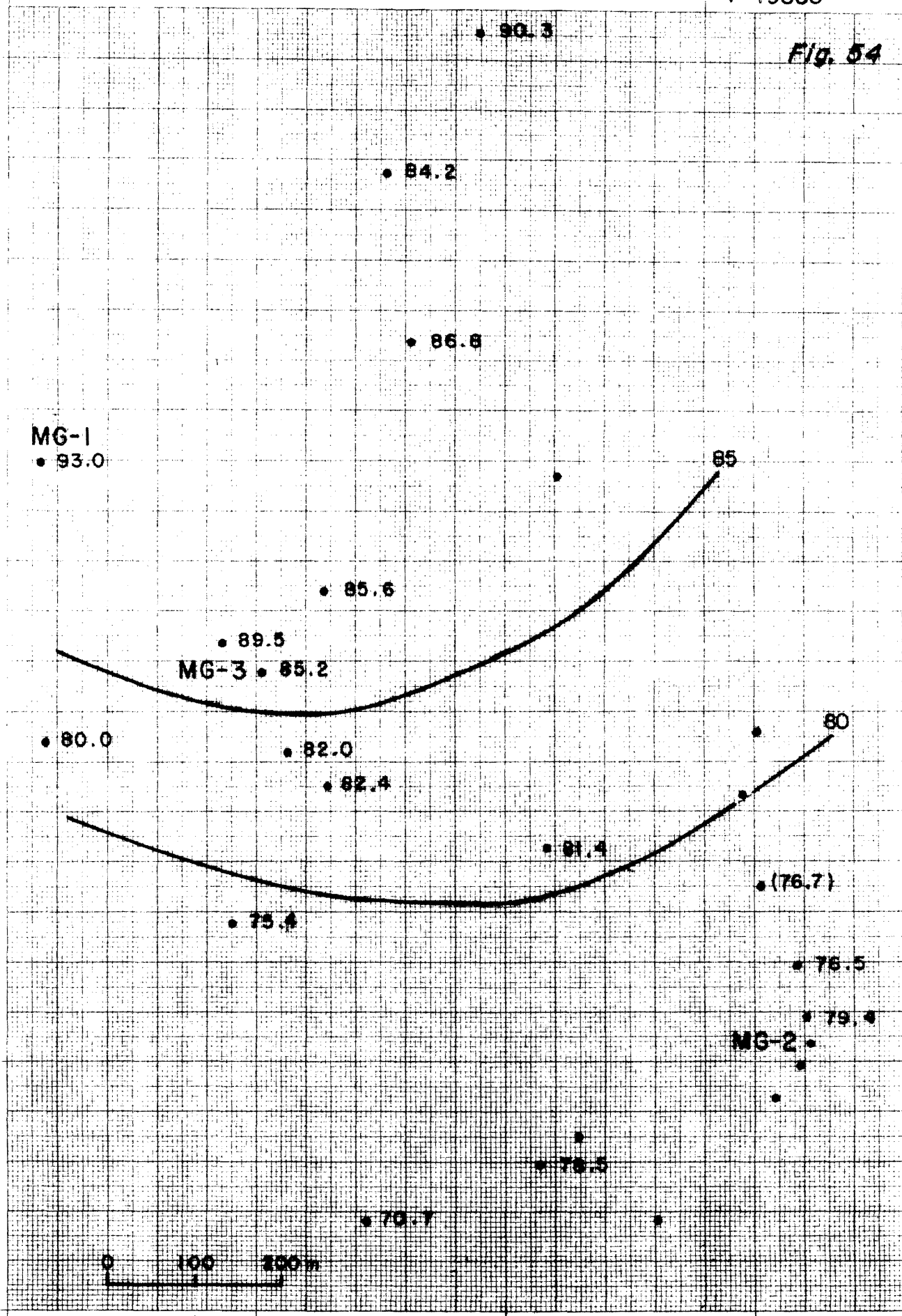
ZHOU / IS

JHD-HSI Mosf.sv.

F-19883

Isotherms at 1300m depth, S-Reykir, Mosfellssveit

Fig. 54



73 25 01 523 A4 1 x 1 mm



Isotherms at 1500m depth, S-Reykir, Mosfellssveit

85 89.8 86(2000)

Fig. 55

83.7

85.5

MG-1

81.7

83.0

MG-3

80

76.5

82.2

MG-2 73.0

76.8

73.6

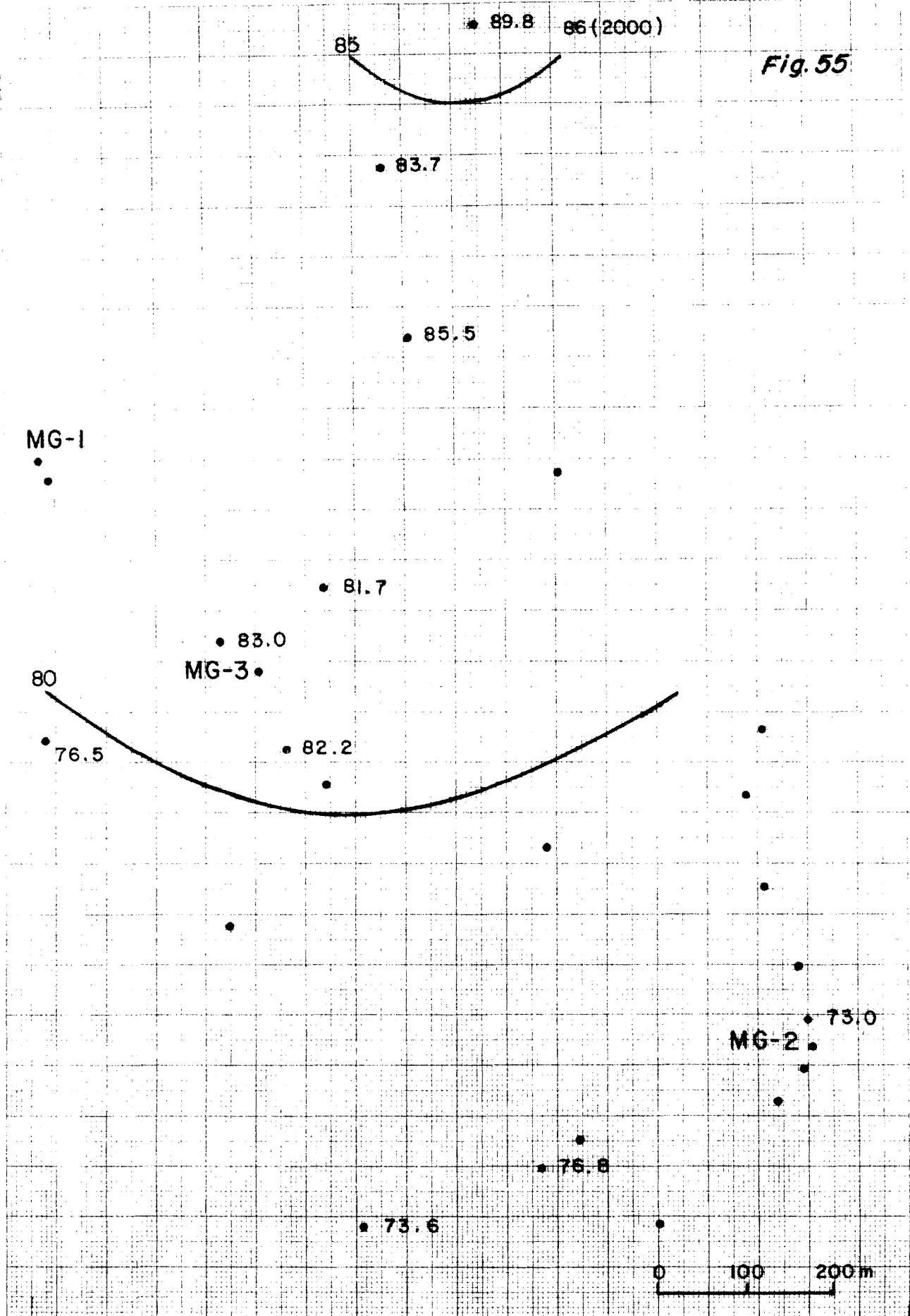




Fig. 56.

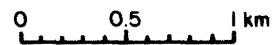
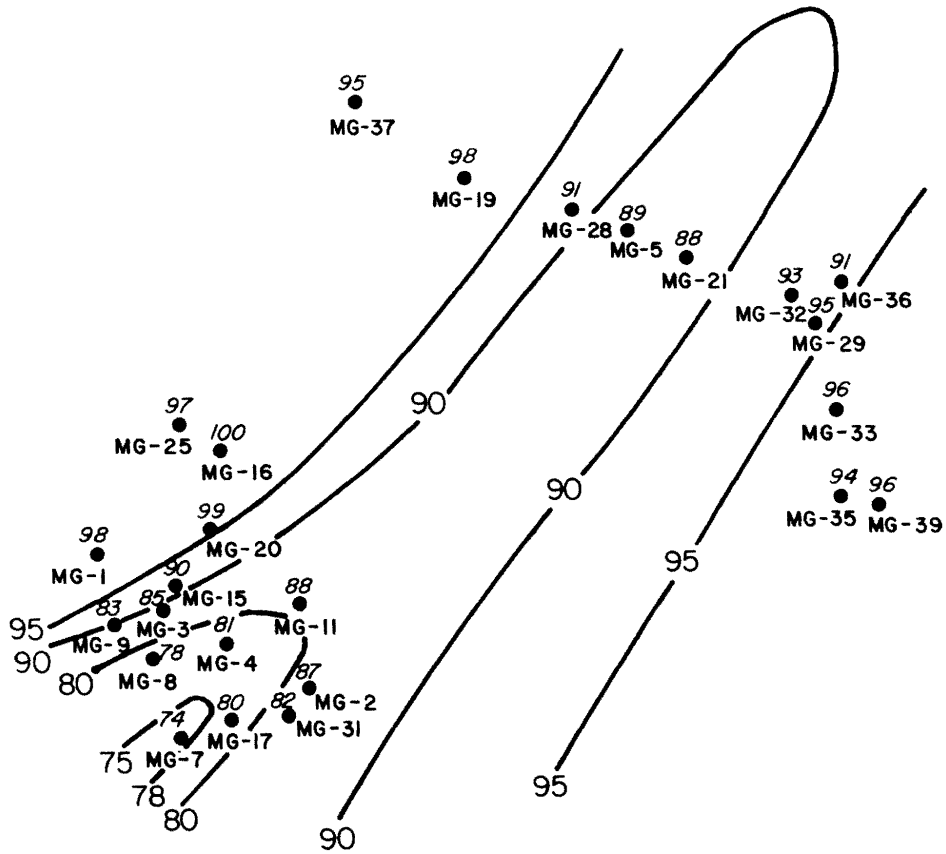


Fig. 57.

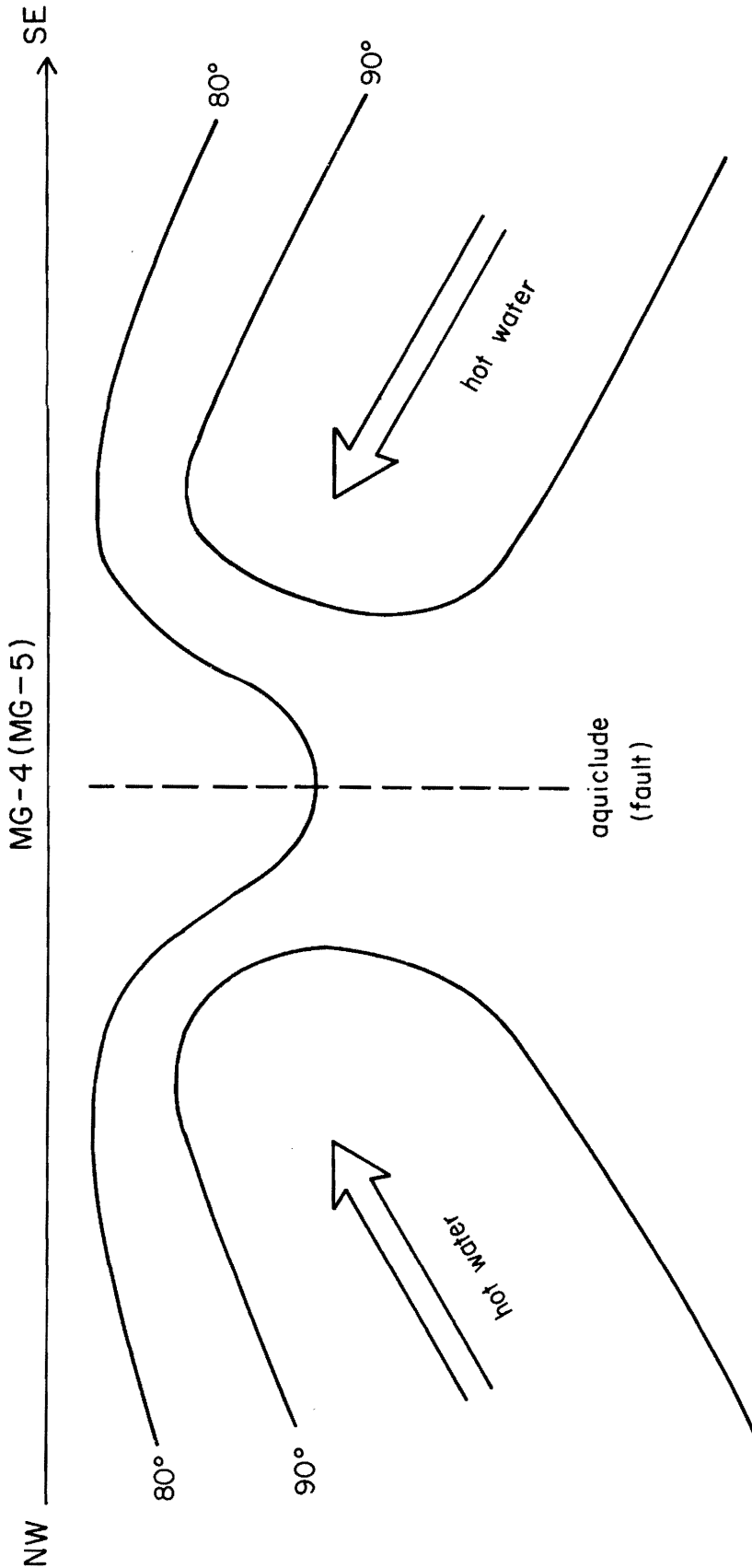
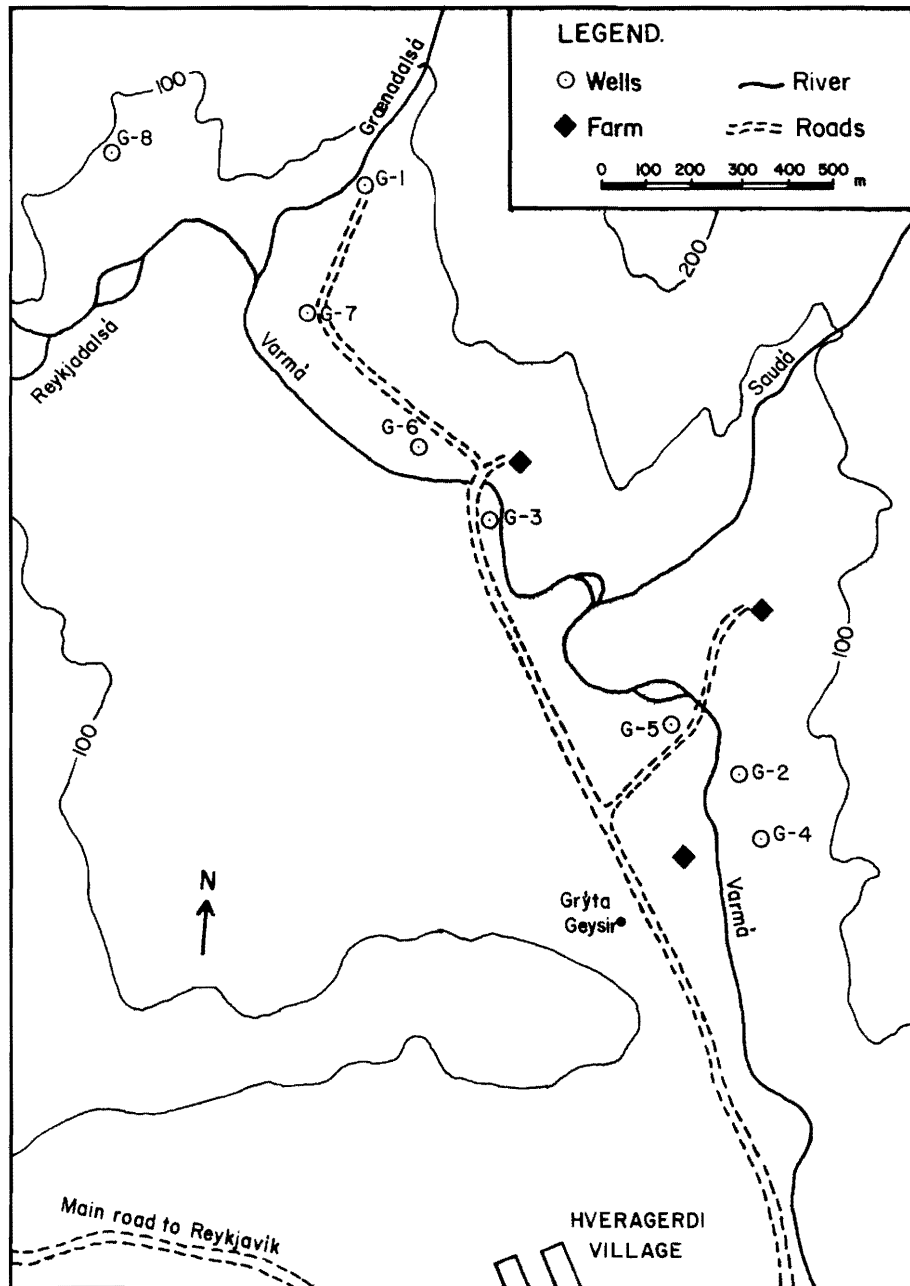




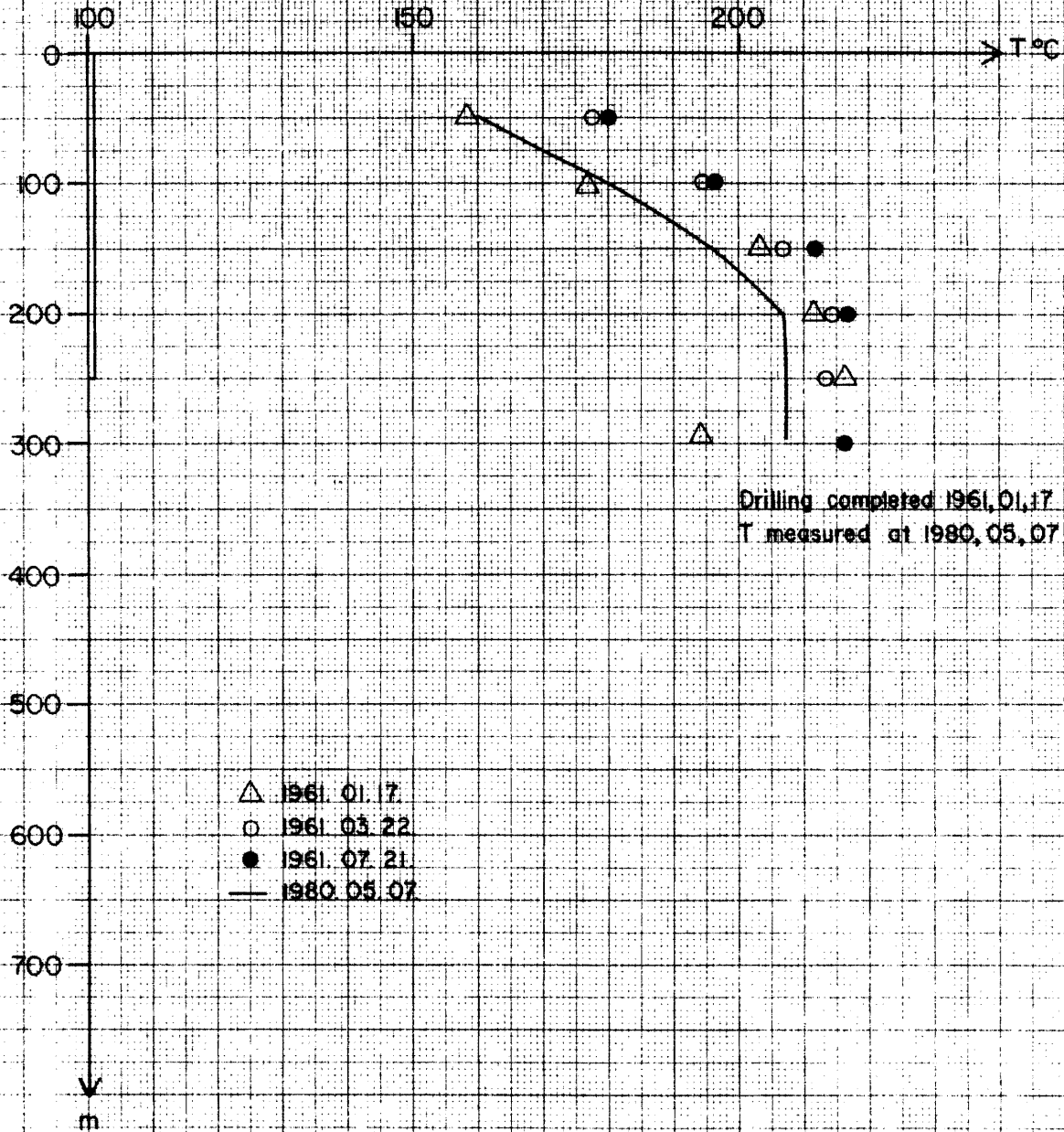
Fig. 58.





Temperature profile of well G-8, Ölfusdalur.

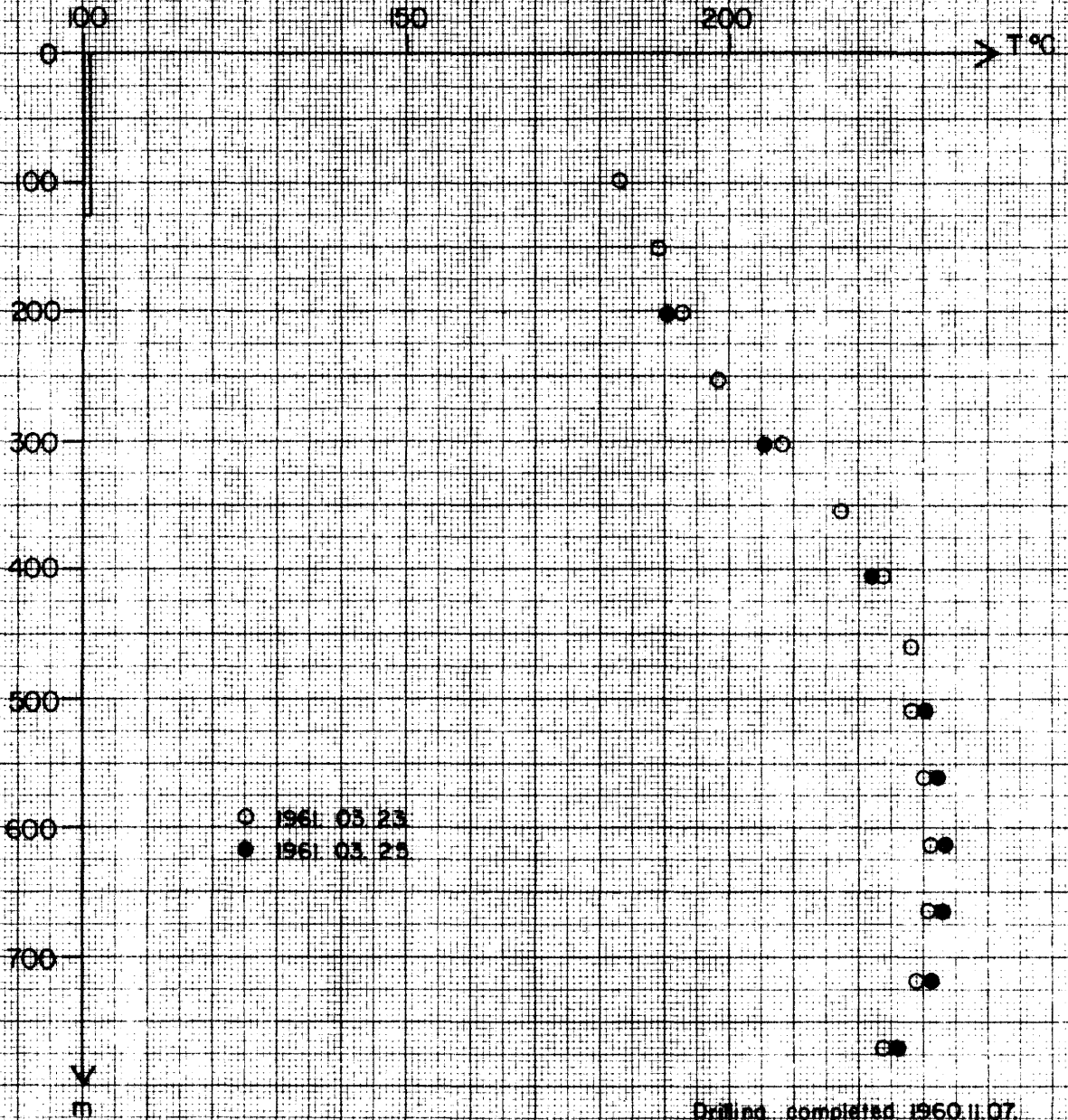
Fig. 59





Temperature profile of well G-1, Ölfusdalur.

Fig. 60

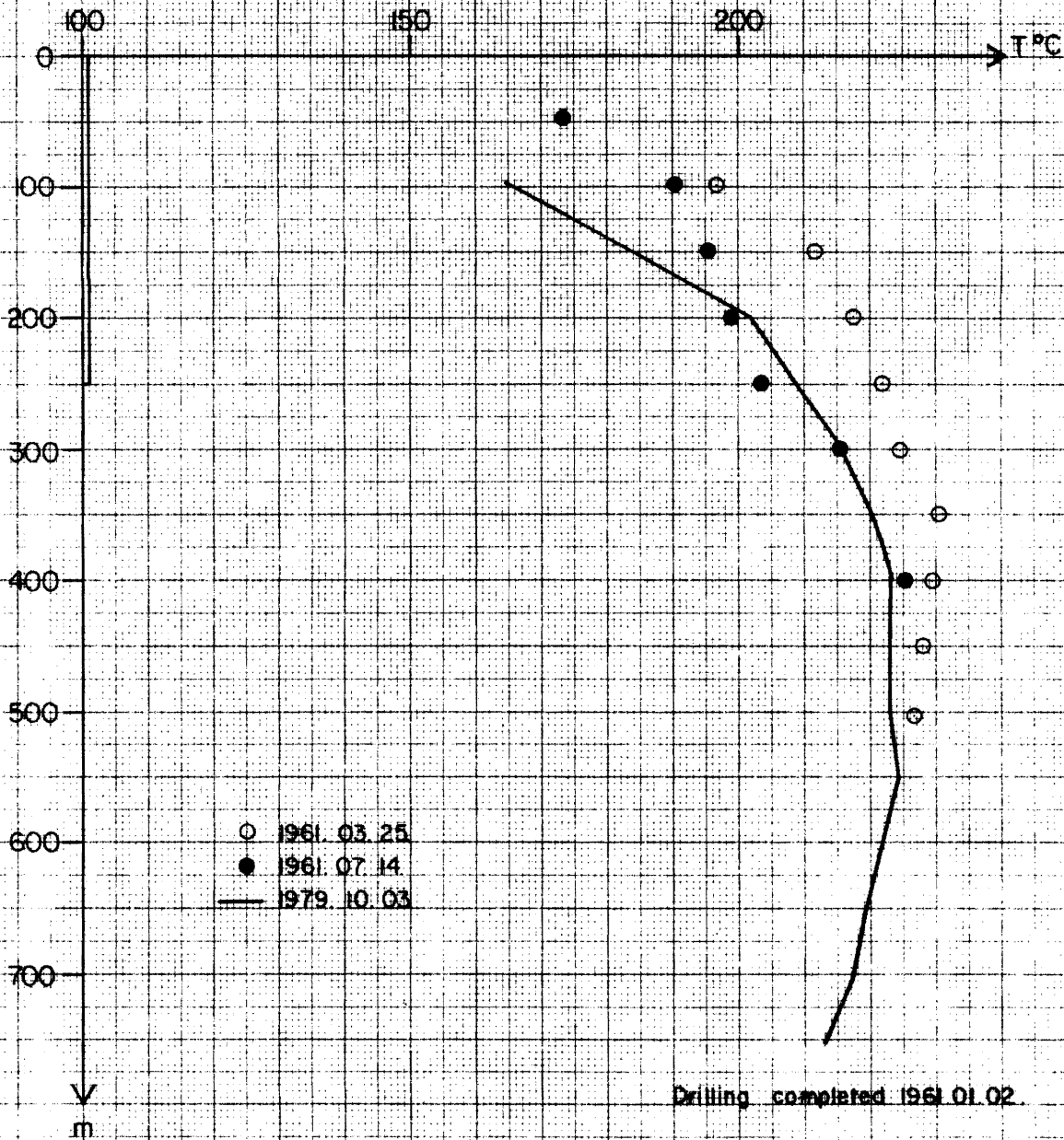


Drilling completed 1960.11.07.



Temperature profile of well G-7, Ölfusdalur.

Fig. 61





'80.09.09.

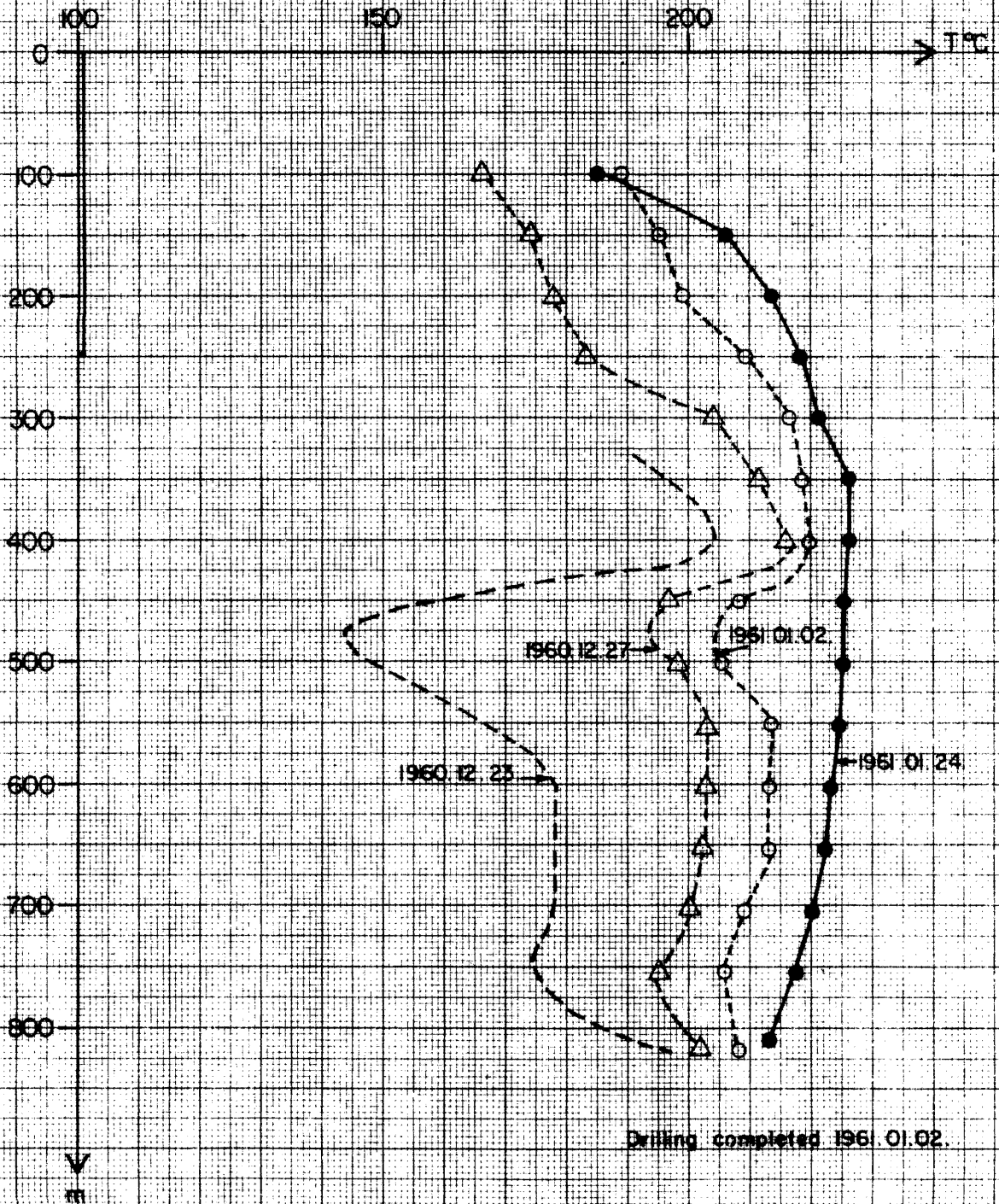
ZHOU/EBF

HSP. Öifus.

F-20002

Temperature profile of well G-7, Öifusdalur.

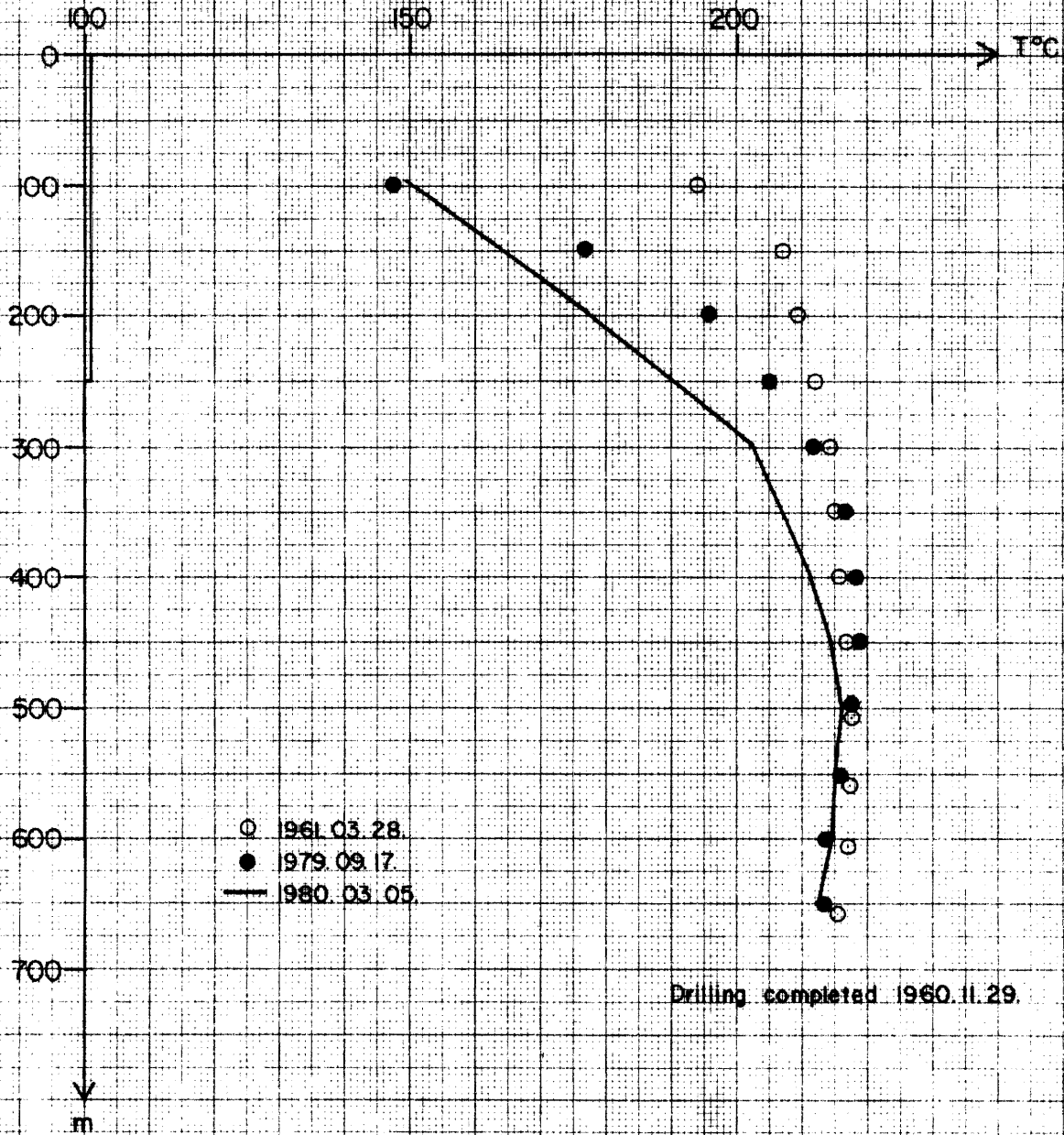
Fig. 52.





Temperature profile of well G-6, Ölfusdalur.

Fig. 63.





'80.09.09.

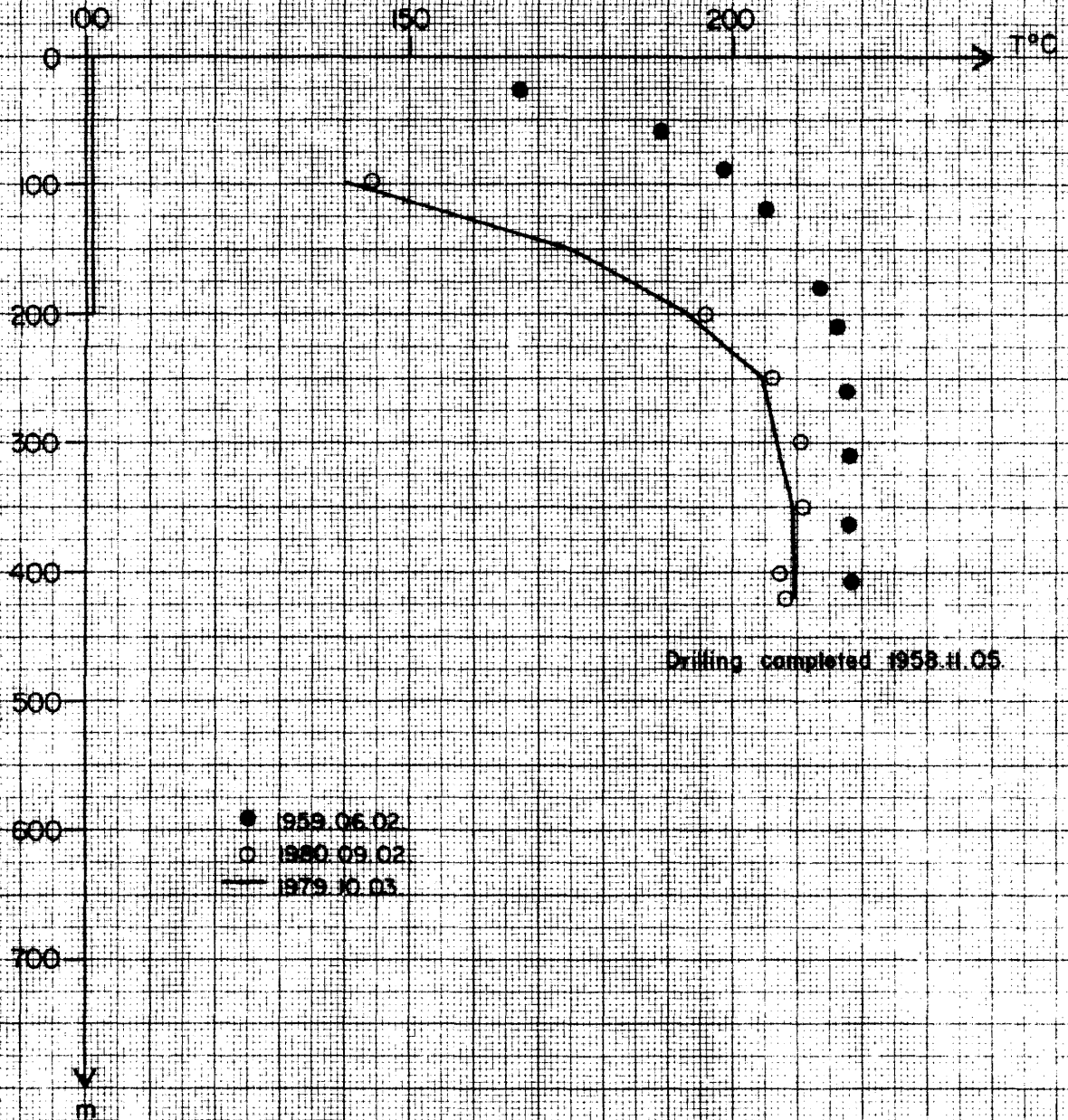
ZHOU/EBF

HSB Ölfus.

F-20004

Temperature profile of well G-3, Ölfusdalur.

Fig. 64





Temperature profile of well G-5, Ölfusdalur.

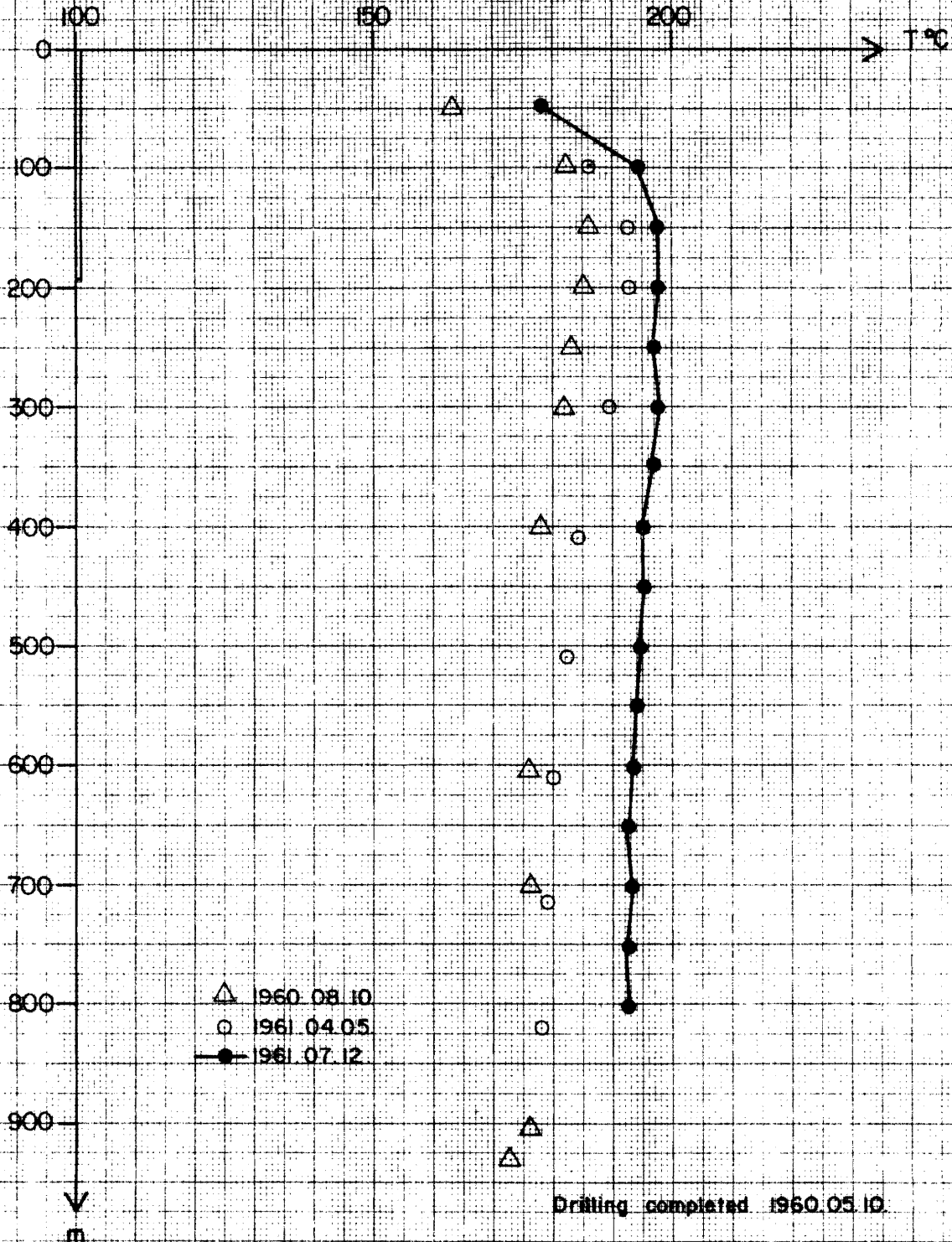
'80.09.09.

ZHOU/EBF

HSP Ölfus.

F-20005

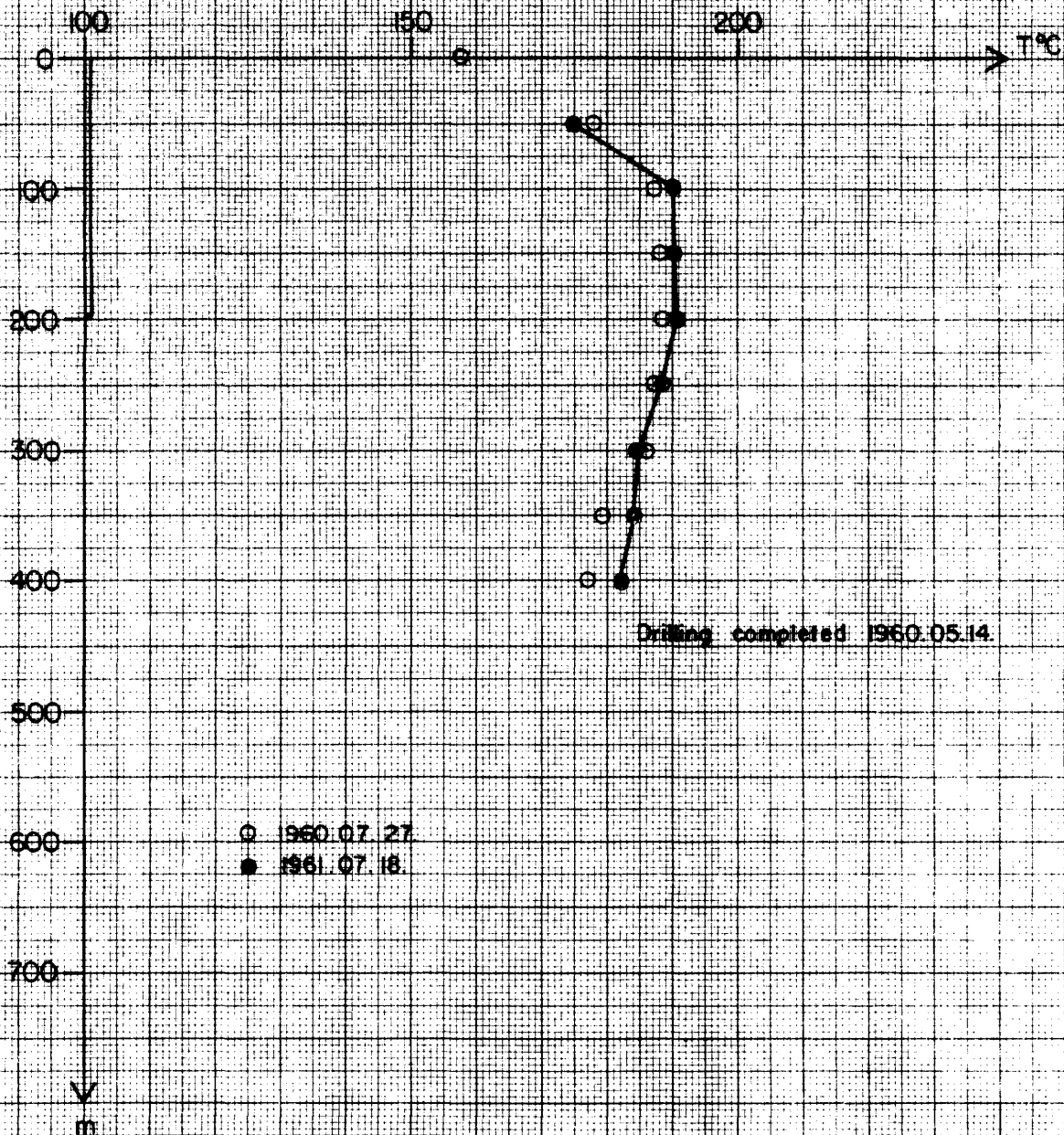
Fig. 65





Temperature profile of well G-2, Ölfusdalur.

Fig. 56





'80.09.09.

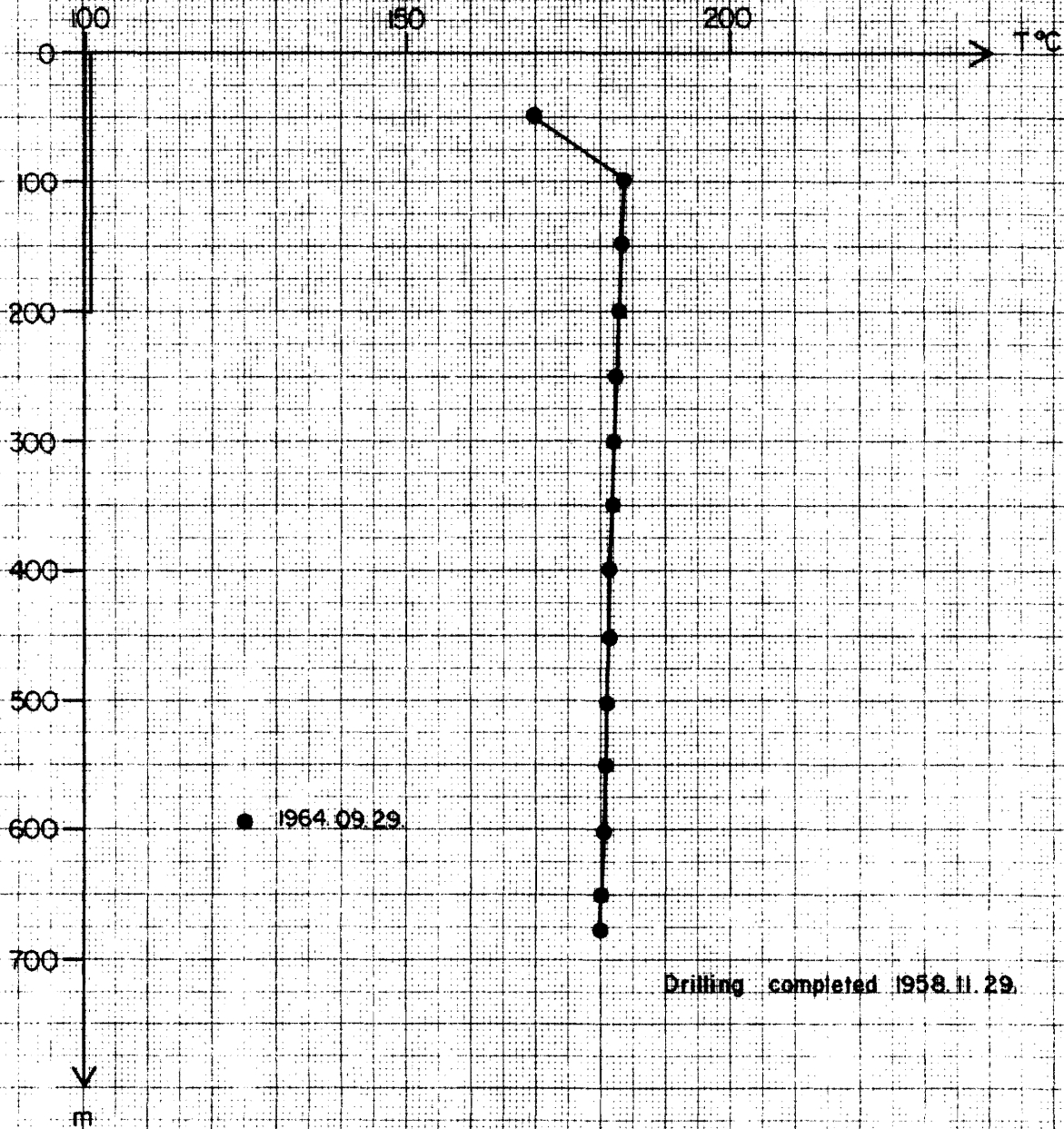
ZHOU / EBF

HSE Ölfus.

F-20007.

Temperature profile of well G-4, Ölfusdalur.

Fig. 67





'80.09.09.

ZHOU / EBF

HSP Ölfus.

F-20008

Temperature profile NW - SE, Ölfusdalur.

Fig. 68

